IMPROOF Workshop
Ghent University, 27-28 January 2020

Chemistry Acceleration in Computational Fluid Dynamics of combustion and heterogeneous catalysis

Alberto Cuoci

Outline

1. **Introduction**

2. **Reduction of chemical complexity**
   - DAC: Dynamic Adaptive Chemistry
   - SPARC: Sample-Partitioning Adaptive Reduced Chemistry

3. **Reduction of number of reactive environments**
   - DCC: Dynamic Cell Clustering (or Cell Agglomeration)
   - KPP: Kinetic Post Processing

4. **Acceleration of ODE solution**
   - ISAT: In Situ Adaptive Tabulation
   - CA: Chemistry Agglomeration
   - ANN + Unsupervised Clustering

Combustion and detailed kinetics

Real fuels and surrogates

need of modeling synergistic effects between the different components

Biofuels

bioalcohols, biodiesel, green diesel, bioethers

Pollutant emissions

NOx, SOx, PAHs, soot

Realistic numerical simulations of pyrolysis and combustion require not only detailed modeling of fluid dynamics, but also a **detailed characterization of chemical reactions**.

The inaccuracy and inadequacy of simple approaches (equilibrium chemistry or global mechanisms) have been clearly demonstrated in recent years.

This has promoted an increasing effort to develop and incorporate **more complex reaction mechanisms** in the numerical simulation of combustion and pyrolysis

Heterogeneous catalytic reactors

Result of the interplay among phenomena at different scales

Microscale

$COOH^*+^* \rightarrow CO^*+OH^*$
$CO^*+OH^* \rightarrow COOH^*+^*$
$COOH^*+^* \rightarrow CO_2^*+H^*$
$CO_2^*+H^* \rightarrow COOH^*+^*$
$CO_2^* + H_2O^* \rightarrow COOH^* + OH^*$
$COOH^* + OH^* \rightarrow CO_2^* + H_2O^*$
$CO_2^*+H^* \rightarrow HCOO^{**}$
$HCOO^{**} \rightarrow CO_2^*+H^*$
$CO_2^* + OH^* + ^* \rightarrow HCOO^{**} + O^*$
$HCOO^{**} + OH^* \rightarrow CO_2^* + H_2O^*$
$CH^* + H^* \rightarrow CH_2^* + ^*$
$CH^* + ^* \rightarrow C^* + H^*$
$C^* + H^* \rightarrow CH^* + ^*$
$CH_3^* + O^* \rightarrow CH_2^* + OH^*$
$CH_2^* + OH^* \rightarrow CH_3^* + O^*$
$CH^* + OH^* \rightarrow CH_2^* + O^*$
$CH_2^* + O^* \rightarrow CH^* + OH^*$
…

~ 10^2 potential steps @ different coverages

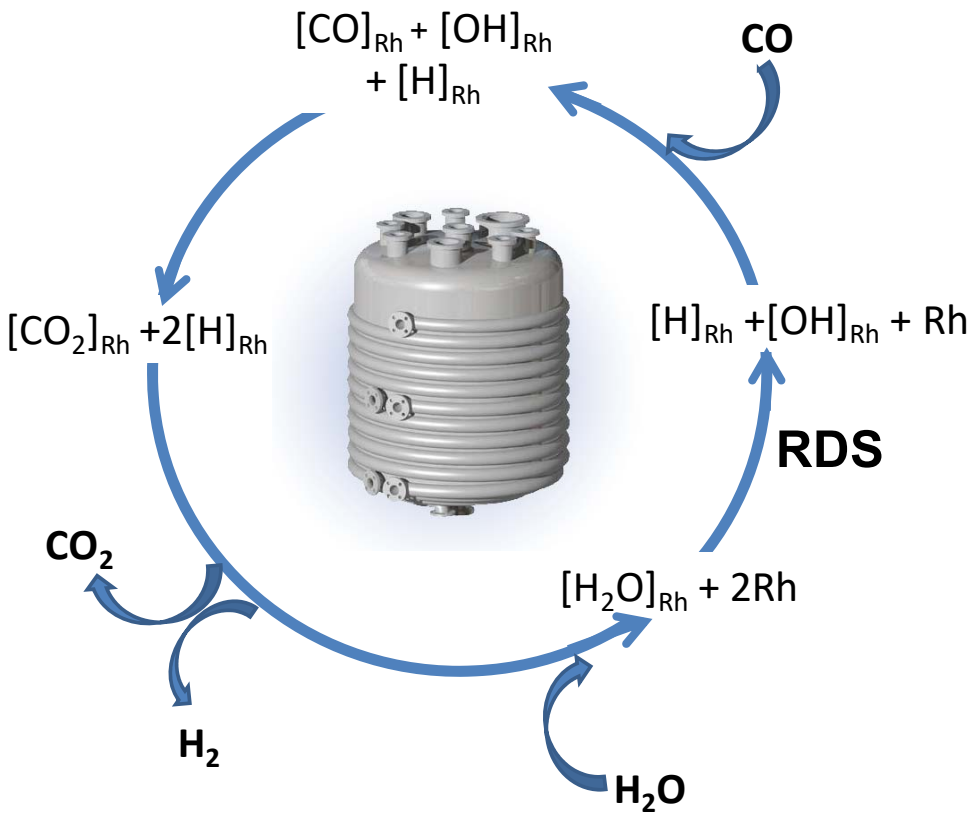

Macroscale

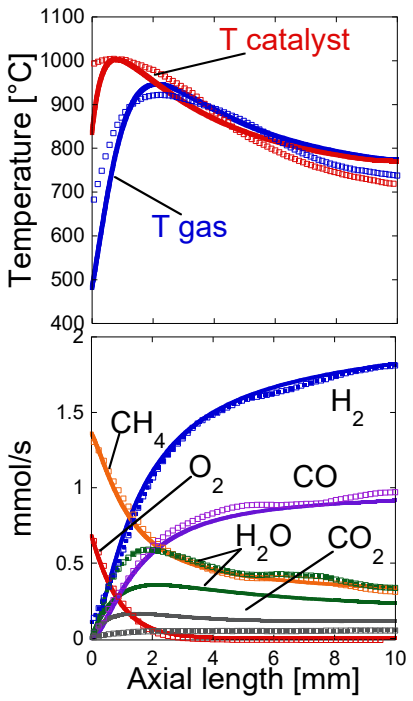

Heterogeneous catalysis and detailed kinetics

New insights into the **complexity of heterogeneous catalysis** reveal the demand for more sophisticated chemistry models and their implementation into CFD simulations

Modeling the **interactions of catalytic surface and surrounding gas-phase** is a very active field, together with the implementation of more adequate and complex kinetic models continue.

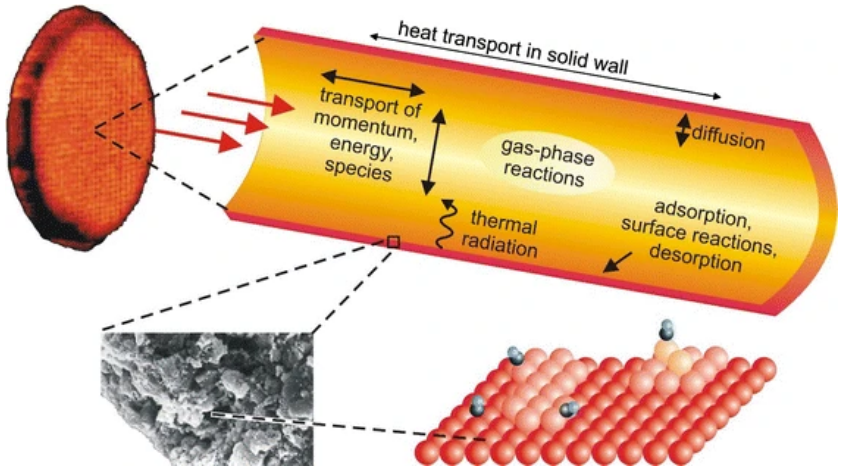

O. Deutschmann, Catalysis Letters, 145, 272–289 (2015)

Examples

- Adsorption and Desorption: Partial Oxidation of CH4 over Rh
- Partial Oxidation of CH4 over Noble Metals
- Gas-Phase Initiated Coking in Dry Reforming of Methane
- Catalytic Reforming of Gasoline
- Catalytic Combustion Monoliths

Detailed kinetic mechanisms in combustion

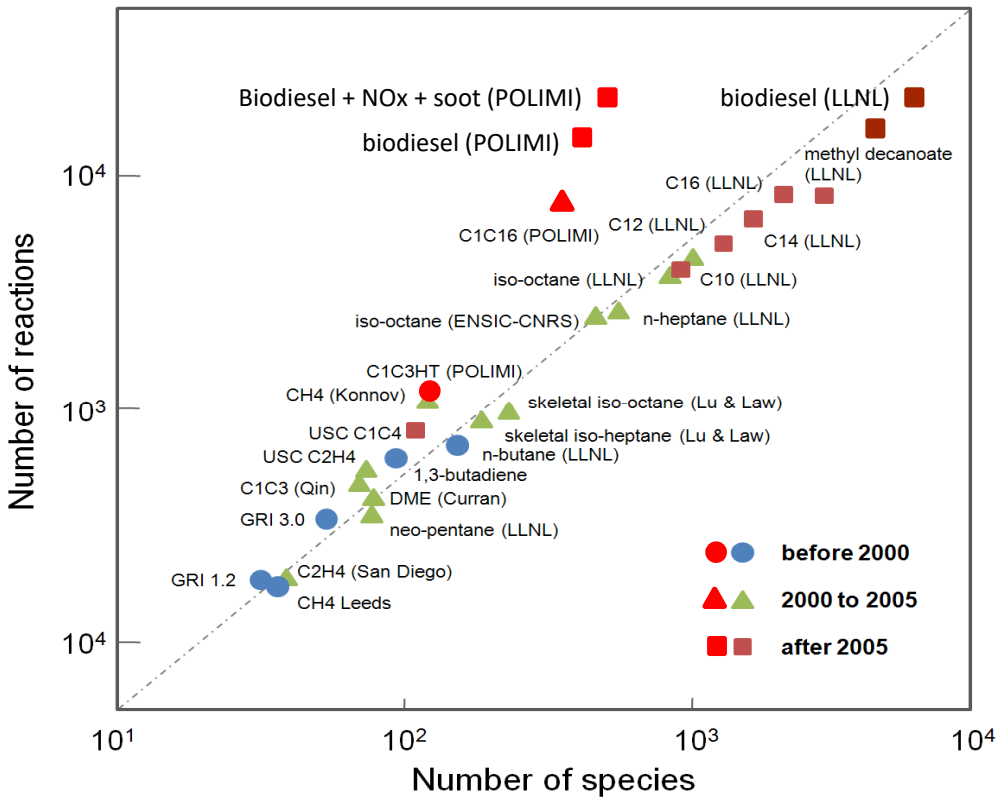

Adapted from: **T.F. Lu, C.K. Law**, *Toward accommodating realistic fuel chemistry in large-scale computations,* Progress in Energy and Combustion Science, 35, p. 192–215 (2009)

increasing effort to incorporate **more complex reaction mechanisms** in simulation of combustion processes

computational cost associated with such mechanisms is usually very high

need of **numerical techniques** and **computational tools** to:

- efficiently make use of large kinetic mechanisms
-easily integrate them in new and/or existing numerical codes

Detailed kinetic mechanisms in heterogeneous catalysis

Examples of detailed microkinetic mechanisms for heterogeneous catalysis

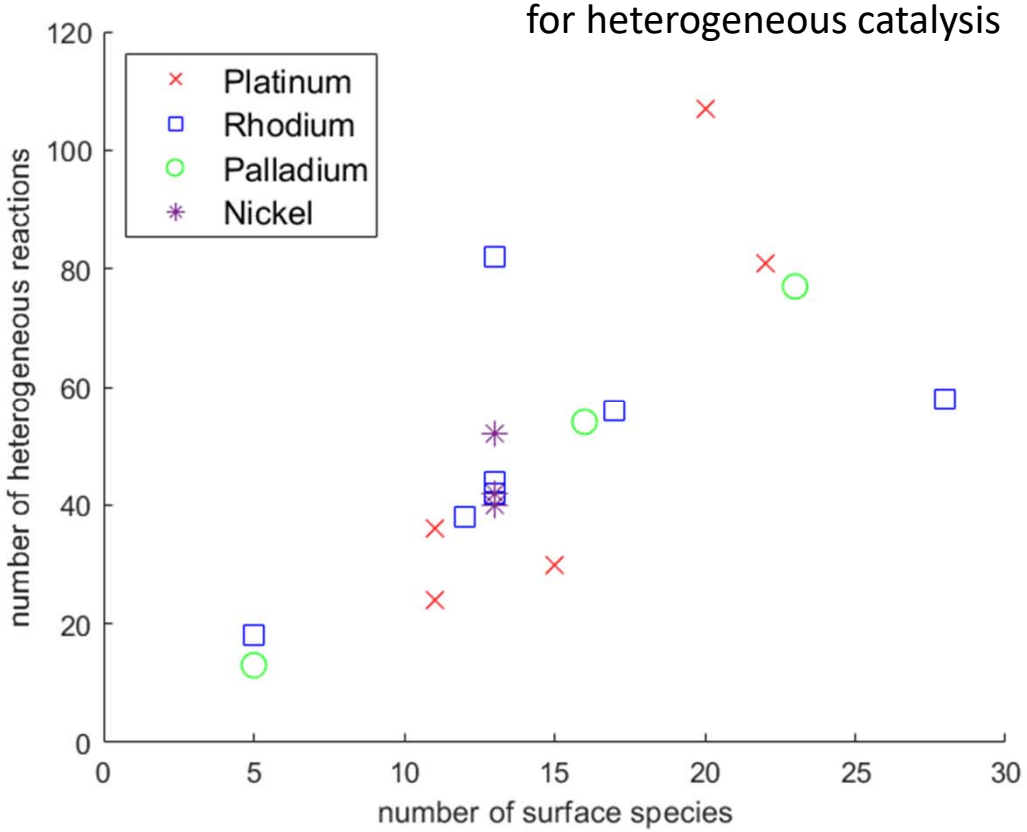

DETCHEM web-site: https://www.detchem.com/mechanisms
CatalyticFOAM web-site: http://www.catalyticfoam.polimi.it/

The direct computation of surface reaction rates from ab-initio and DFT, promoted the development of heterogeneous, catalytic mechanisms with **increasing level of detail and complexity**

Microkinetic models – based on first-principles (electronic structure) calculations – have demonstrated an unparalleled power in the detailed description of the elementary steps at the catalyst surface

Example: laminar coflow flames

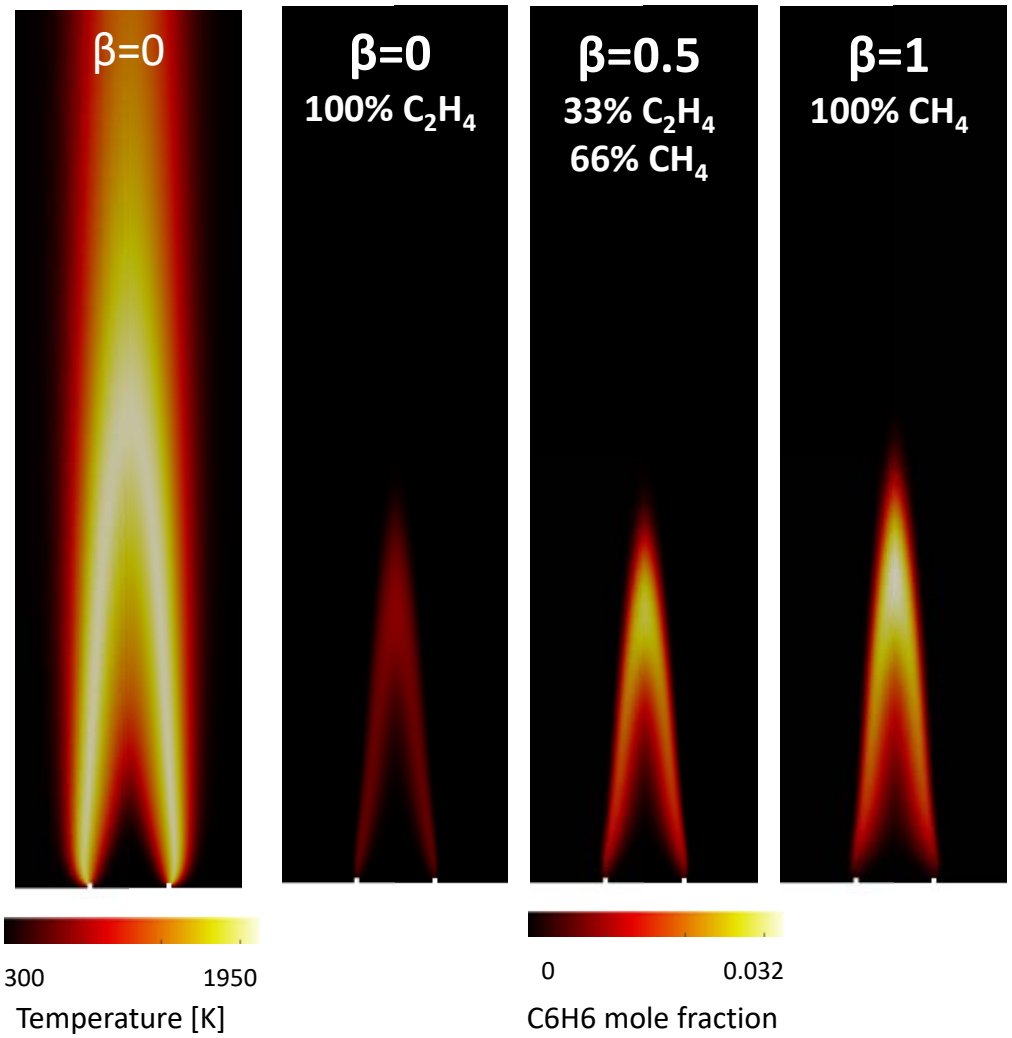

Fuel: CH4/C2H4
Air: O2/N2 (23.2%, 76.8% mass)
Vfuel: 12.52 cm/s
Vair: 10.50 cm/s
Fuel nozzle diameter: 11.1 mm
Chamber diameter: 110 mm

Computational details
Domain: 2D axisymmetric (55 x 200 mm)
Computational grid: ~25,000 cells
Discretization: second order centered

Kinetic mechanism
POLIMI_SOOT_1412:
292 species, ~15,800 reactions

The concentrations of C2H4 and CH4 are identified by the mixture parameter β:

$$\beta = \frac{X_{CH4}}{X_{CH4} + 2X_{C2H4}}$$

Cuoci, A., Frassoldati, A., Faravelli, T., Ranzi, E., *A computational tool for the detailed kinetic modeling of laminar flames: Application to C2H4/CH4 coflow flames* (2013) Combustion and Flame, 160 (5), pp. 870-886

Example: CPOX of methane over Pt gauze

Homogeneous Chemistry

84 species, 1698 reactions

Ranzi et al., PECS 2014

Heterogeneous Chemistry

13 surface species, 82 reactions

UBI-QEP and DFT refinements

M. Maestri et al., AIChE J., 2009

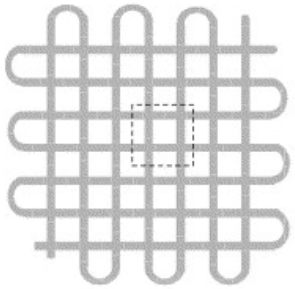

T_{in}=600 K

T_{gauze}=1000-1200 K

P=1.3 bar

CH_4/O_2/HE

0.143/0.057/0.80

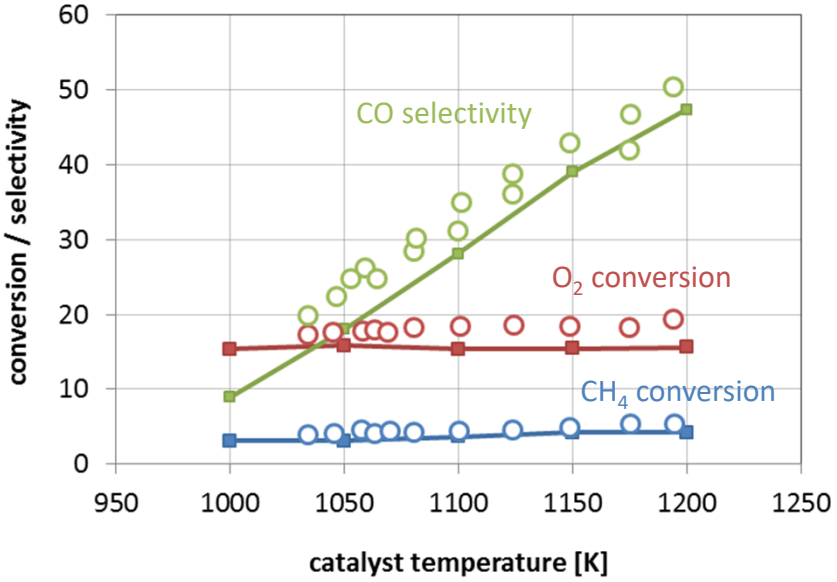

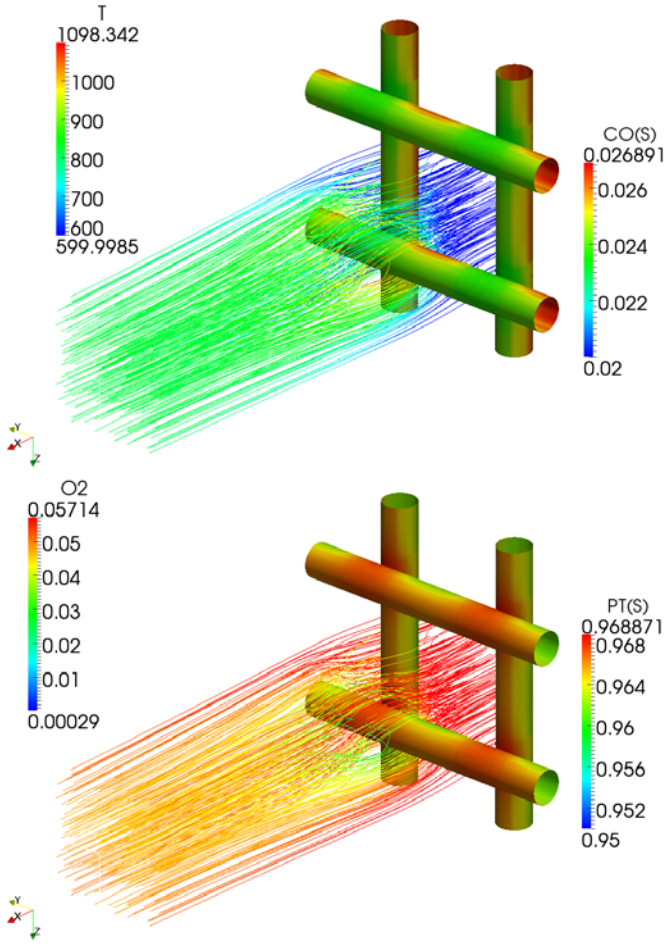

M. Maestri, A. Cuoci, *Coupling CFD with detailed microkinetic modeling in heterogeneous catalysis*, Chemical Engineering Science, 96(7), 106-117 (2013)

Detailed kinetics in CFD: challenges

1. Coupling
Hundreds of species resulting in a large number of coupled transport equations

2. Non-linearity
The transport equations of species and energy are very non-linear, because of reaction rates expressions (power-law and exponential)

3. Stiffness
The characteristic times of species involved in detailed chemistry can differ by several order of magnitudes.

Detailed kinetics

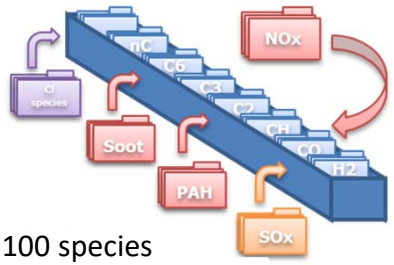

~ 100 species
~ 1,000 reactions

Unsteady flame

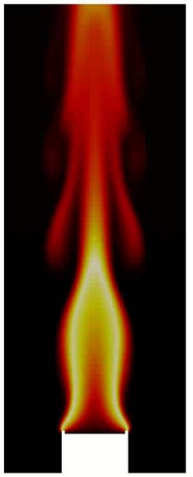

Inlet mixture: C_3H_8 + Air
Temperature: 1800 K

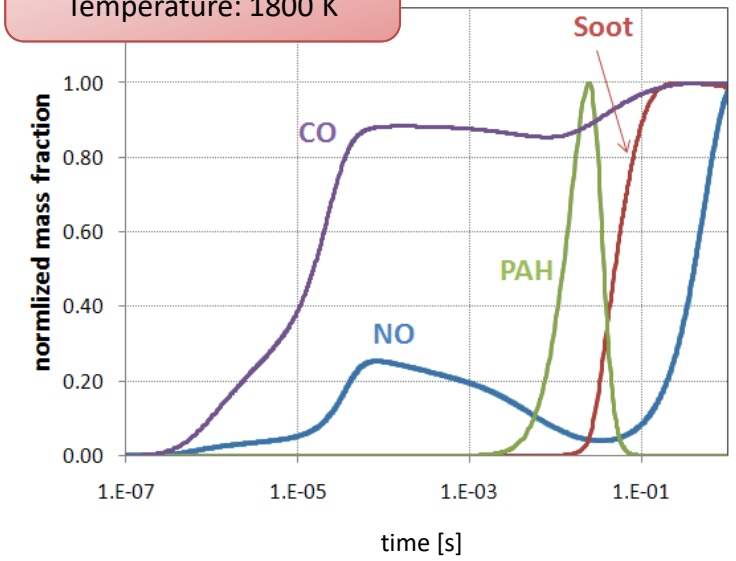

Chemistry is stiff

LLNL-NC7 Mechanism
Species: 654
Reactions: 2,837

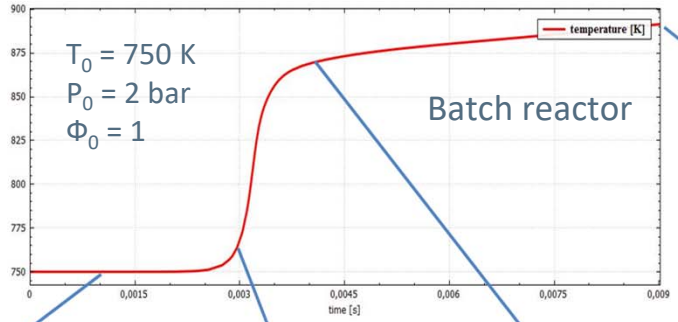

Distribution of characteristic times calculated through the eigenvalue analysis of the Jacobian matrix associated to the system of species and energy equations

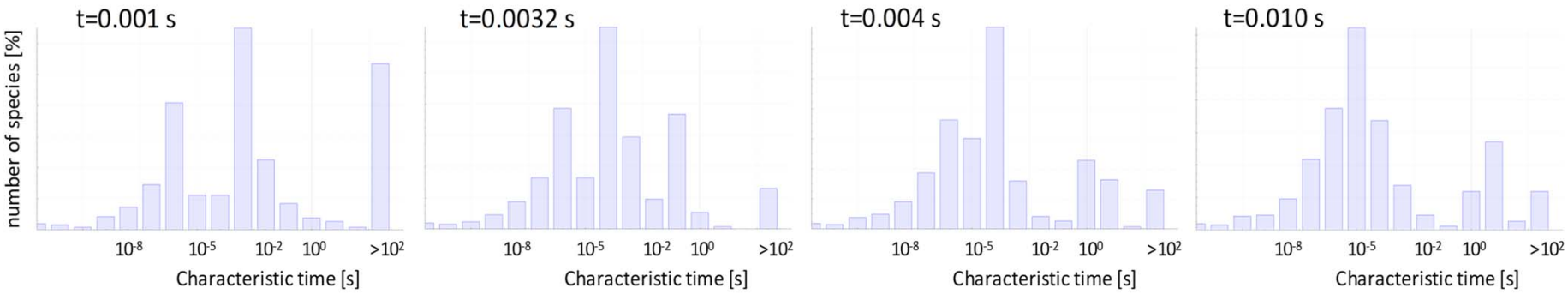

Implicit treatment of chemistry (I)

$$\frac{d\boldsymbol{\psi}}{dt} = \mathbf{M} + \mathbf{S}$$

Transport (convection + diffusion)

Chemistry (reactions)

$$\begin{cases} \Delta\boldsymbol{\psi}_1^n = \Delta t \mathbf{M}^n \\ \Delta\boldsymbol{\psi}_2^n = \Delta t \mathbf{S}^n \end{cases}$$

Transport step (Δt)

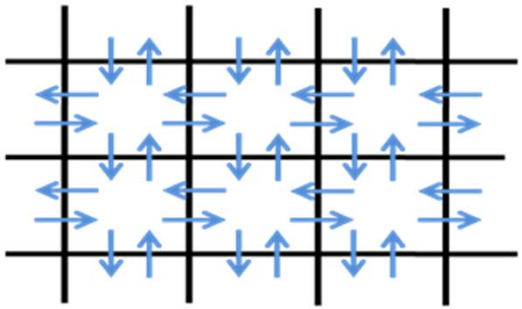

$$\frac{d\boldsymbol{\psi}}{dt} = \mathbf{M}$$

Chemical step (Δt)

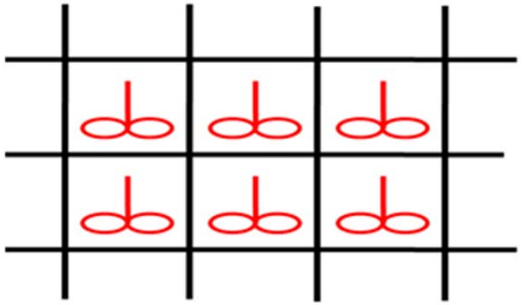

$$\frac{d\boldsymbol{\psi}}{dt} = \mathbf{S}$$

Strang, *On the construction and comparison of difference schemes.* SIAM Journal of Numerical Analysis, 5, p. 506-517 (1968)

Ren, Pope, *Second-order splitting schemes for a class of reactive systems.* Journal of Computational Physics, 227 p. 8165-8176 (2008)

Implicit treatment of chemistry (II)

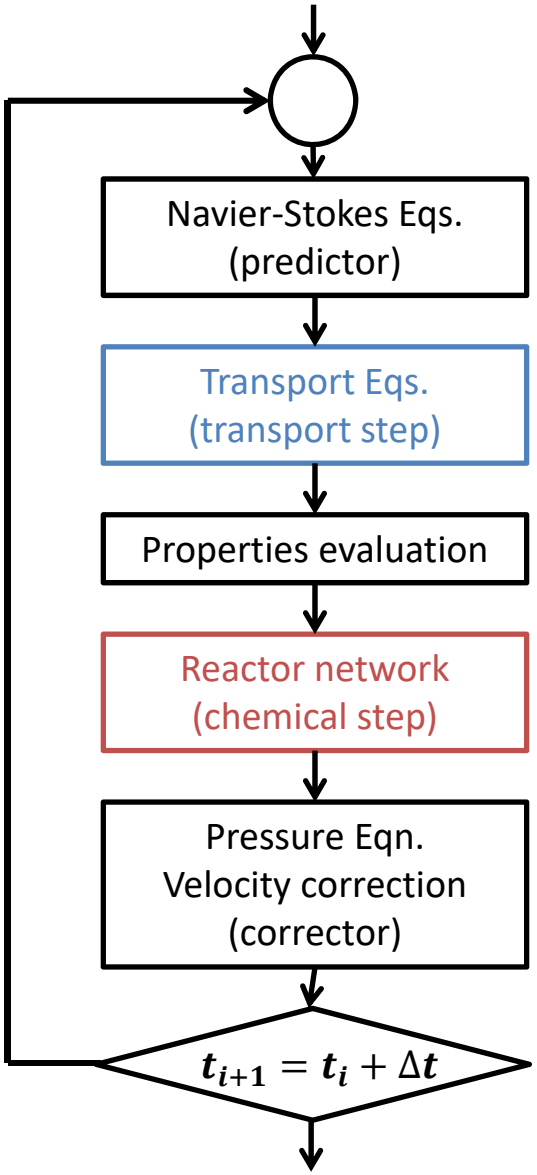

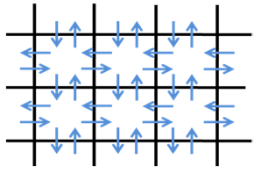

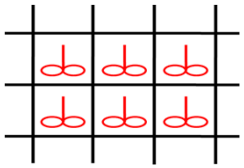

The chemical step corresponds to the solution of **independent ODE systems** with IC (i.e. independent batch reactors).

Because of non-linearity and stiffness, the use of implicit ODE solvers is basically mandatory!

However, **implicit ODE solvers** are computationally very expensive and their computational cost increases more than linearly with the number of species:

$$C \sim n^{2 \div 3}$$

Chemistry Acceleration
to reduce the computational cost of chemical step (without compromising the accuracy)

Chemistry Acceleration (I)

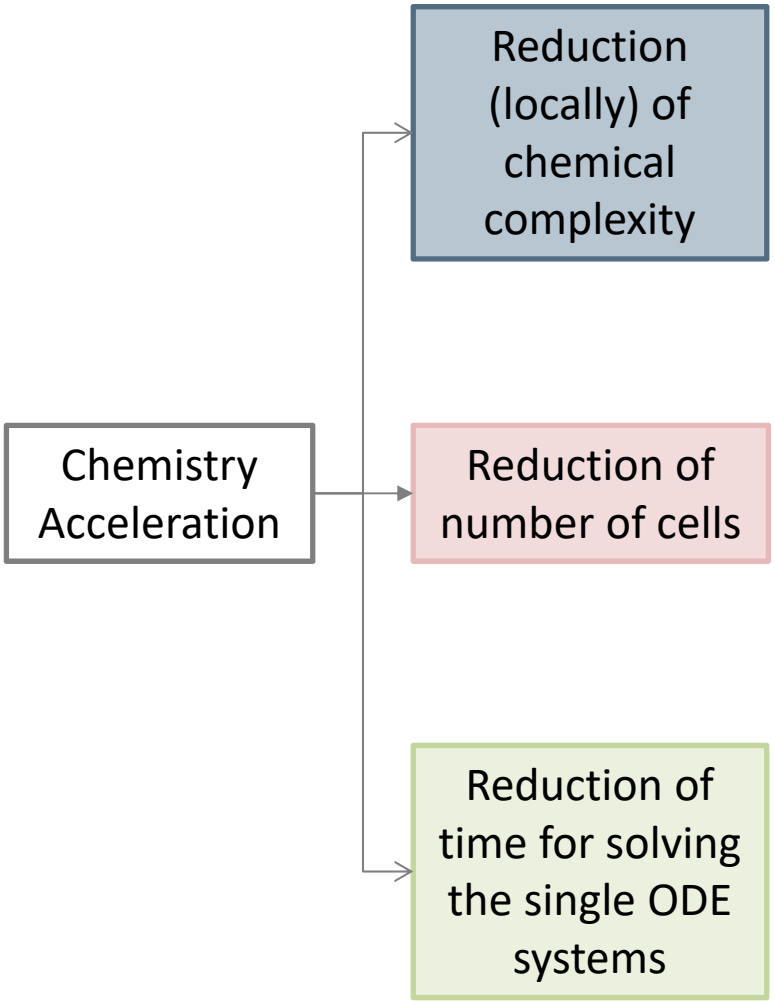

Classification problem

Reduction of kinetic mechanisms by removal of species, classification of thermochemical state and clustering of species

Classification problem

Group (cluster) together cells having a similar thermochemical state to reduce the total number of ODE systems to be solved

Regression & Classification problem

Numerical techniques to replace/improve the solution of expensive ODE systems.

Chemistry Acceleration (II)

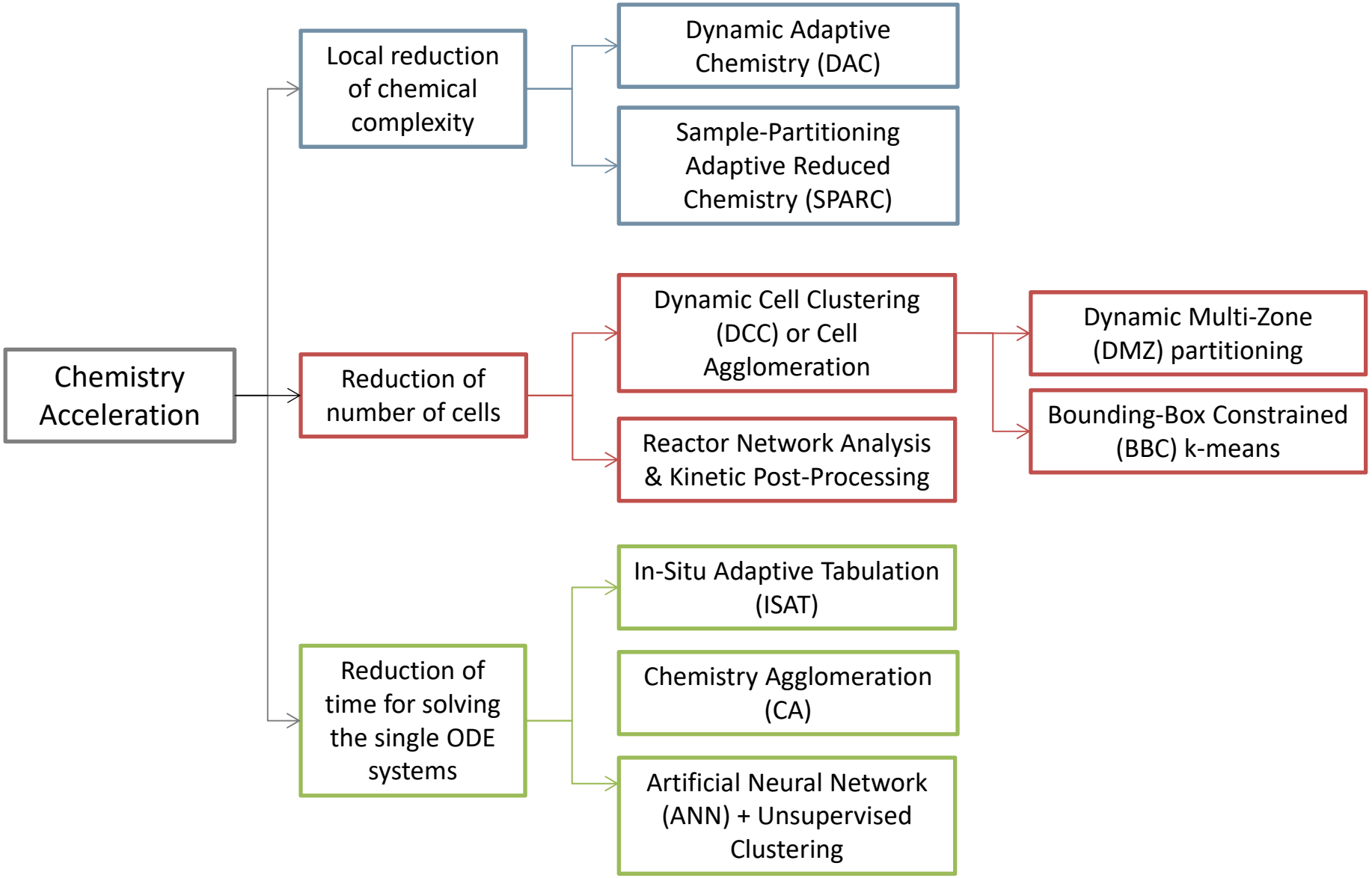

Chemistry Acceleration and Machine Learning

		Chemistry Acceleration							
		Reduction of chemistry		Reduction of cells			ODE Acceleration		
		DAC	SPARC	DMZ	BBC	RNA	ISAT	CA	ANN+UC
Classification	Unsupervised		X	X	X			X	X
Classification	Supervised	X				X	X	X	
Regression	ANN		X						X
Regression	Other		X			X	X		

The **flexibility of Machine Learning (ML)** models to easily capture nonlinear, multi-dimensional characteristics in data, makes them very useful in different aspects of reacting flows.

Chemistry Acceleration

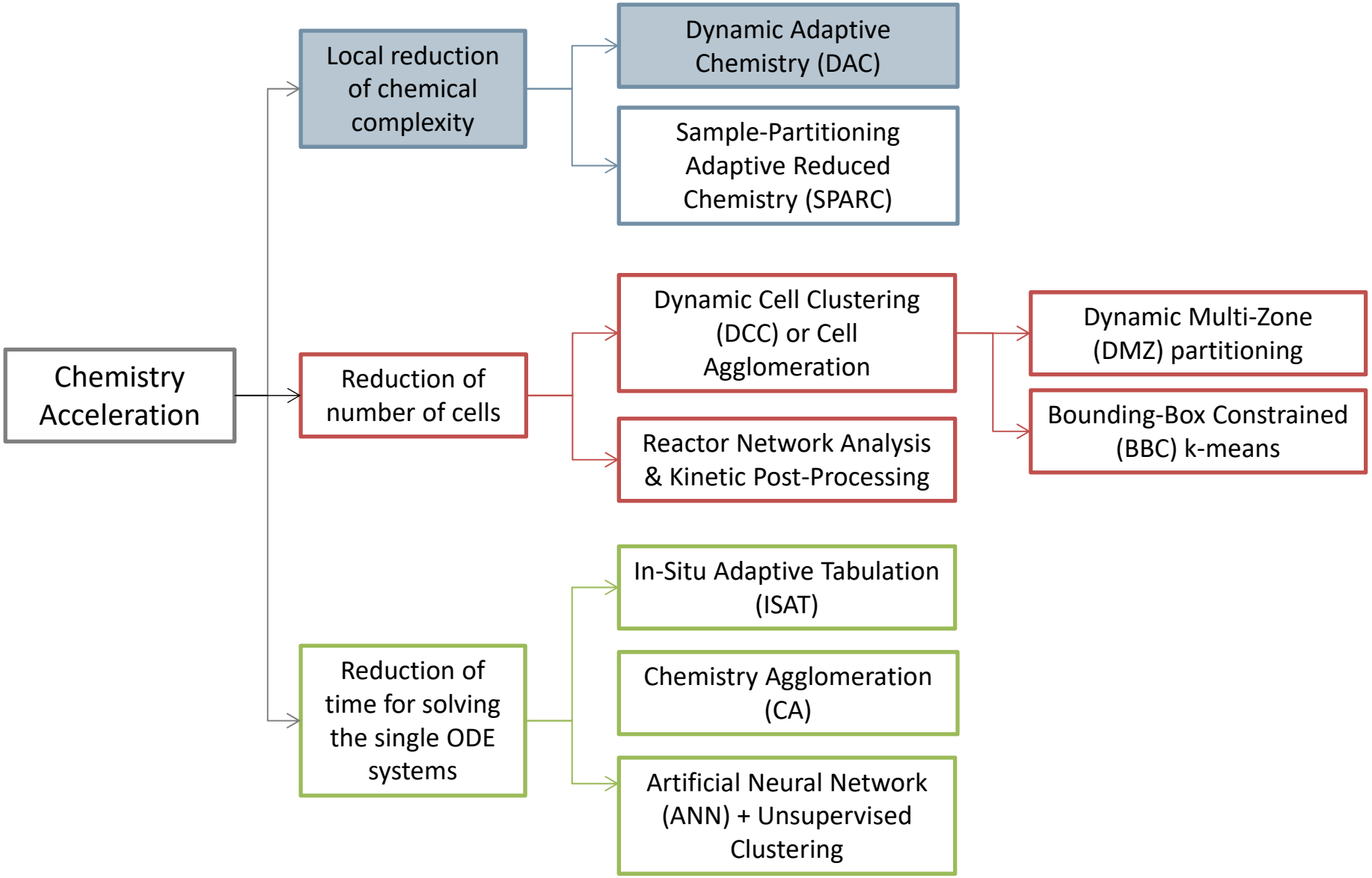

Adaptive Chemistry: an example (I)

Burner-Stabilized Stagnation Flame

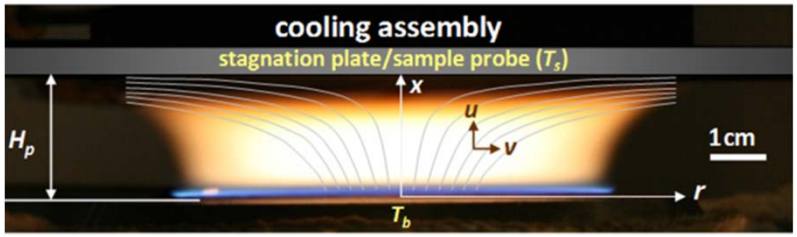

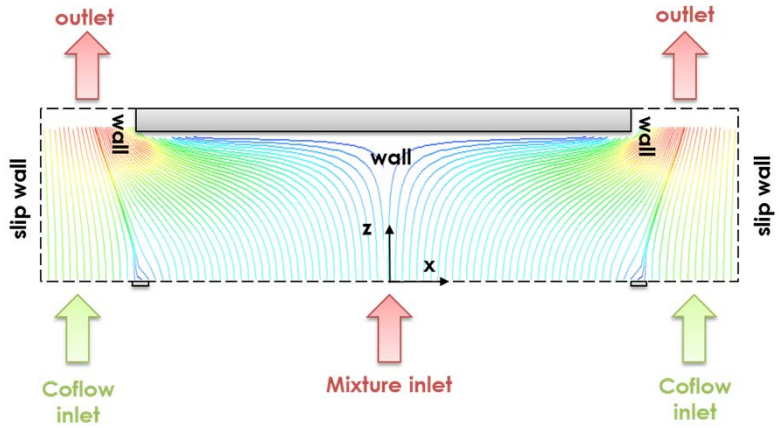

C. Saggese, S. Ferrario, J. Camacho, A. Cuoci, A. Frassoldati, E. Ranzi, H. Wang, T. Faravelli, *Kinetic modeling of particle size distribution of soot in a premixed burner-stabilized stagnation ethylene flame* (2015) Combustion and Flame, 162(9), pp. 3356-3369

Detailed kinetic mechanism: 292 species and ~15,800 reactions

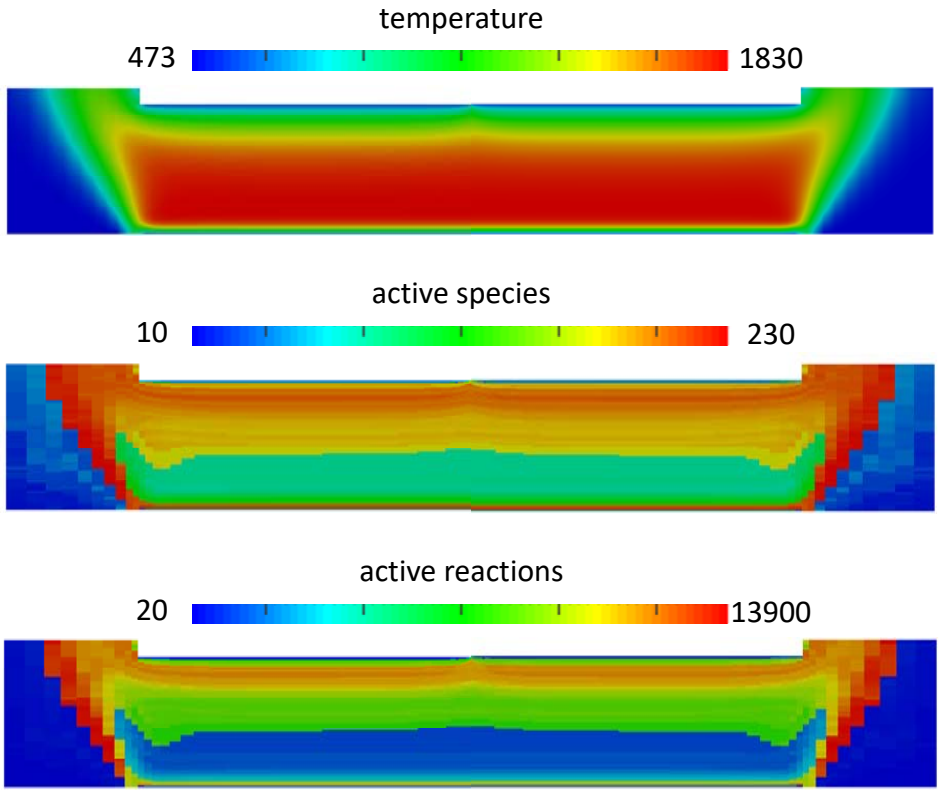

Dynamic Adaptive Chemistry (DAC) (I)

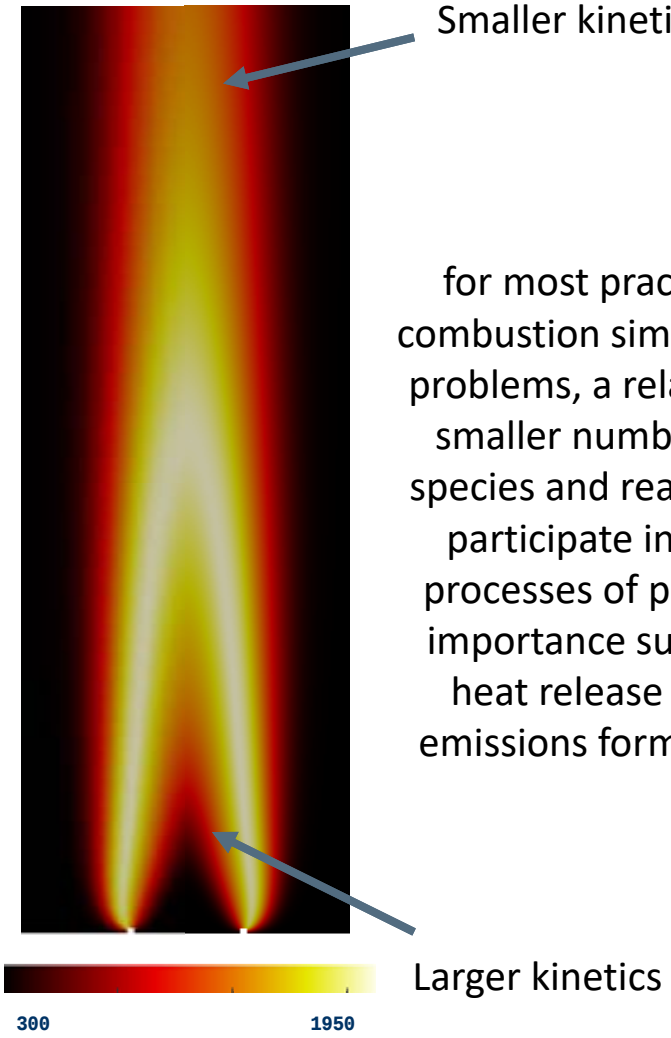

for most practical combustion simulation problems, a relatively smaller number of species and reactions participate in the processes of pivotal importance such as heat release and emissions formation

Dynamic Adaptive Chemistry

The detailed mechanism is reduced **locally and instantaneously** into accurate sub-mechanisms at each hydrodynamic time step of the calculation ("on the fly")

no a priori information regarding simulation conditions is needed.

For comprehensiveness, more species is better
For computational cost, less species is better

Liang L., Stevens J.G., Farrell J.T., *A dynamic adaptive chemistry scheme for reactive flow computations*, Proceedings of The Combustion Institute, 32, p. 527–534 (2009)
Liang L., Stevens J.G., Raman S., Farrell J.T., *The use of dynamic adaptive chemistry in combustion simulation of gasoline surrogate fuels*, Combustion and Flame, 156, p. 1493–1502 (2009)

Dynamic Adaptive Chemistry (DAC) (II)

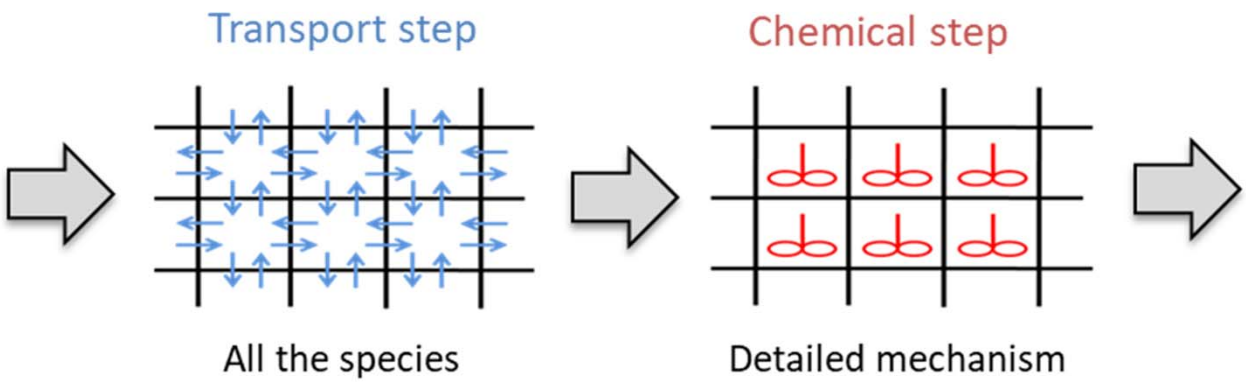

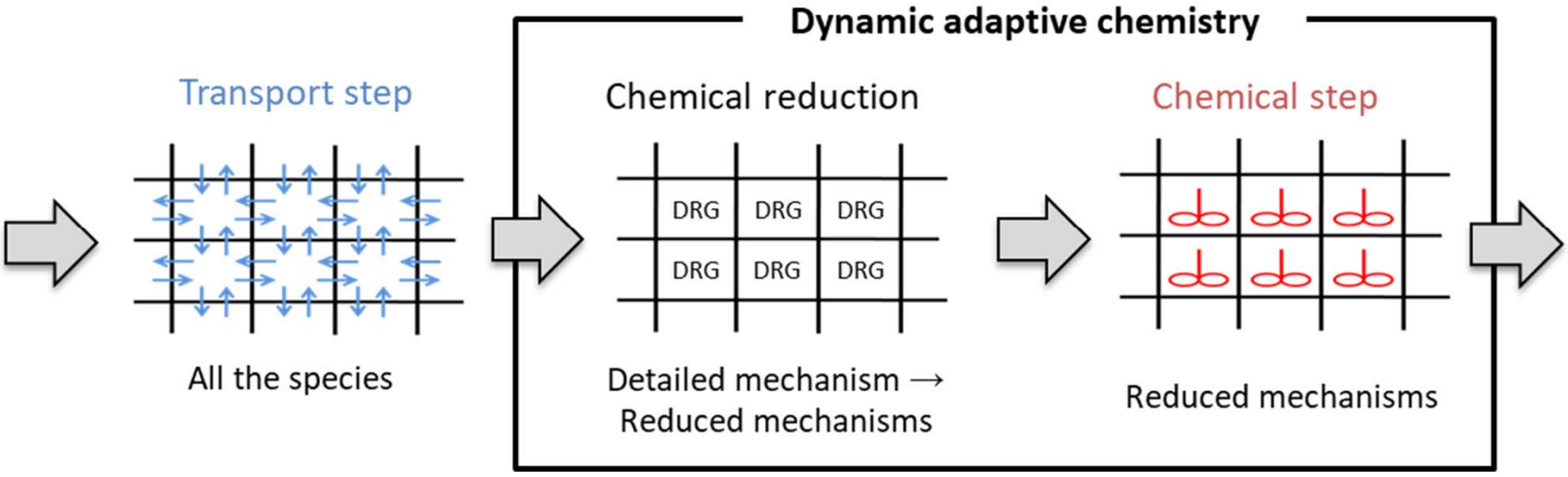

Automatic reduction of kinetic mechanisms

Target species

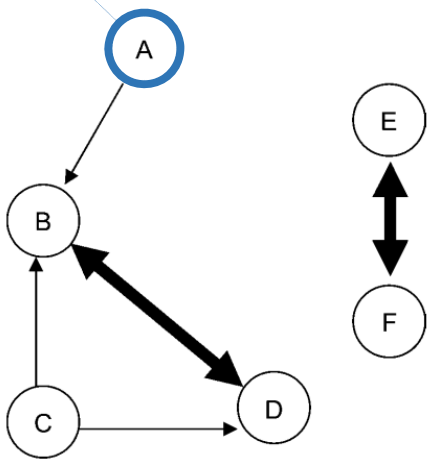

Mechanisms reduction

Directed Relation Graph

Strongly linked species

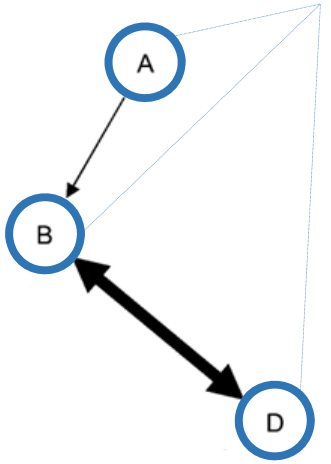

Original mechanism

Species: A , B , C , D , E , F

Optimized Reduced mechanism

Important Species: A , B , D

Adapted from: **T.F. Lu, C.K. Law**, *Toward accommodating realistic fuel chemistry in large-scale computations,* Progress in Energy and Combustion Science, 35, p. 192–215 (2009)

DRG: Directed Relation Graph

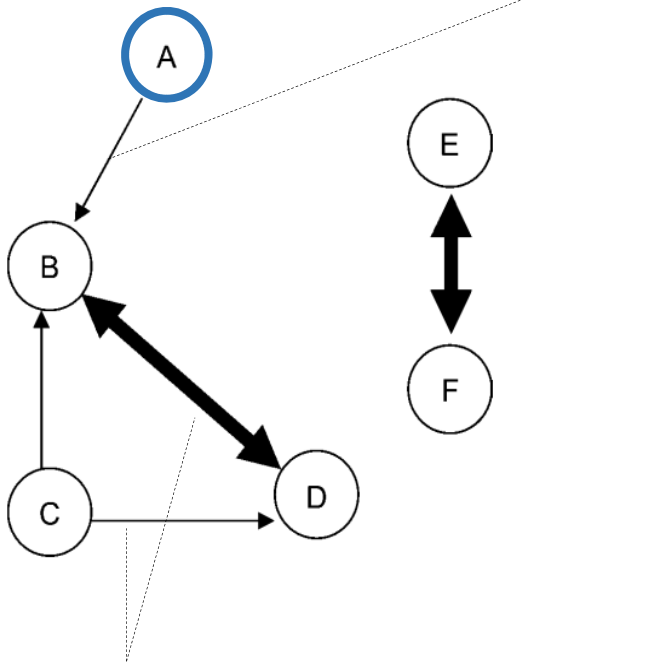

The greater I_{ij} the thicker the Edge

If there exist an edge connecting A to B, it means that B must be kept in order to correctly predict the rate production of A:

$$R_A = \sum_i \upsilon_{A,i} r_i$$

To quantify the direct influence of the species J on the species A, a normalized contribution of species J to the A production rate is defined:

$$I_{AJ} = \frac{\sum_i |\upsilon_{A,i} r_i \delta_{Ji}|}{\sum_i |\upsilon_{A,i} r_i|} > \varepsilon$$

$$\delta_{Ji} = \begin{cases} 1 & \text{If the species } J \text{ participate to reaction } i \text{ with A} \\ 0 & \text{Otherwise} \end{cases}$$

Dynamic Adaptive Chemistry: an example (I)

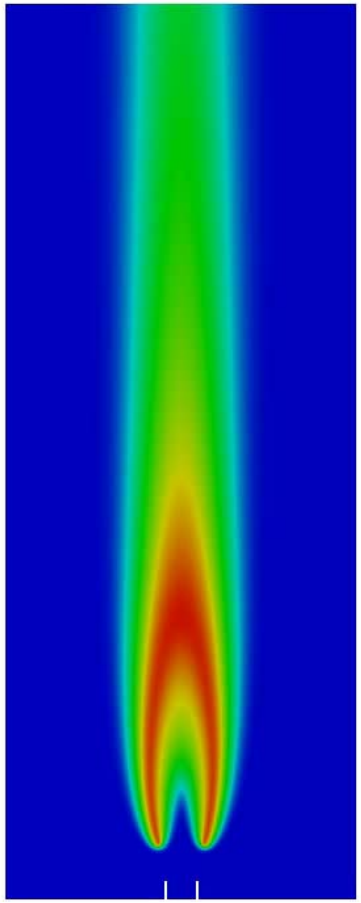

POLIMI C1C3HT mechanism
Species: 115
Reactions: 2141

Fuel mixture:
34% C_2H_4, 66% N_2
Coflow stream:
21% O_2, 79% N_2

The **transient behavior** is induced by a 2**0 Hz perturbation** in the fuel velocity profile

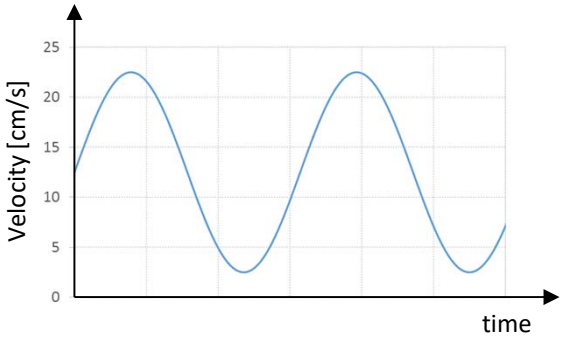

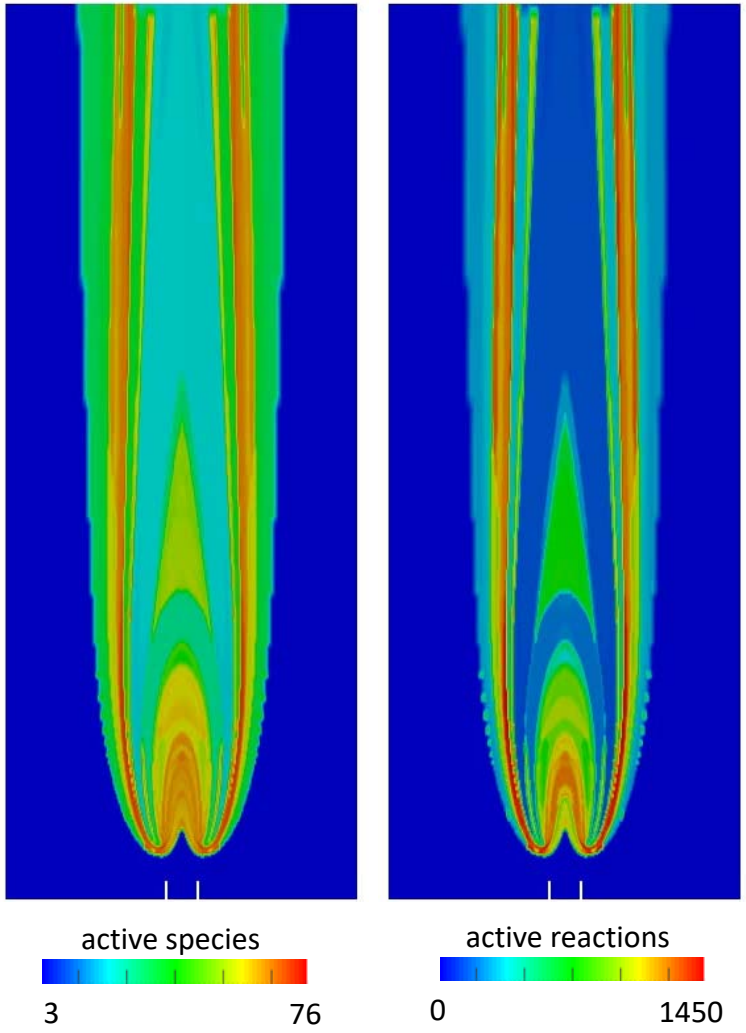

Dynamic Adaptive Chemistry: an example (II)

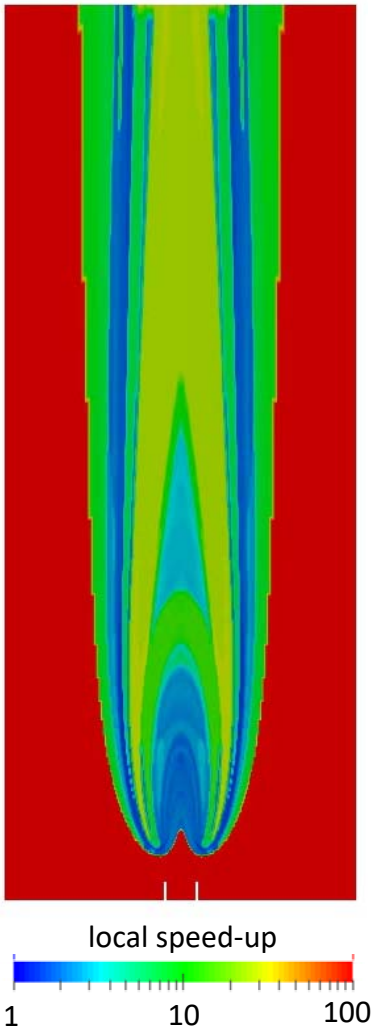

POLIMI kinetic mechanism
Species: 115
Reactions: 2141

Fuel mixture:
34% C_2H_4, 66% N_2
Coflow stream:
21% O_2, 79% N_2

The **transient behavior** is induced by a 2**0 Hz perturbation** in the fuel velocity profile

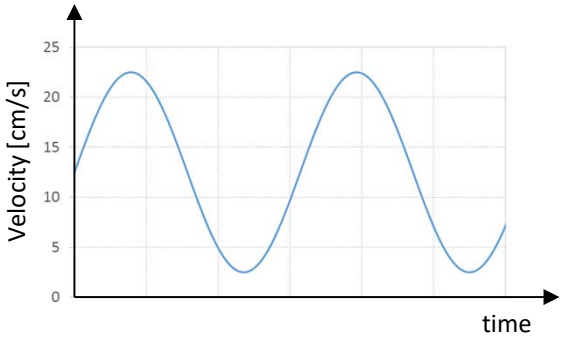

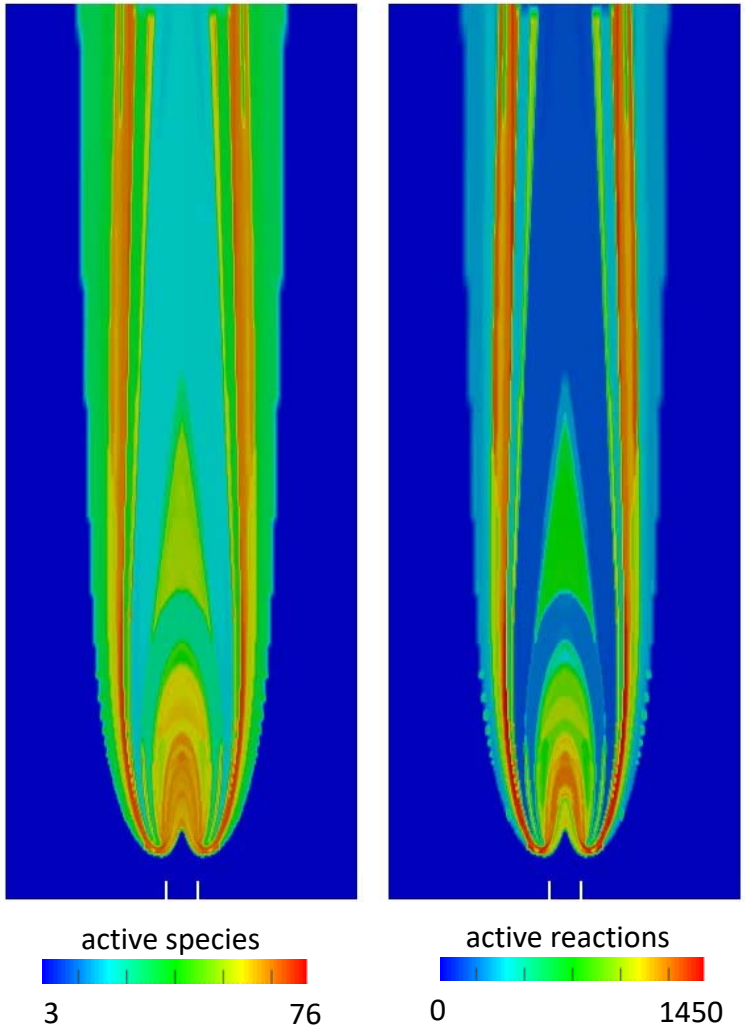

Computational performances: accuracy

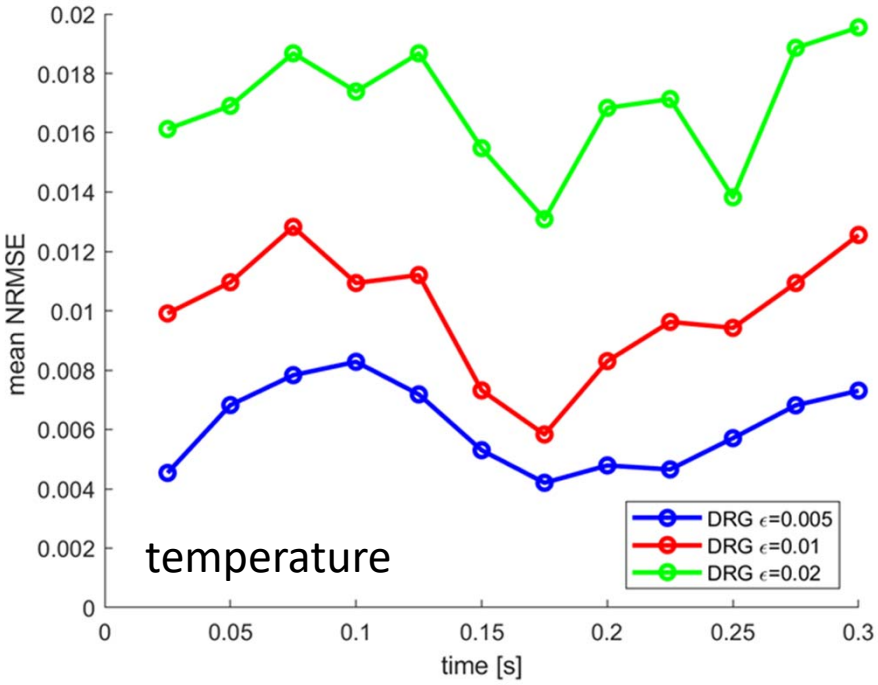

$$NRMSE = \frac{1}{\bar{y}}\sqrt{\frac{1}{N}\sum\left(y_i - y_i^{DRG}\right)^2}$$

Error measuring the difference between the detailed and the DRG solution

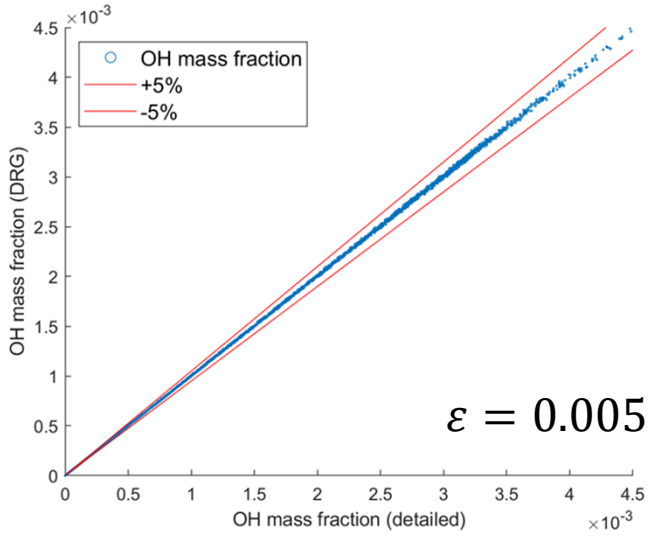

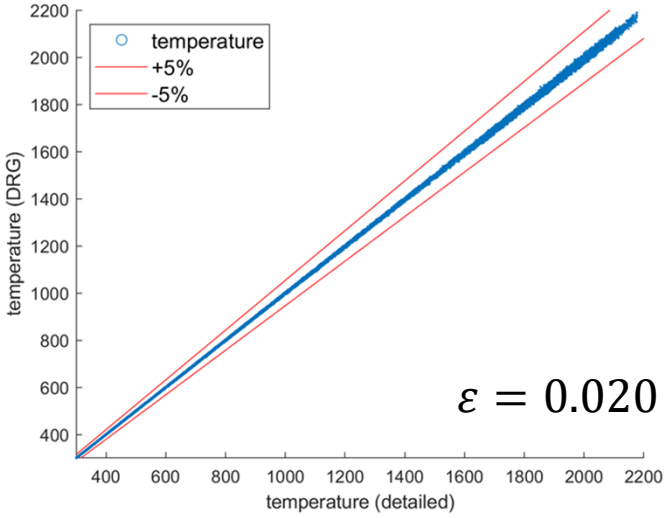

Computational performances: CPU time

$\varepsilon = 0.005$

Very accurate reduction

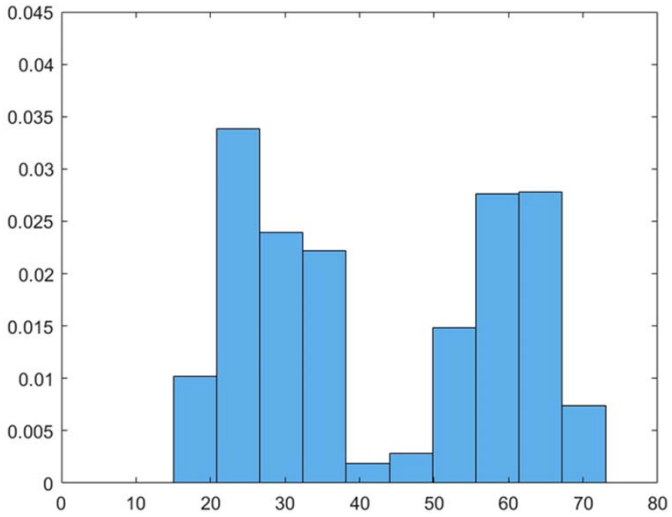

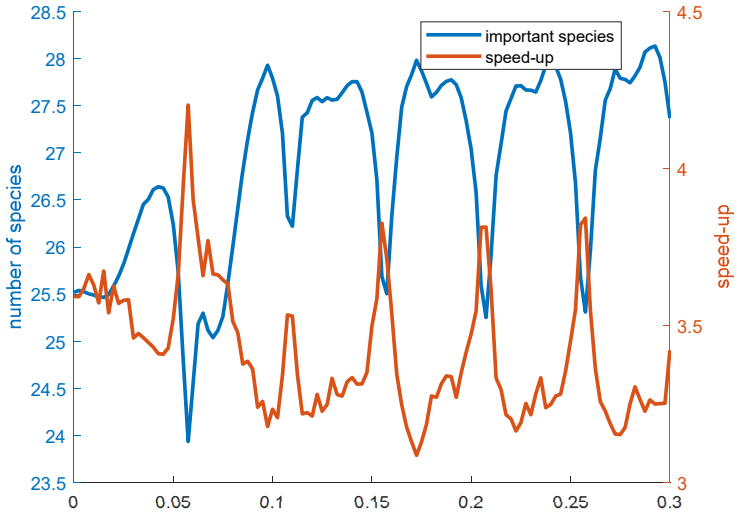

$\varepsilon = 0.02$

Coarse reduction

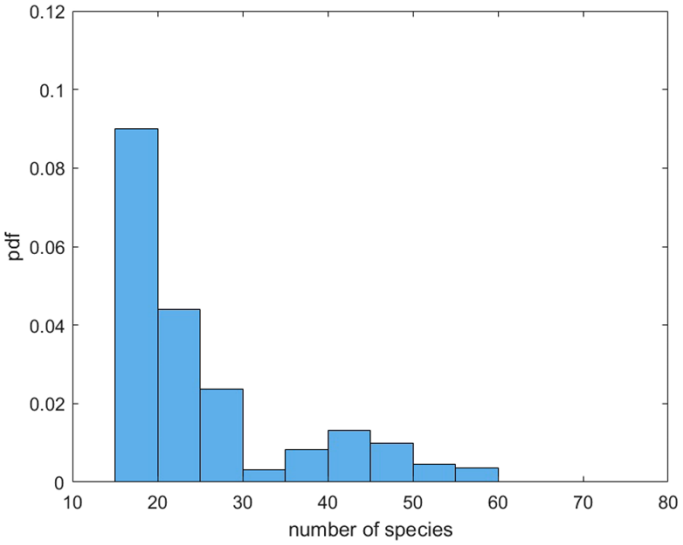

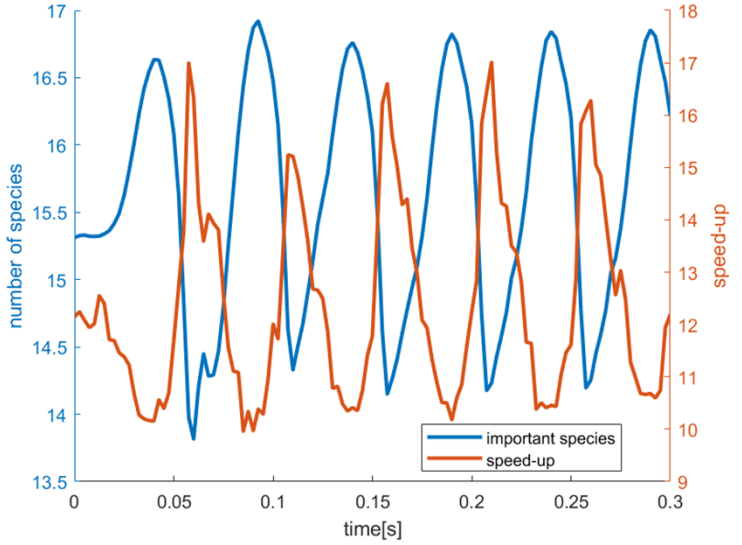

Computational performances: speed-up

Dynamic Adaptive Chemistry is able to speed-up the chemical step only
The CPU time associated to the transport step is unaffected

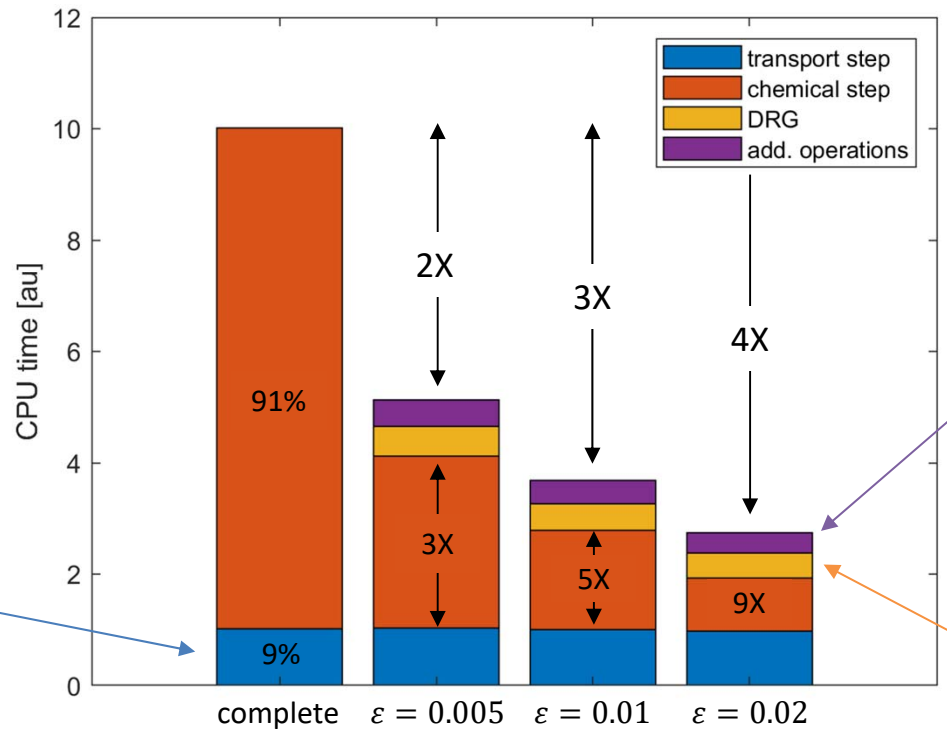

Maximum theoretical global speedup 10X

Additional operations are required to properly setup the ODE solvers to accommodate the reduced mechanisms

The time for performing DRG is almost independent of the tolerance ε

Other graph-based reduction methods

- DRG aided sensitivity analysis (DRGASA) (Zheng et al., 2007; Sankaran et al. 2007)
- Path flux analysis (PFA) (Sun et al., 2009)
- **DRGEP Directed Relation Graph with Error Propagation (Pepiot et al. 2008)**
- DRGEP with sensitivity analysis (DRGEPSA) (Niemeyer et al. 2010)
- Transport flux based DRG (on-the-fly reduction) (Tosatto et al. 2011)
- DRG with expert knowledge (DRGX) (Lu et al. 2011)
- Species-Targeted Sensitivity Analysis (STSA) (Stagni et al., 2015)

DRGEP: Directed Relation Graph with Error Propagation (I)

Graph vertices represent species and **directed edges** between vertices represent the coupling of species. The dependence of one species on another is based on a contribution to overall production or consumption rate.

$$I_{AJ} = \frac{\sum_i |\upsilon_{A,i} r_i \delta_{Ji}|}{\max(P_A, C_A)}$$

Direct interaction coefficient (DIC)

A **Depth First Search (DFS)** is performed starting at user-selected target species (e.g., fuel, oxidizer, important radicals or pollutants) to find the dependency pathways for all species relative to the targets.

A path-dependent interaction coefficient (PIC) represents the error propagation down a certain pathway:

$$I_{AJ,p} = \prod_{i=1}^{n-1} I_{S_i S_{i+1}}$$

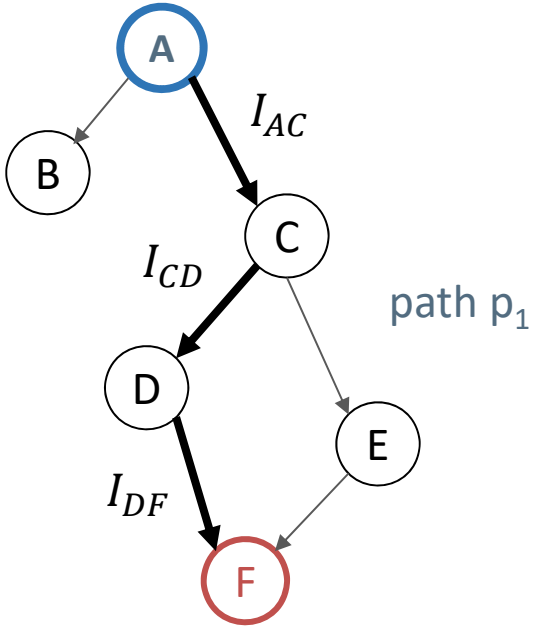

$$I_{AF,p_1} = I_{AC} + I_{CD} + I_{DF}$$

P. Pepiot, H. Pitsch, *An efficient error-propagation-based reduction method for large chemical kinetic mechanisms* (2008), Combustion and Flame 154(1-2), p. 67-81

DRGEP: Directed Relation Graph with Error Propagation (II)

Graph vertices represent species and **directed edges** between vertices represent the coupling of species. The dependence of one species on another is based on a contribution to overall production or consumption rate.

$$I_{AJ} = \frac{\sum_i |\upsilon_{A,i} r_i \delta_{Ji}|}{\max(P_A, C_A)}$$

Direct interaction coefficient (DIC)

A **Depth First Search (DFS)** is performed starting at user-selected target species (e.g., fuel, oxidizer, important radicals or pollutants) to find the dependency pathways for all species relative to the targets.

A path-dependent interaction coefficient (PIC) represents the error propagation down a certain pathway:

$$I_{AJ,p} = \prod_{i=1}^{n-1} I_{S_i S_{i+1}}$$

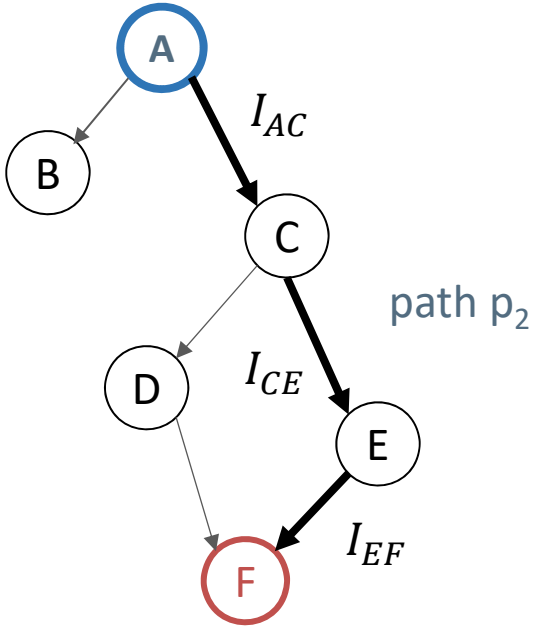

$$I_{AF,p_1} = I_{AC} + I_{CE} + I_{EF}$$

P. Pepiot, H. Pitsch, *An efficient error-propagation-based reduction method for large chemical kinetic mechanisms* (2008), Combustion and Flame 154(1-2), p. 67-81

DRGEP: Directed Relation Graph with Error Propagation (III)

An overall interaction coefficient (OIC) is then defined as the maximum of all PICs between the targets and each species of interest:

$$R_{AJ} = \max_{all\ paths\ p} \left(I_{AJ,p}\right) < \varepsilon_{EP}$$

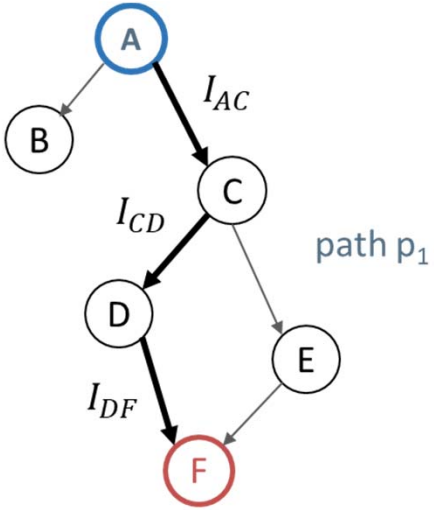

$$I_{AF,p_1} = I_{AC} + I_{CD} + I_{DF}$$

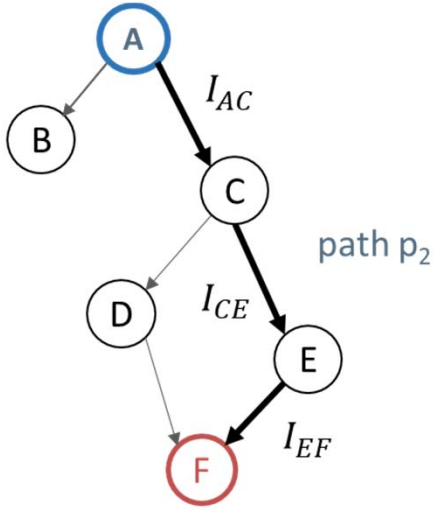

$$I_{AF,p_1} = I_{AC} + I_{CE} + I_{EF}$$

The removal of species with OICs below a threshold is considered negligible to the overall production/consumption rates of the target species and therefore such species are unimportant for the given conditions and can be removed from the reaction mechanism.

DRG vs DRG-EP

More advanced reduction techniques, such as DRGEP, are able to produce more compact reduced mechanisms

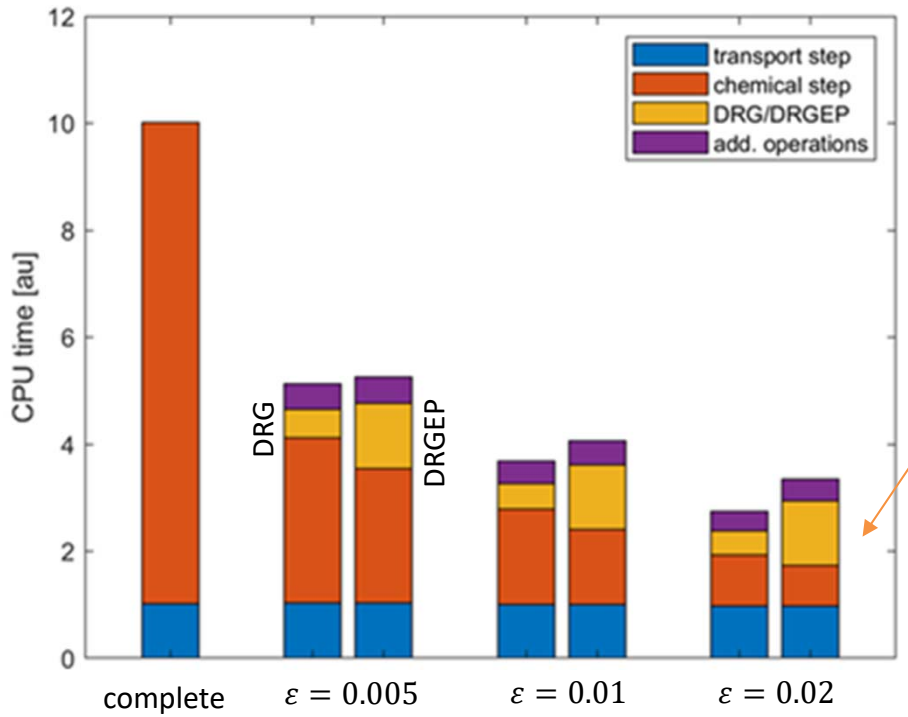

However their cost is larger, thus the overall impact on the simulation is not necessarily positive if compared to DRG

Chemistry Acceleration

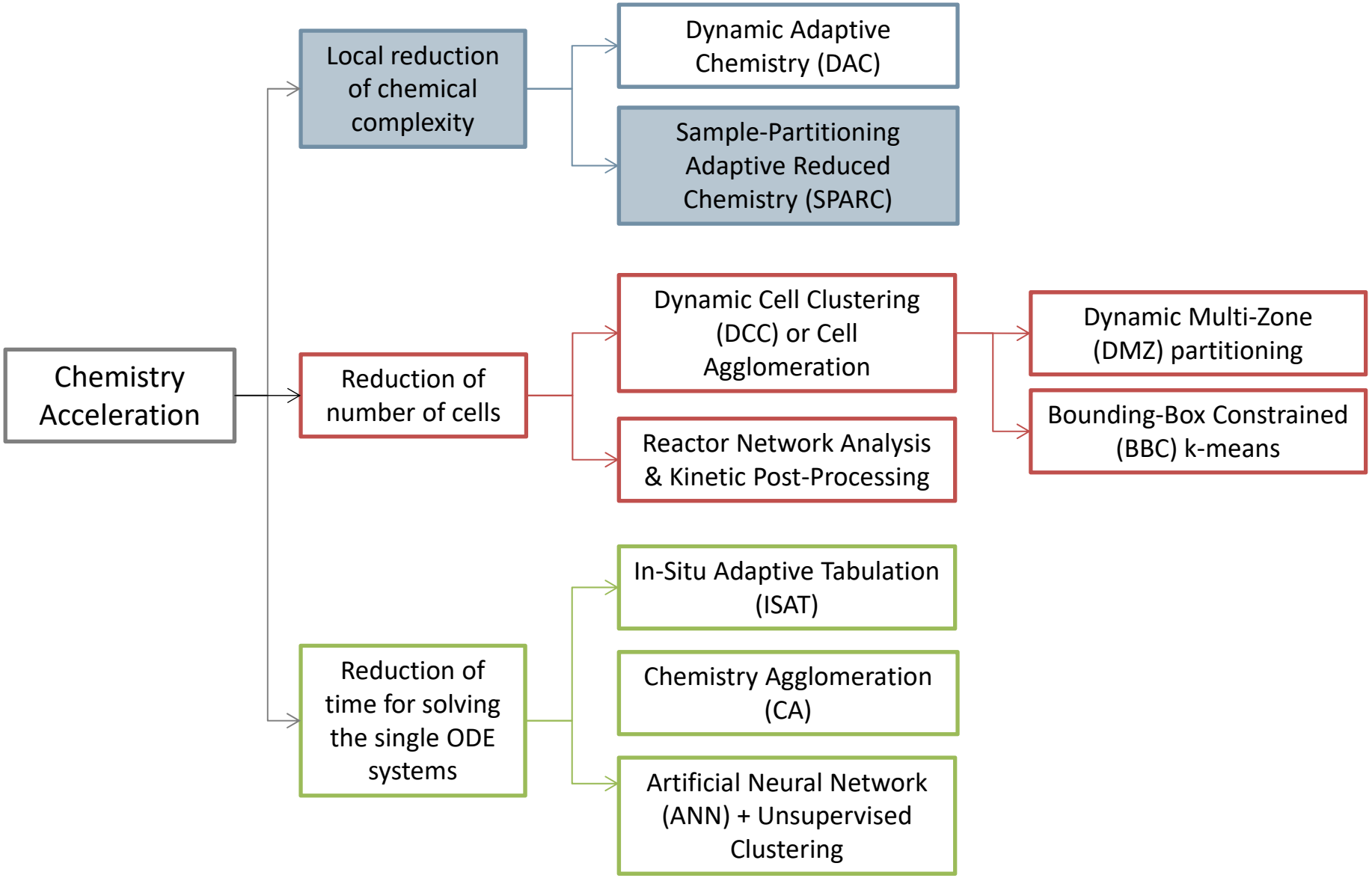

Pre-partitioned Adaptive Chemistry

Dynamic Adaptive Chemistry (DAC)

The **computational overhead** needed for the on-the-fly reduction of the mechanism can be **significant**, strongly reducing the efficiency of DAC

Pre-partitioned Adaptive Chemistry

- A **library of reduced mechanisms** is built in a pre-processing step, covering the composition space which is expected to be visited by the reactive systems of interest.
- During the CFD simulation, before carrying out the chemical step, each cell is **classified**, i.e. the reduced mechanism available in the library is identified instantaneously and applied

D.A. Schwer, P. Lu, and W.H. Green, Combustion and Flame, 133(4):451-465, 2003.
I. Banerjee and M.G. Ierapetritou, Combustion and Flame, 144(3):619-633, 2006.
Y. Liang, S.B. Pope, and P. Pepiot, Combustion and Flame, 162(9), 2015.
L.L.C. Franke, A.K. Chatzopoulos, and S. Rigopoulos, Combustion and Flame, 185:245-260, 2017

SPARC: Sample-Partitioning Adaptive Reduced Chemistry

Training phase

1. • Data generation
2. • Clustering based on Local Principal Component Analysis (LPCA)
3. • Generation of reduced kinetic mechanisms via DRG-EP

Simulation

4. • CFD simulation based on reduced mechanisms

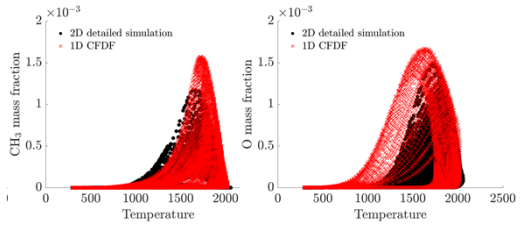

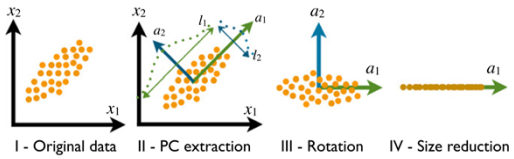

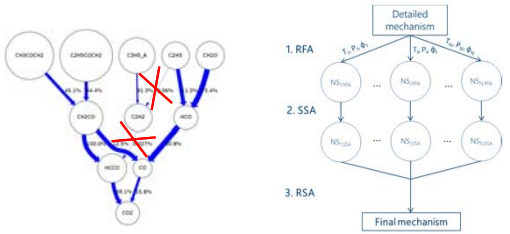

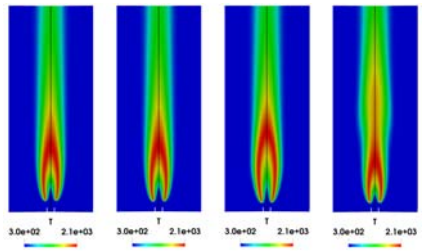

D'Alessio G., Parente A., Stagni A., Cuoci A., *Adaptive chemistry via pre-partitioning of composition space and mechanism reduction*, Combustion and Flame, 211, p. 68-82 (2020)

SPARC: Sample-Partitioning Adaptive Reduced Chemistry

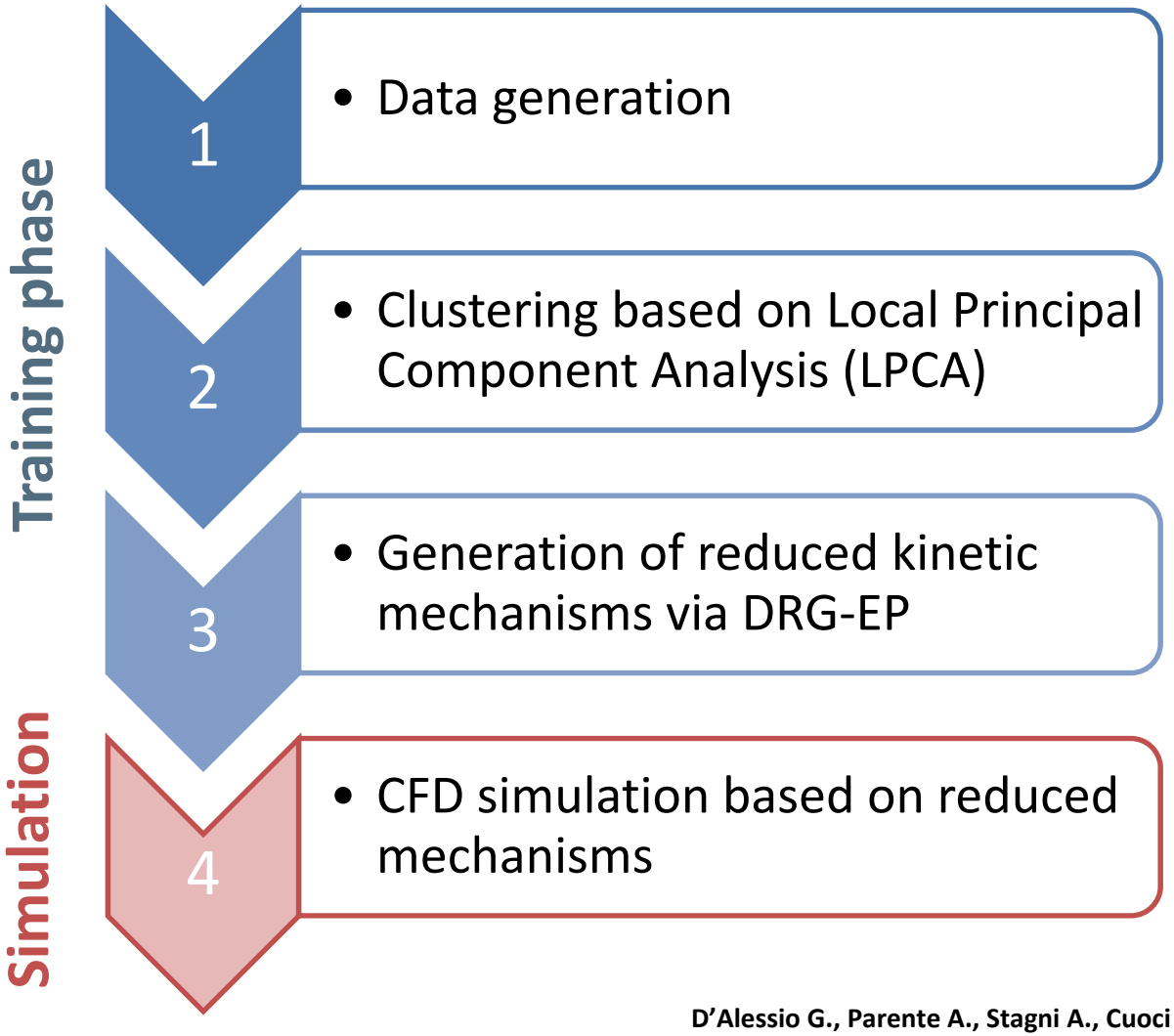

Choice of a proper **training dataset** is the most important step

Unsupervised classification
It is convenient to reduce the number of variables via PCA

Reduction is done off-line, so more advanced (expensive) techniques can be used)

Fast **on-the-fly classification** (i.e. identification of the cluster) is required

D'Alessio G., Parente A., Stagni A., Cuoci A., *Adaptive chemistry via pre-partitioning of composition space and mechanism reduction*, Combustion and Flame, 211, p. 68-82 (2020)

Principal Component Analysis (PCA)

$$\mathbf{X} = \begin{bmatrix} x_{11} & x_{12} & \dots & x_{1Q} \\ x_{21} & x_{22} & \dots & x_{2Q} \\ \vdots & \vdots & \ddots & \vdots \\ x_{n1} & x_{n2} & \dots & x_{nQ} \end{bmatrix} = \begin{bmatrix} T^1 & Y_1^1 & \dots & Y_p^1 \\ T^2 & Y_1^2 & \dots & Y_p^2 \\ \vdots & \vdots & \ddots & \vdots \\ T^n & Y_1^n & \dots & Y_p^n \end{bmatrix}$$

Instantaneous snapshot

State variable

Rows represent observations and columns correspond to the problem variables (T, and species mass fraction).

Covariance matrix

$$\mathbf{S} = \mathbf{X}^\mathbf{T}\mathbf{X} \longrightarrow \mathbf{S} = \mathbf{A}\mathbf{L}\mathbf{A}^\mathbf{T}$$

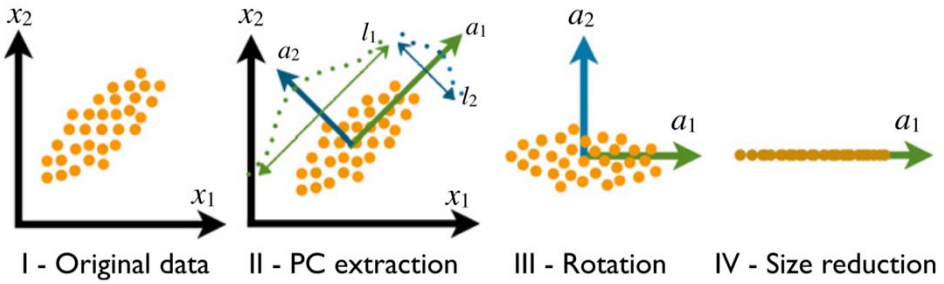

PC (Principal Components): eigenvectors of S, i.e. the columns of A

Eigenvalues: i.e. the diagonal of the L matrix, the portion of variance they account for.

Adapted from: **A. Parente**, *Data-driven simulation of combustion problems*, Invited Lecture, NC19 Aachen (Germany)

Unsupervised Clustering via LPCA and k-means

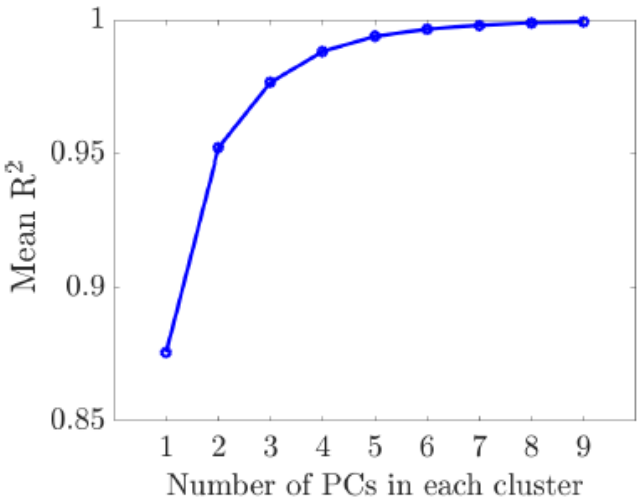

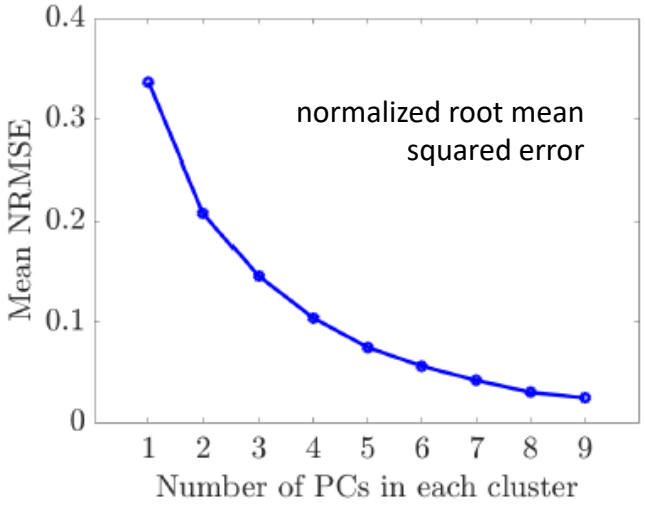

1. Initialization

The initial clusters centroids are chosen from a **k-means solution**. The eigenvector matrix in each cluster is initialized as the identity matrix.

2. Partition

Each observation is assigned to a cluster by means of the calculation of a reconstruction error.

3. Update

The cluster centroids are updated on the basis of the partitioning carried out at step 2.

4. Local-PCA

LPCA is performed in each cluster found at step 2.

On-the-fly classification via ANN (I)

The on-the-fly classification step has an important role in the overall approach, since the non-optimal choice of the mechanism can compromise the accuracy of the simulation.

If the chemical mechanism consists of a large number of species, the classification can be a difficult task to accomplish since the **use of distances in high-dimensional spaces can sometimes lead to poor results** (Aggarwal, 2001).

ANN represent a valid alternative to improve the classification efficiency, as they do not rely on the use of the metrics in high-dimensional spaces.

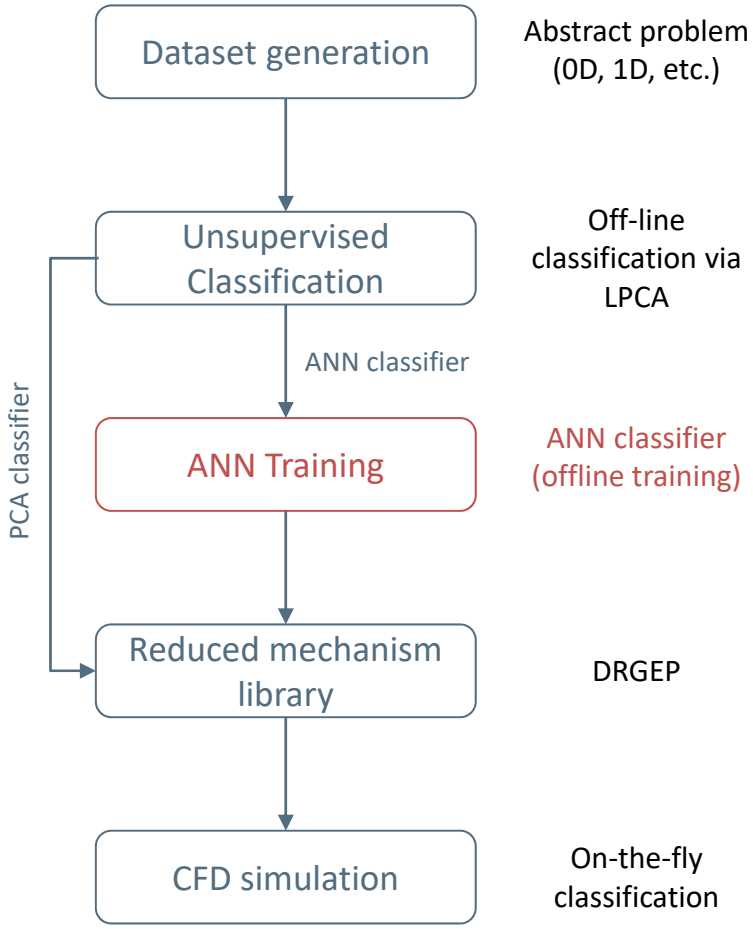

D'Alessio G., Cuoci A., Parente A., Submitted to Proceedings of the Combustion Institute (2020)

On-the-fly classification via ANN (II)

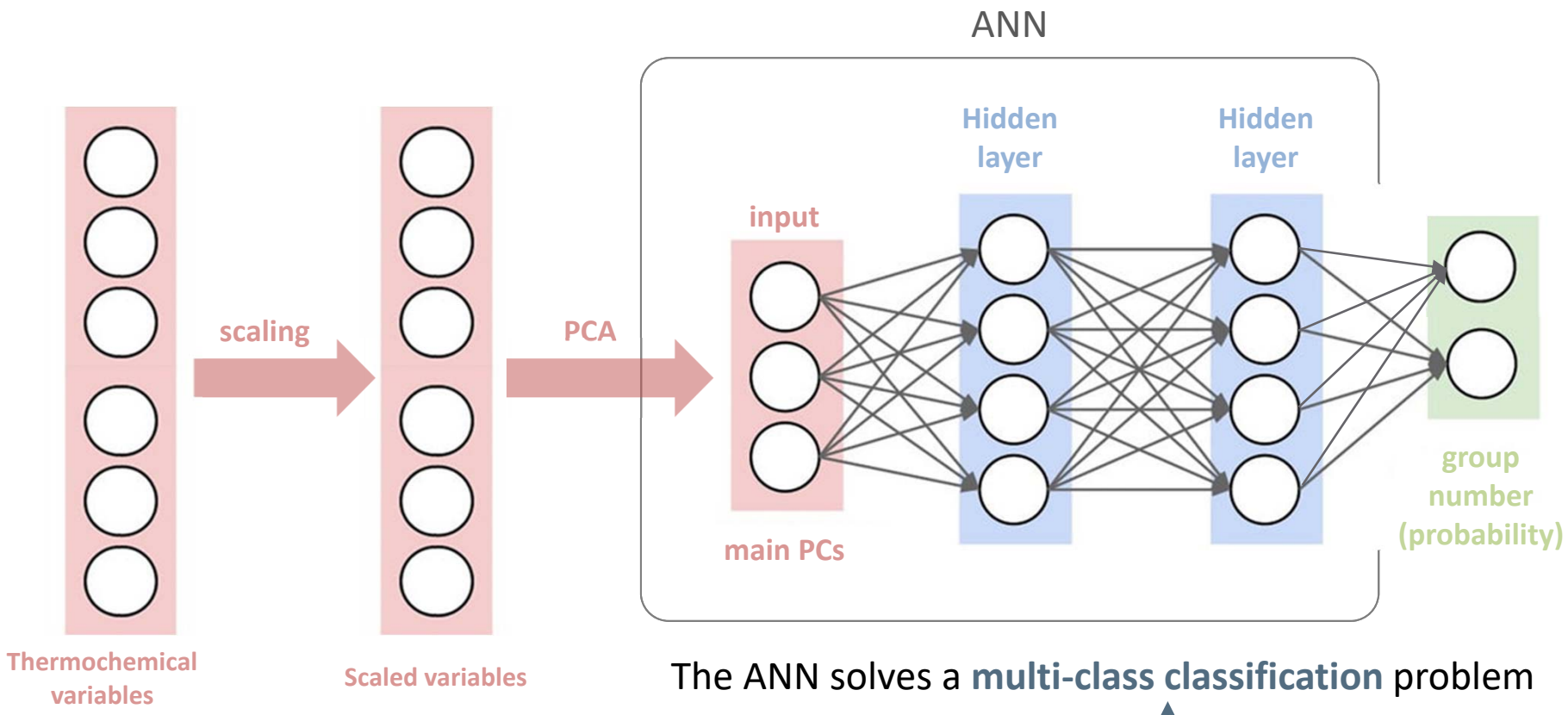

The ANN solves a **multi-class classification** problem

Important to assess on-the-fly the quality of the classification

A test case: $nC_7H_{16}/CH_4/N_2$ laminar flame

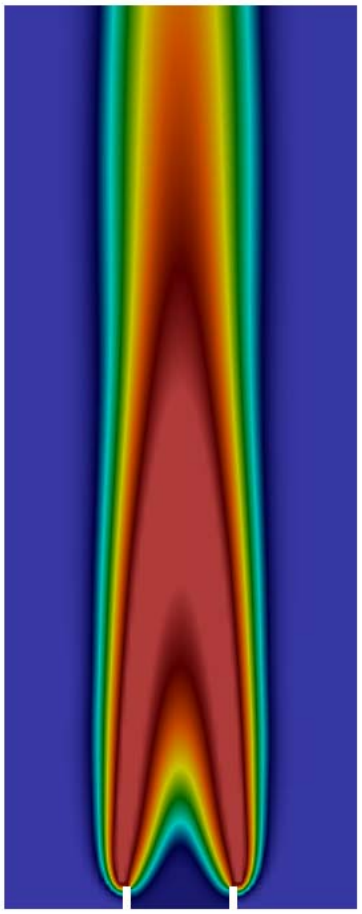

Fuel stream
Composition: 2.47% nC_7H_{16}, 48.7% CH_4, 48.7% N_2
Velocity: 10.12 cm/s (parabolic)

Oxidizer stream
Composition: 21% O_2, 79% N_2
Velocity: 12.32 cm/s (flat)

Geometry
Fuel nozzle diameter: 11 mm
Thickness: 0.90 mm
Coflow diameter: 50 mm

Numerical simulation

Axisymmetric 2D Mesh
Domain: 40 x 100 mm
Cells: ~10,000

Kinetic mechanism
POLIMI_PRF_PAH_HT_1412
176 species and 6067 reactions

CFD code
`laminarSMOKE` (based on the operator splitting approach)

D'Alessio G., Cuoci A., Parente A., Submitted to Proceedings of the Combustion Institute (2020)

Training dataset

The training data set must cover adequately the composition space that is expected to be visited during the simulation of the system under investigation

The samples were generated by means of **1D counterflow diffusion flames (CFDF)**, adopting a wide range of strain rates randomly chosen from 15 to 1000 1/s

By changing the strain rate, a wide range of composition states can be obtained, from **thermodynamic equilibrium to extinction**.

The resulting data set consists of about 220,000 observations, corresponding to 440 different CFDF flames.

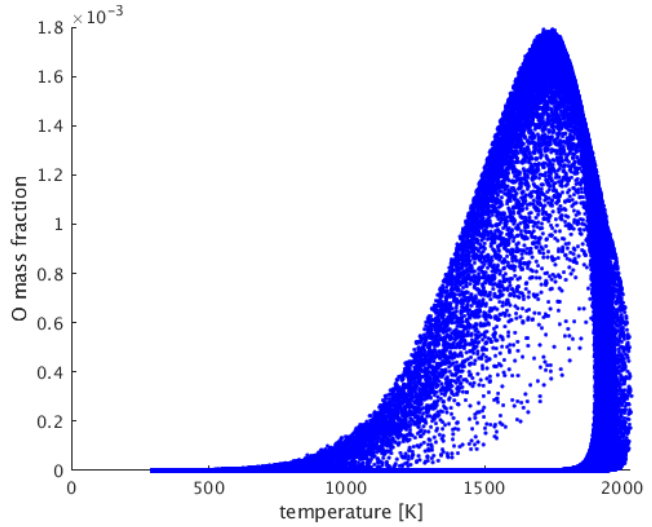

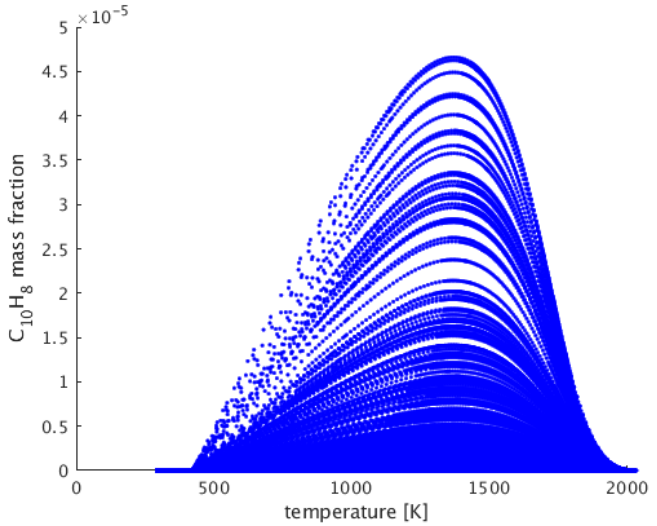

Results: accuracy

The ANN used for the classification consisted of **2 hidden layers with 200 and 400 neurons**, respectively, chosen after an optimization of the hyper-parameters to achieve a satisfactory accuracy in the class prediction.

The activation functions chosen for the hidden layers were both **ReLU (Rectified Linear Unit)**, with a **softmax activation** for the output layer as required in case of multi-class classification tasks.

Early stopping was adopted in the offline training to prevent the network overfitting.

Averaged normalized root mean square error over time

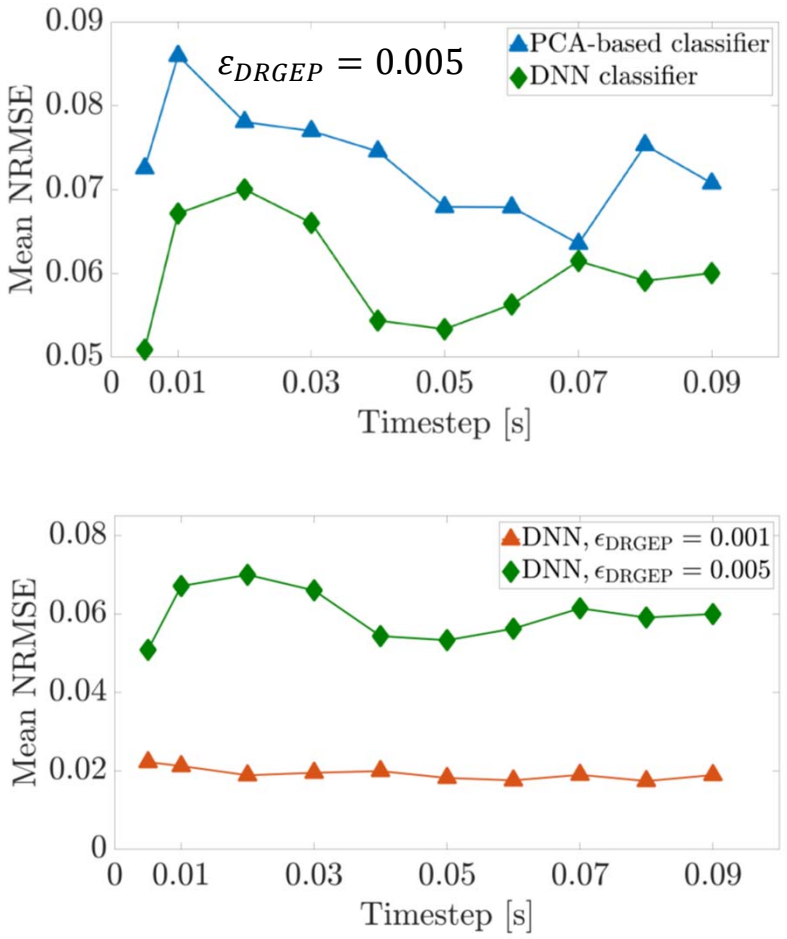

Results: CPU time and speed-up

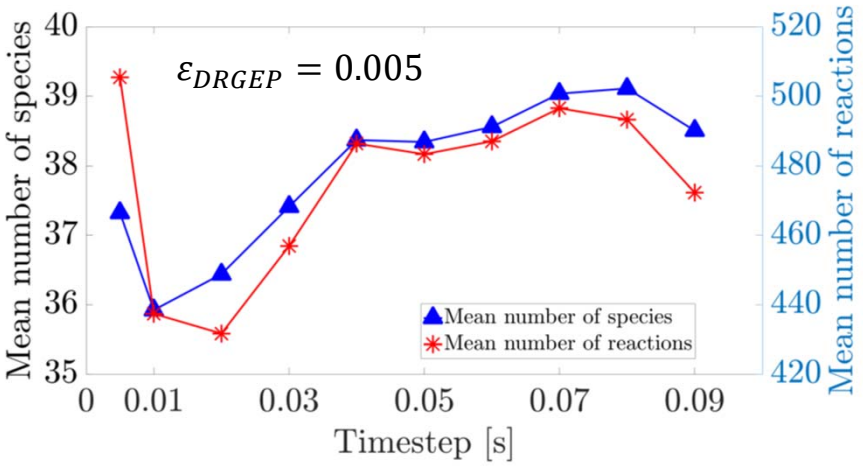

The reduction in terms of number of species is remarkable (only 25% of species are retained)

A stronger reduction in the number of active reactions is evident: less than 10% of the original reactions are retained.

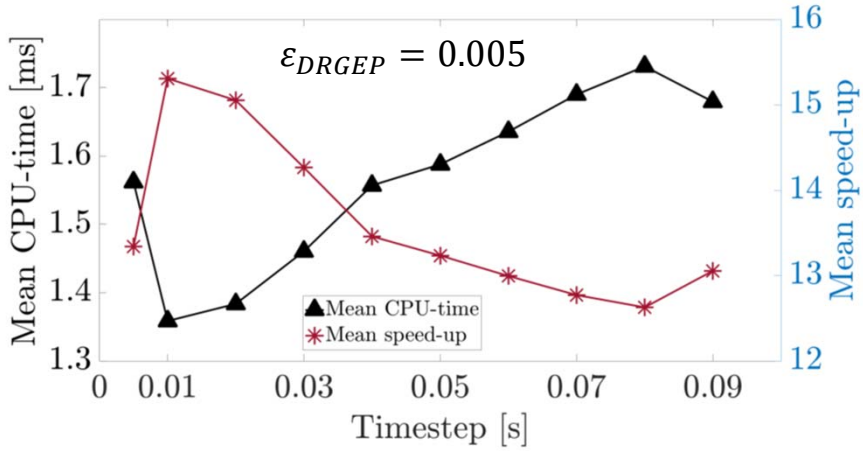

The computational speed-up of the ANN adaptive simulation is in a range between 13 and 15 for the chosen reduction tolerance. The value can vary in time because the number of species and reactions can also change in time depending on the local flame chemistry

Results: comparison with full-chemistry

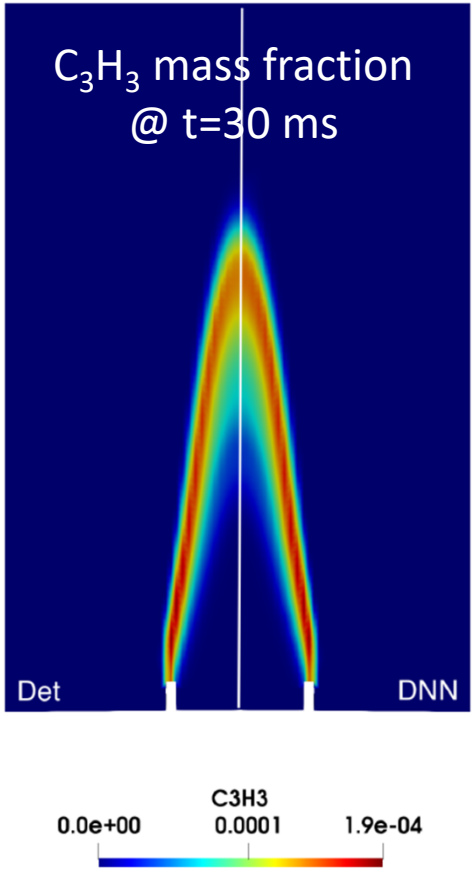

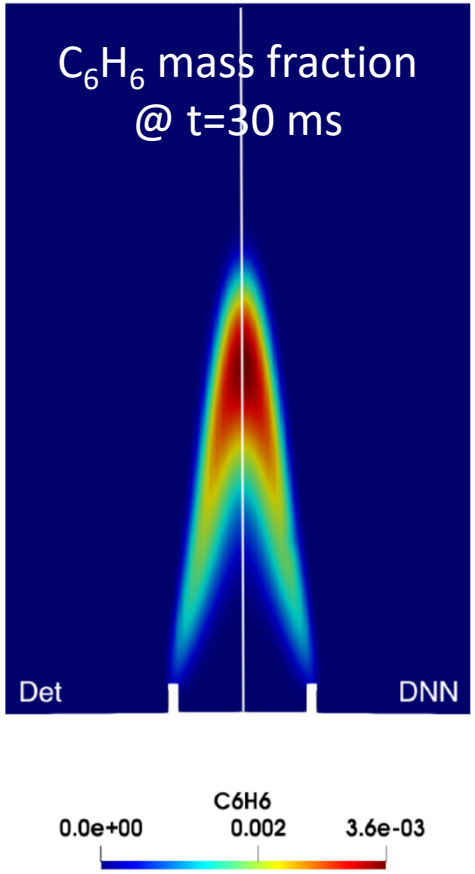

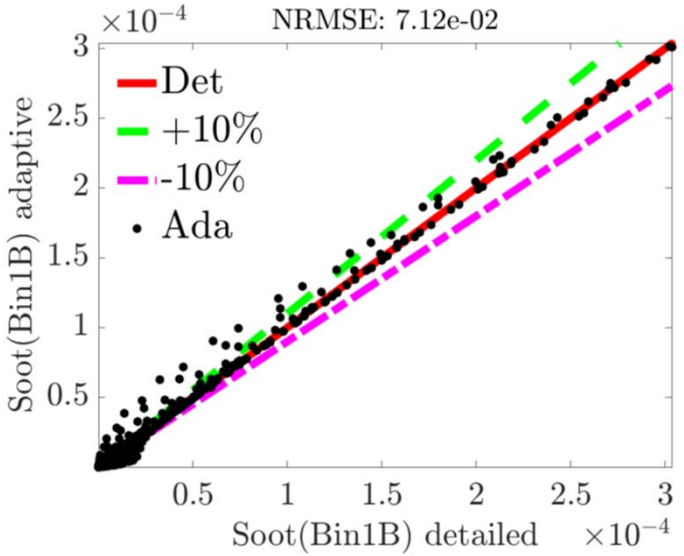

BIN1B (C_{20}) is the heaviest species in the mechanism and it is a soot precursor

A satisfactory level of agreement is observed not only for main species, but also for radicals (such as propargyl) and heavy species (such as benzene and soot precursors).

Comparison with conventional DRG/DRGEP

The main advantage of SPARC with respect the conventional DAC approach is in the reduction of CPU times for additional operations and on-the-fly classification

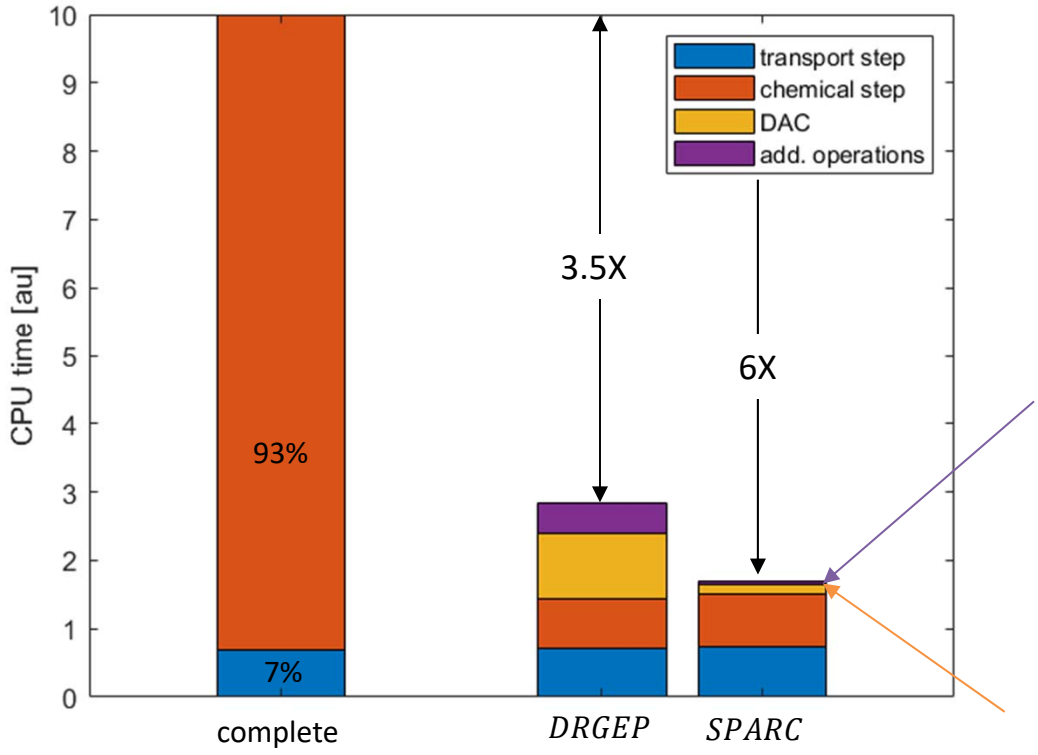

The cost of additional operation is now negligible, since the possible reduced mechanisms are pre-defined

This includes the time for performing the PCA in each cells and classify the points via ANN

Chemistry Acceleration

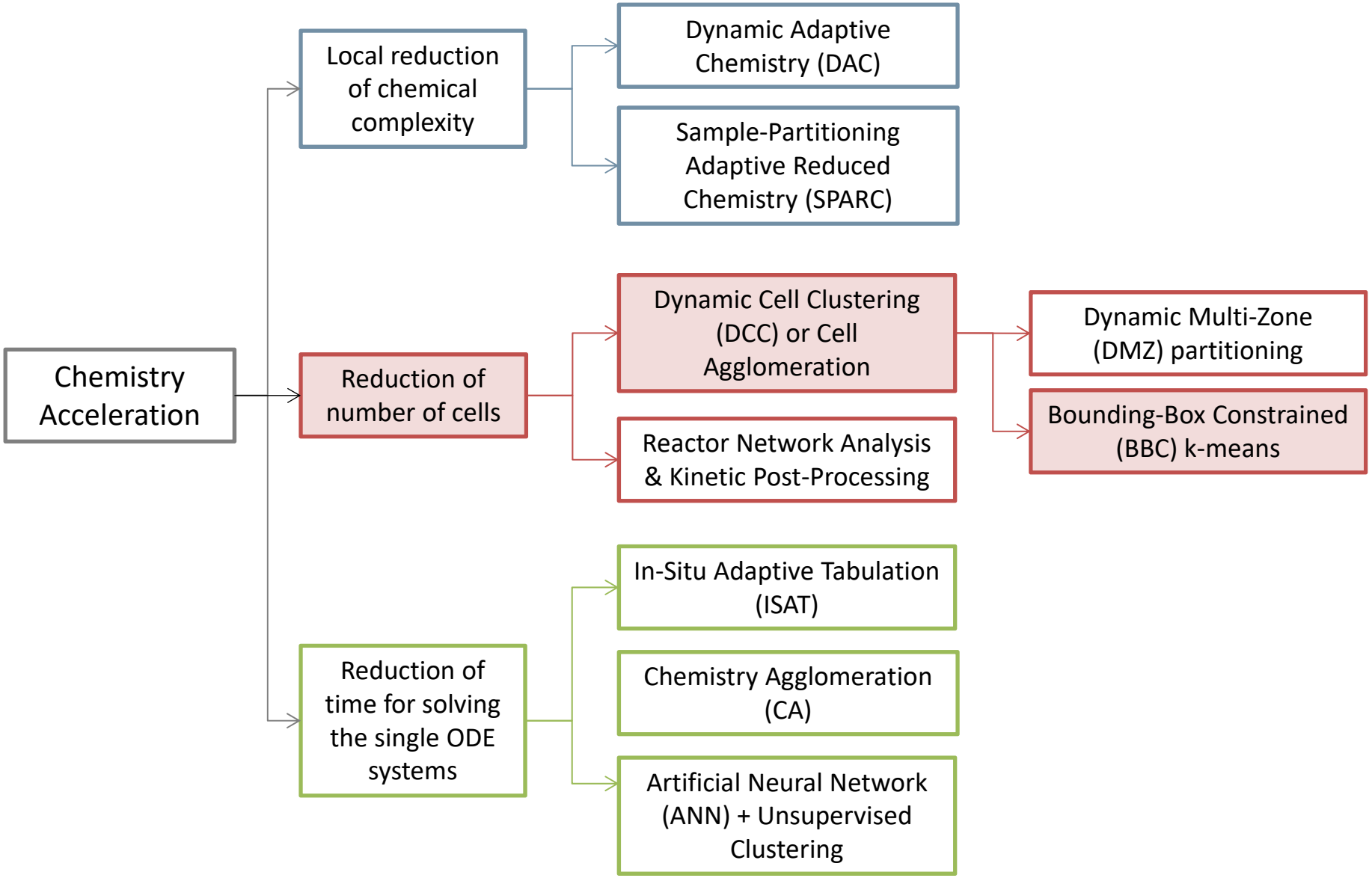

Dynamic Cell Clustering (DCC) (I)

Dynamic Cell Clustering (DCC) dynamically groups/clusters regions of the domain that have similar thermochemical conditions. This reduces the number of detailed chemistry calculations executed at every time step, as calculations are now executed for a group of cells (i.e. the cluster), and not for each and every cell.

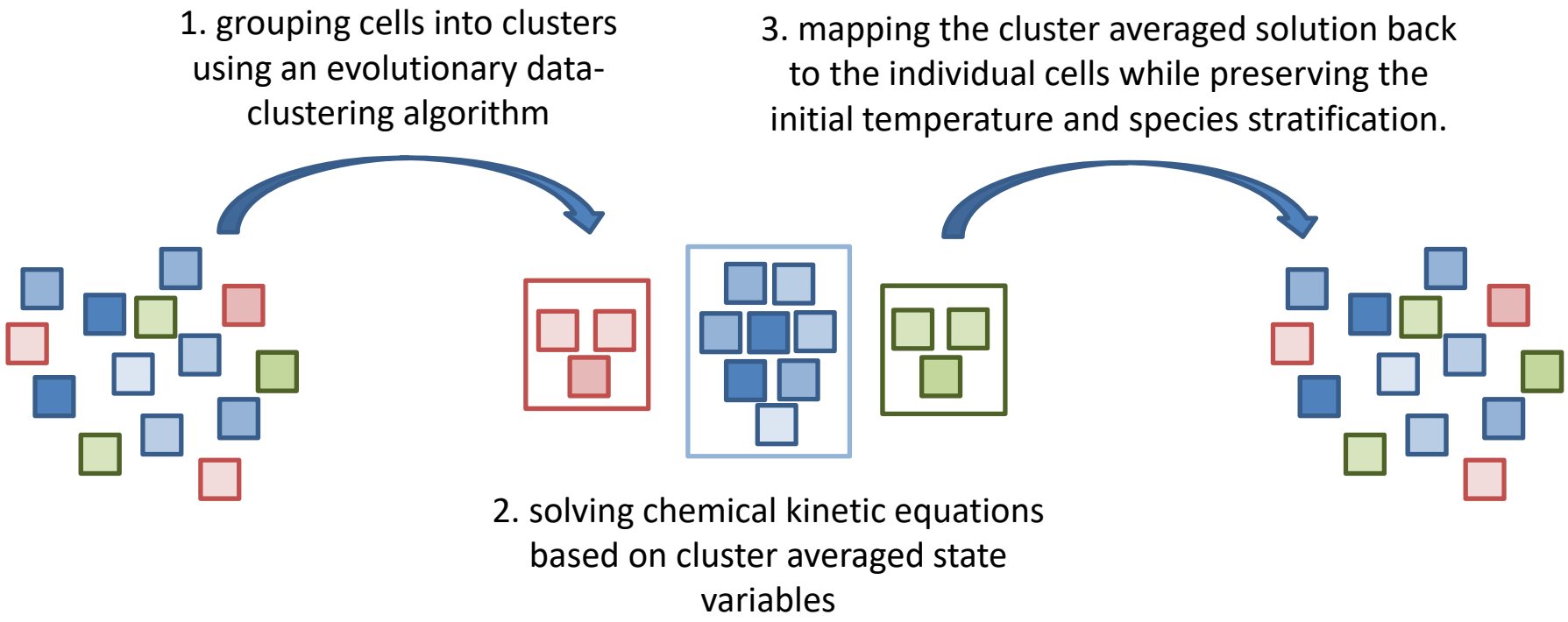

Clustering of cells

Unsupervised clustering algorithms

A number of clusters is defined by the user and a proper algorithm, for example the **k-means**, based on a proper definition of distance, is adopted to classify the points among the clusters

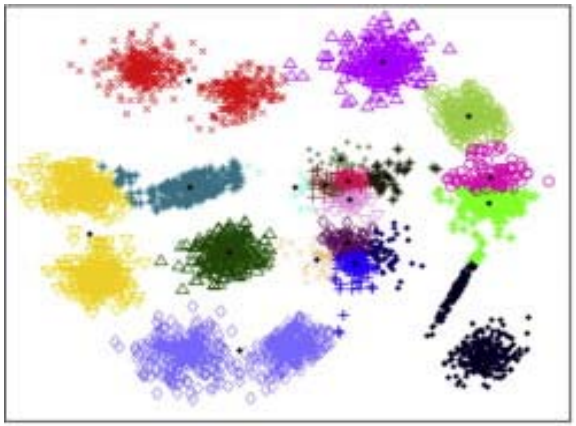

k-means, k = 20

Need to define a priori the number of clusters
Higher computational cost

Binning algorithms

Uniform Cartesian meshes in the T-P-composition space are constructed

Each cell in the T-P-space including at least one point becomes a cluster

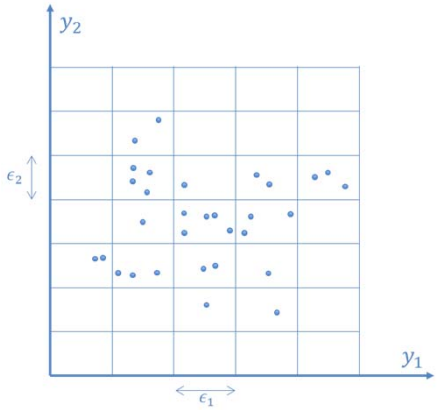

No need to define a priori the number of clusters
Typically a high number of clusters is obtained, especially in high-D spaces

Bounding Box Constrained (BBC) k-means (I)

The **BBC k-means algorithm** aims at a smarter initialization of cluster centers and at a reduced computational cost of operations involved during each iteration of clustering.

The BBC approach does not require to fix in advance the number of clusters, but it is able to **automatically find an optimal number of cluster**.

The starting point is represented by a proper selection of **D features** and the **normalization** of data in the [0,1] box.

Perini F., *High-dimensional, unsupervised cell clustering for computationally efficient engine simulations with detailed combustion chemistry,* Fuel 106, p. 344–356 (2013)

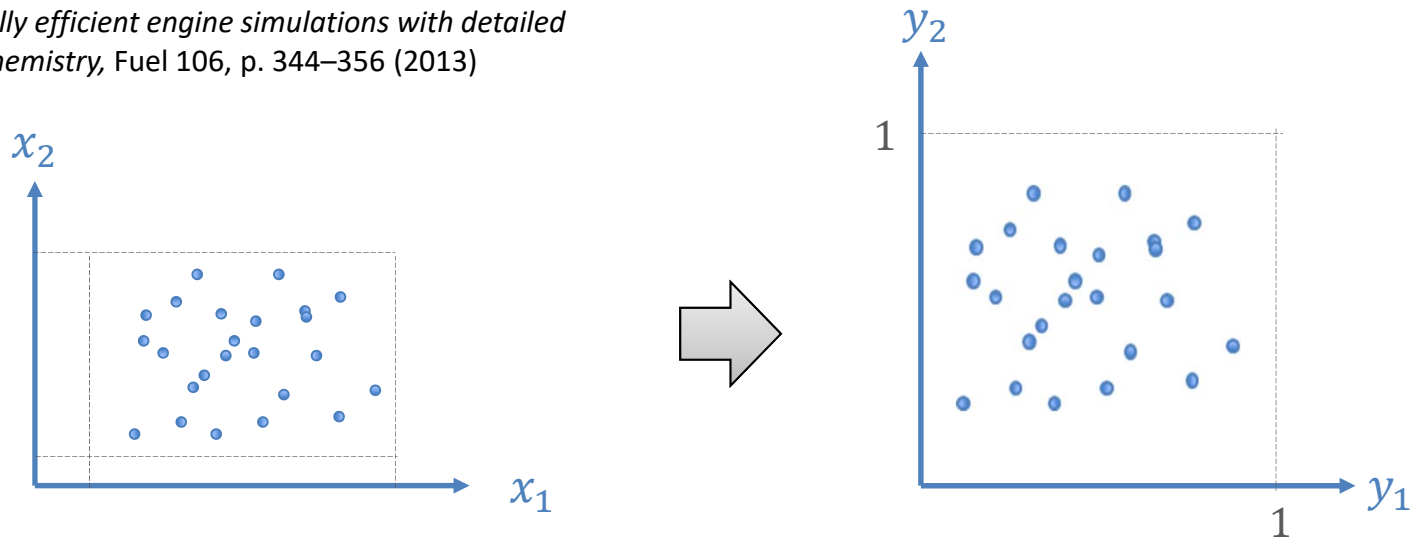

Bounding Box Constrained (BBC) k-means (II)

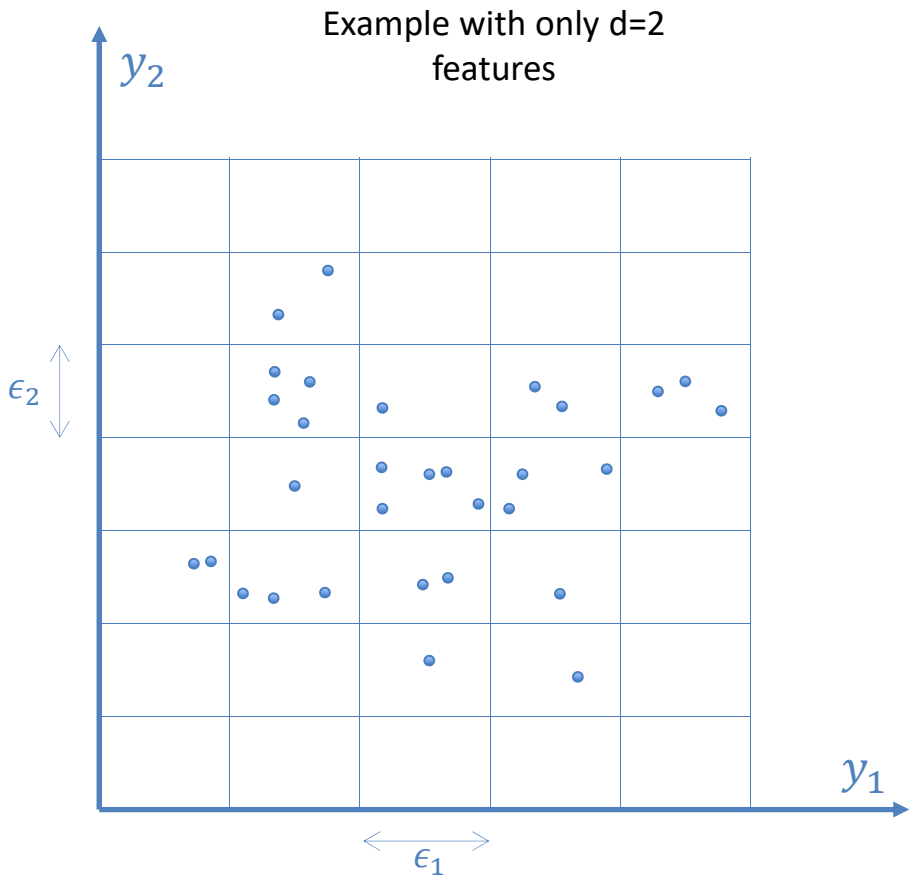

Instead of defining the number of clusters, we define for each feature *d* a grid with uniform step ϵ_d

Each vertex in the grid represents a potential cluster center initialization

Bounding Box Constrained (BBC) k-means (II)

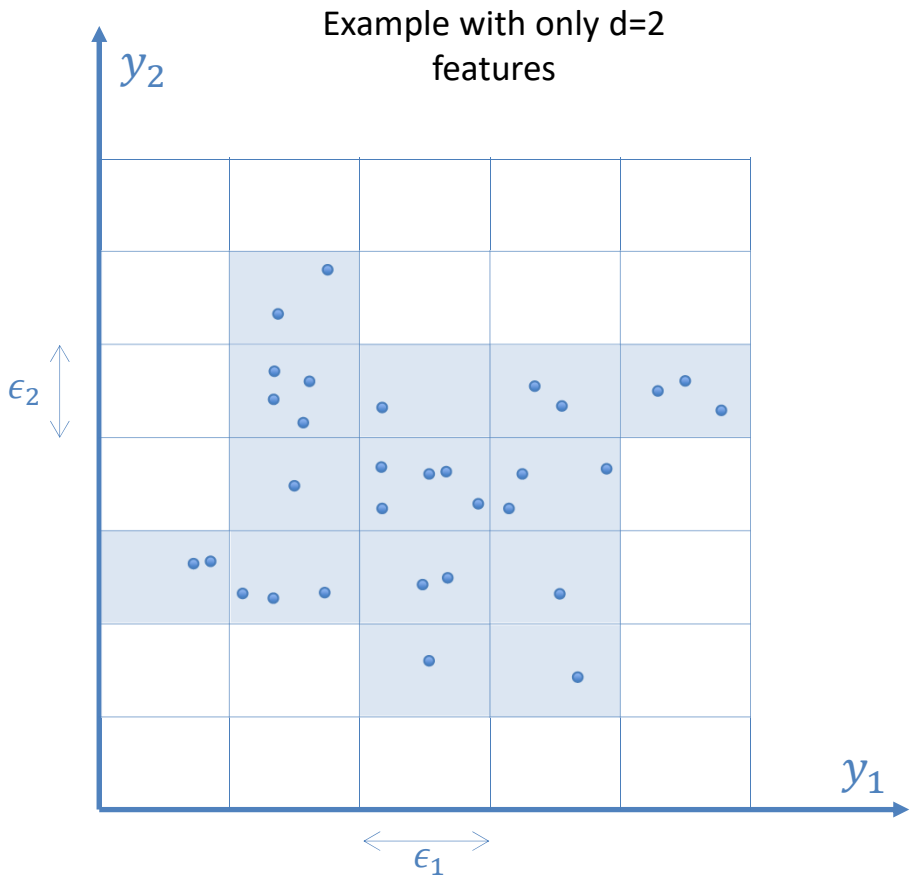

Instead of defining the number of clusters, we define for each feature *d* a grid with uniform step ϵ_d

Each vertex in the grid represents a potential cluster center initialization

We can now recognize a number of active cells, i.e. cells in which we have at least 1 pattern (or feature vector)

Bounding Box Constrained (BBC) k-means (II)

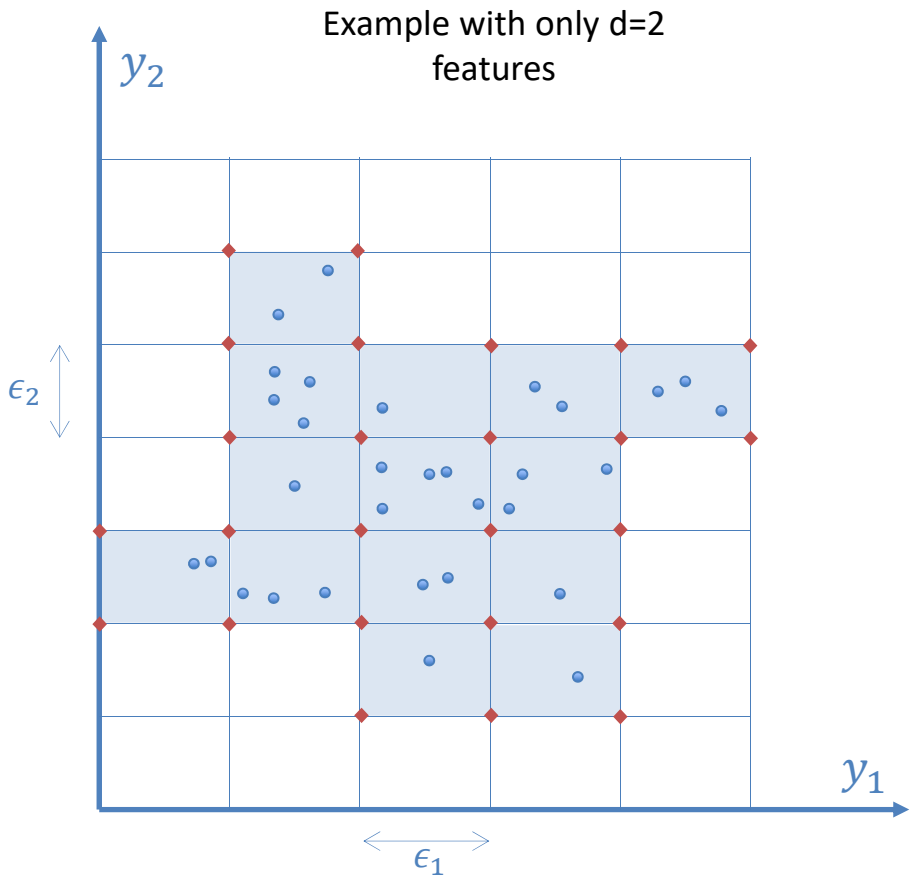

Instead of defining the number of clusters, we define for each feature *d* a grid with uniform step ϵ_d

Each vertex in the grid represents a potential cluster center initialization

We can now recognize a number of active cells, i.e. cells in which we have at least 1 pattern (or feature vector)

As a matter of fact, **only the vertices of the active cells**, which contain at least one point image, can become cluster centers

This idea is the seed for the bounding-box clustering (BBC)

Bounding Box Constrained (BBC) k-means (II)

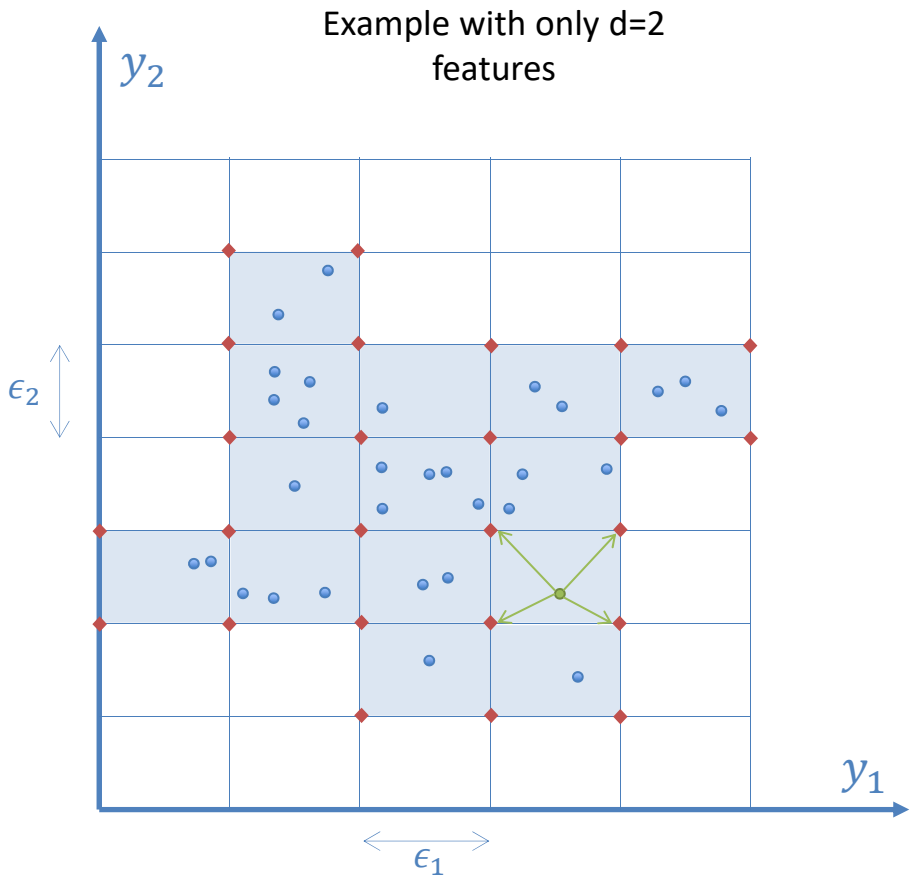

The BBC algorithm exploits the idea that, if the cluster centers have been uniformly initialized across the zones of the space unity hyper-box that are covered with point images, each of them will lay in the surroundings of its initialization value even after the end of the iterative clustering process.

Each pattern can be assigned to its surrounding cluster centers only, i.e. those which define the pattern's grid-like bounding box vertexes at the initialization.

Example: catalytic heterogeneous reactor

Partial Oxidation (POX) of methane

The CH_4 micro-kinetic model has 21 gas species and 13 adsorbed species involved in 82 surface reactions

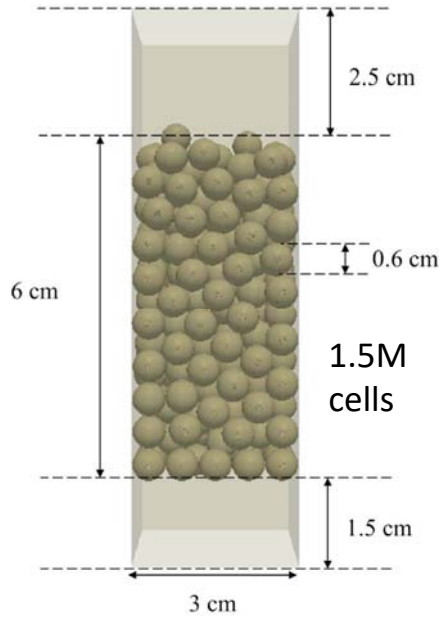

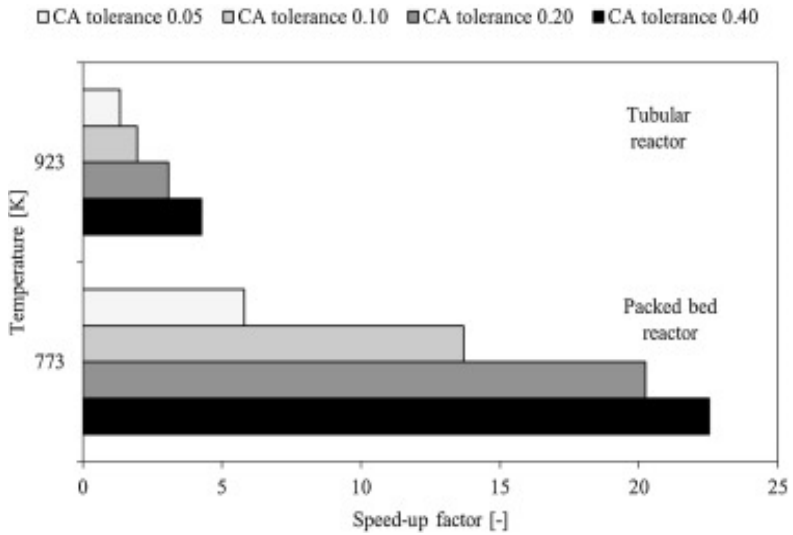

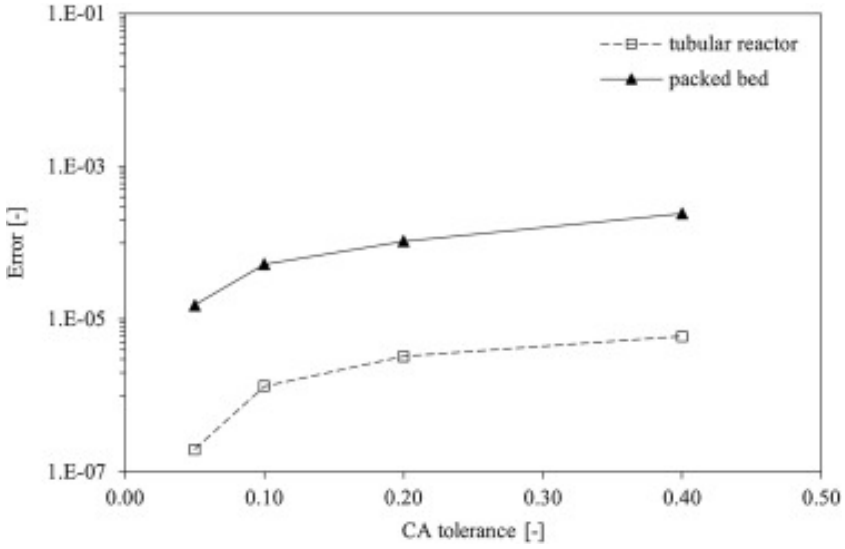

Rebughini S., Cuoci A., Dixon A.G., Maestri M. *Cell agglomeration algorithm for coupling microkinetic modeling and steady-state CFD simulations of catalytic reactors*, Computers and Chemical Engineering 97, p. 175-182 (2017)

Example: pulsating laminar coflow flame

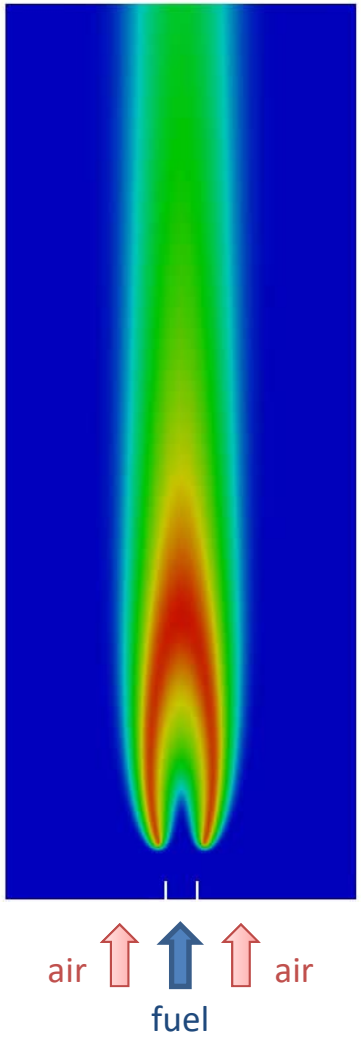

POLIMI kinetic mechanism
Species: 115
Reactions: 2141

Fuel mixture:
34% C_2H_4, 66% N_2
Coflow stream:
21% O_2, 79% N_2

The **transient behavior** is induced by a 2**0 Hz perturbation** in the fuel velocity profile

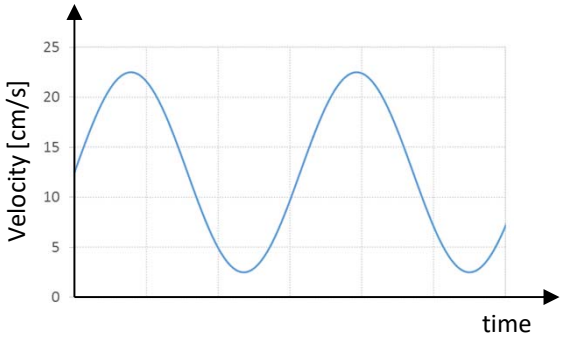

Total number of cells: 25,000
Number of active cells: 13,000

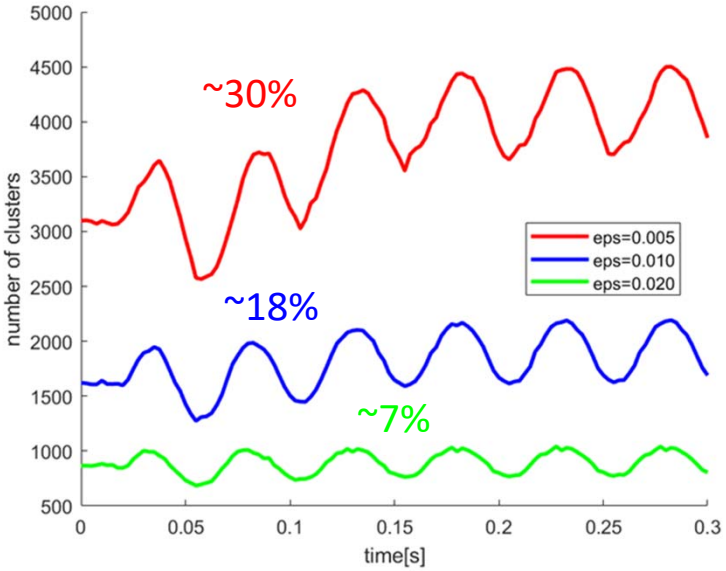

Set of features:
T, CH4, O2, OH, CO

Tolerance: $\varepsilon = 0.005 - 0.02$

Computational performances: speed-up

The cost of the chemical step decreases linearly with the number of aggregated cells

The cost of the agglomeration step (identification of similar cells and redistribution of results) increases with the number of considered **features**

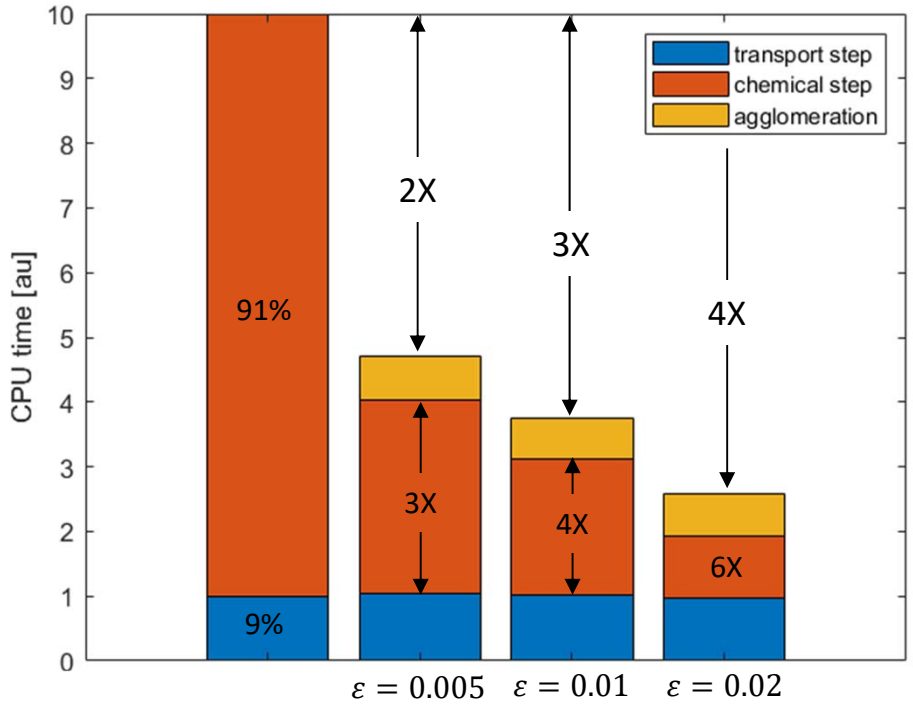

Set of features:
T, CH4, O2, OH, CO

Computational performances: accuracy

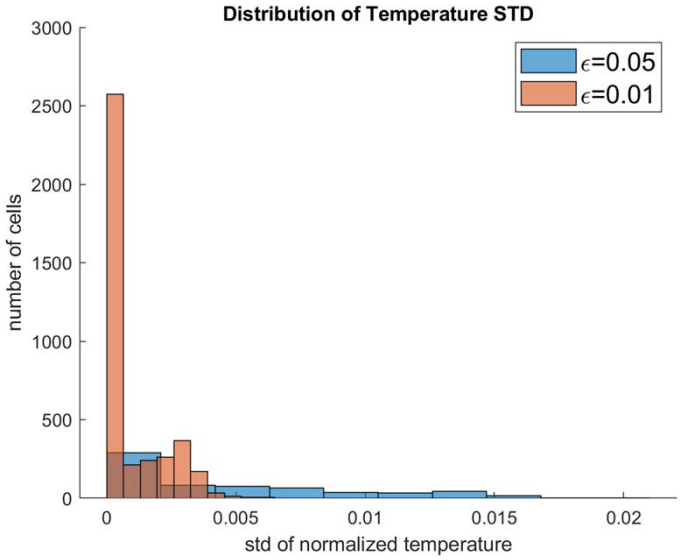

It is important to measure the internal **chemical homogeneity** in each agglomerated cell

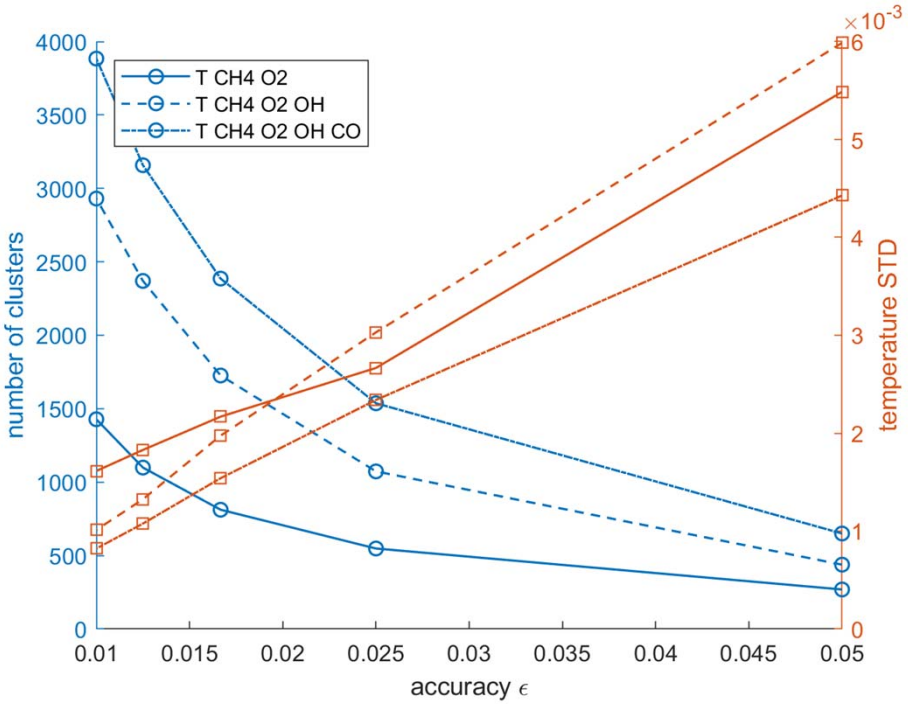

Ill clusters

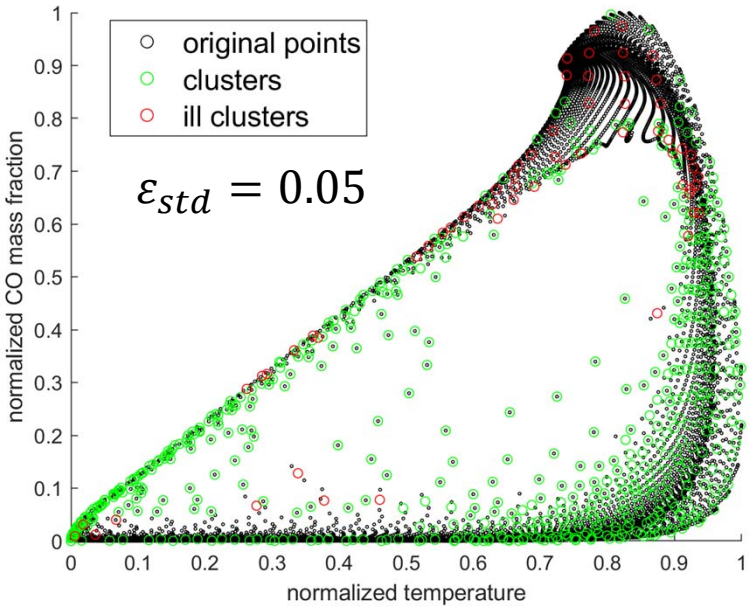

Only agglomerated cells which are sufficiently homogeneous are considered (green points)

$$std(y_i) \leq \varepsilon_{std}$$

y_i is the normalized temperature and a number of selected species

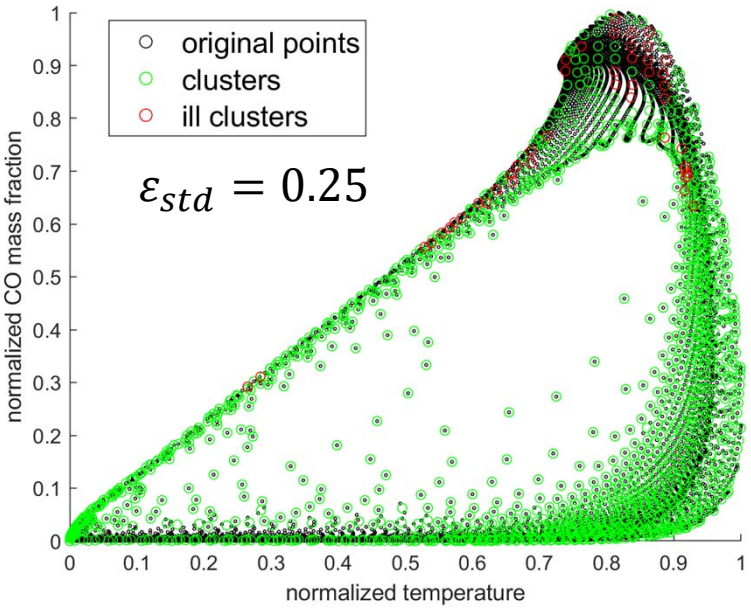

If the homogeneity condition is not satisfied (red points), 2 options are considered:

1. The agglomerated cell is rejected (i.e. no agglomeration is performed)
2. An additional level of refinement (binning) is adopted

How to properly choose the D features?

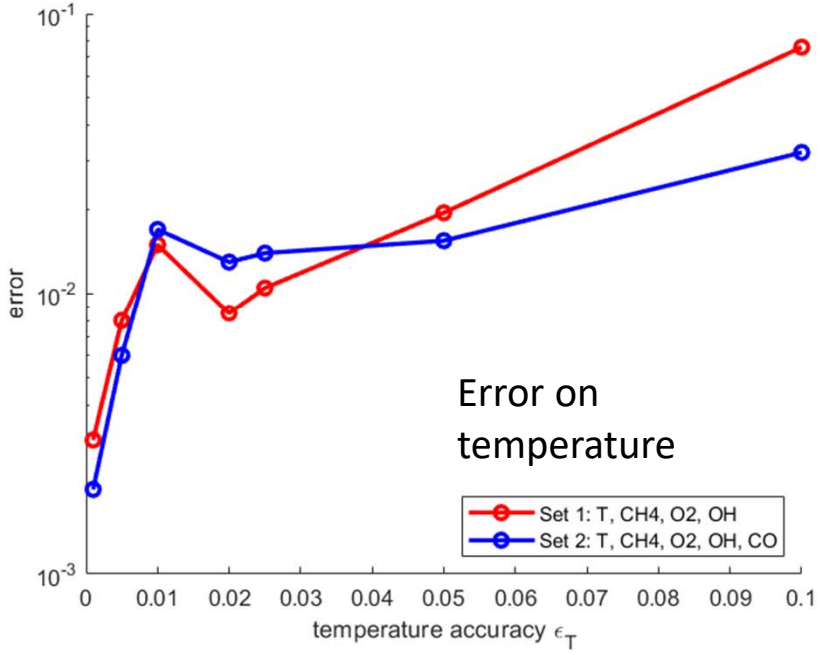

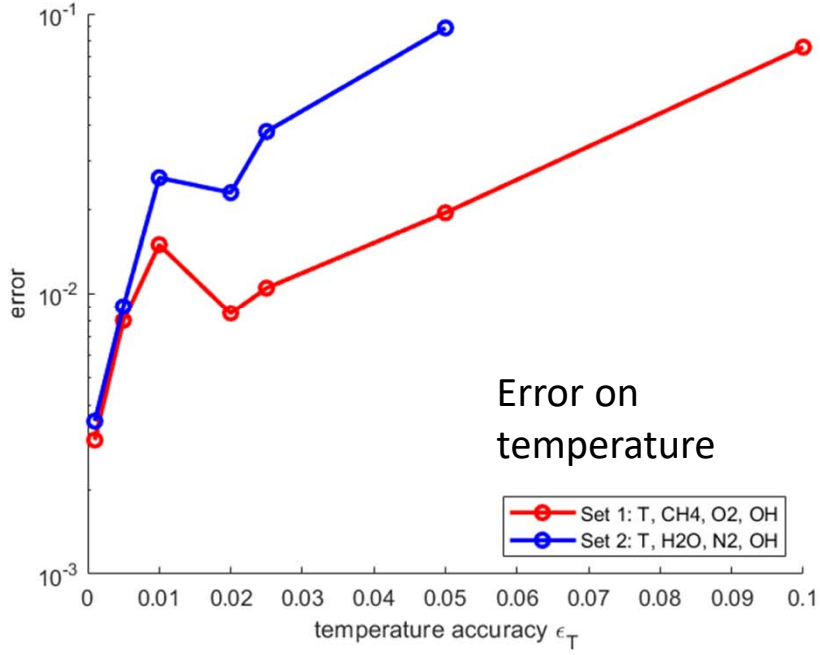

- How to select the proper set of species for the binning algorithm?
- How many species?

Principal Components (PCs) as binning features (I)

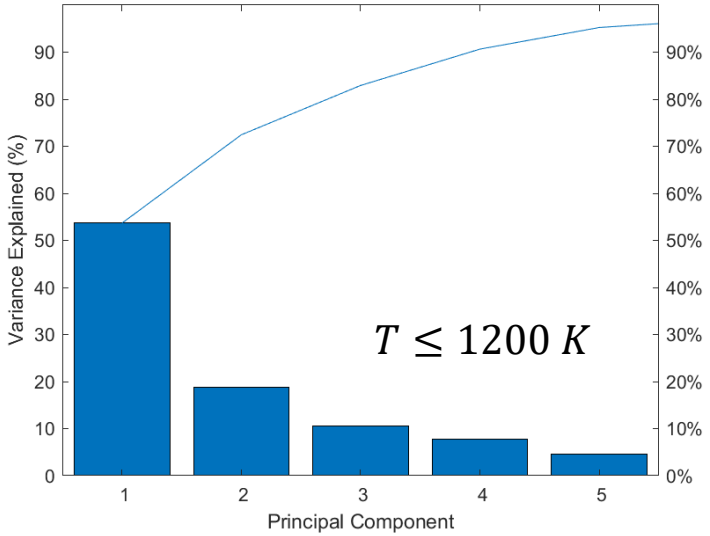

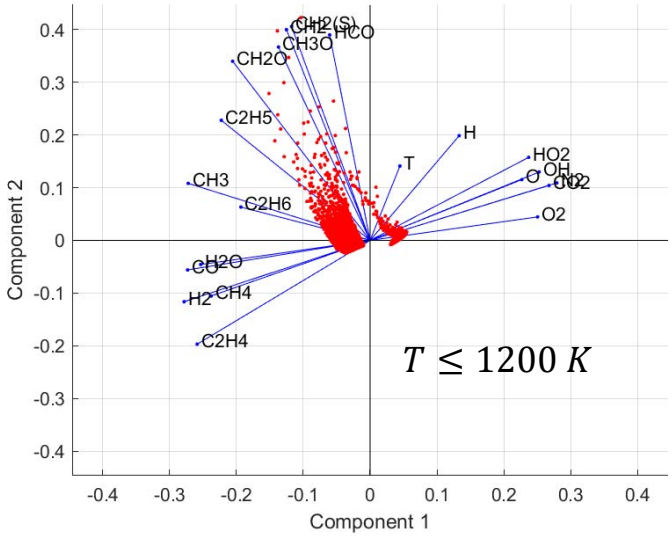

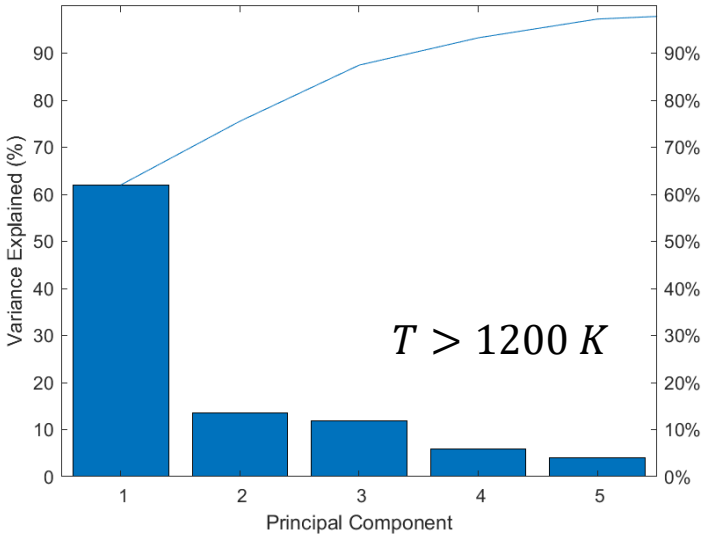

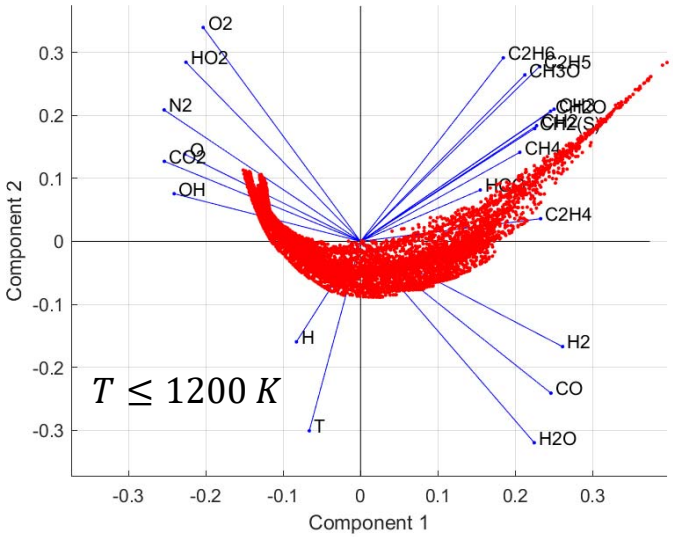

Principal Components (PCs) as binning features (II)

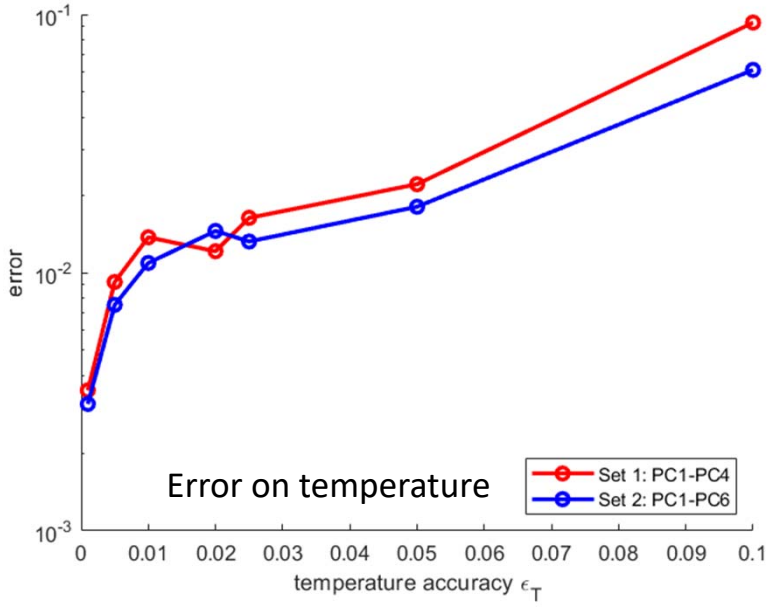

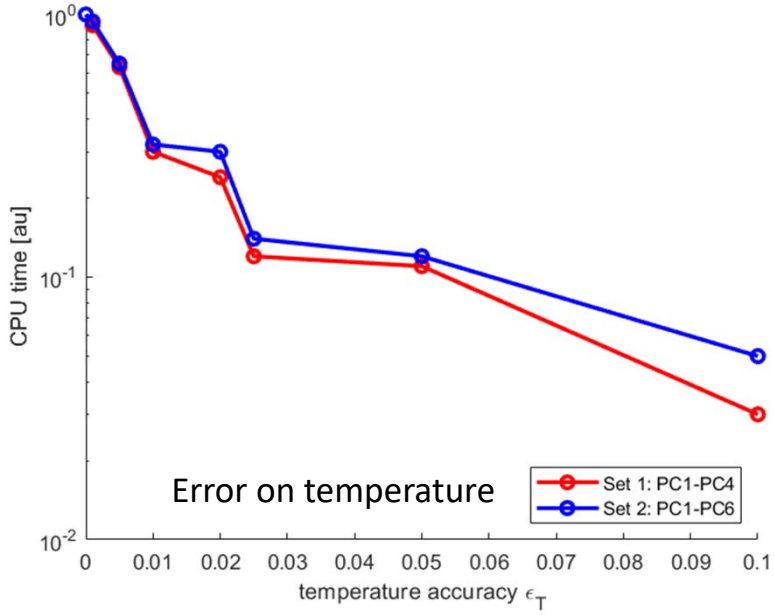

The first N Principal Components are automatically chosen, so the only degree of freedom is N

The sensitivity to the number N of PCs is relatively small (if a sufficiently large number N of PCs is chosen)

An additional CPU cost has to be considered to perform the PCA on-the-fly

Chemistry Acceleration

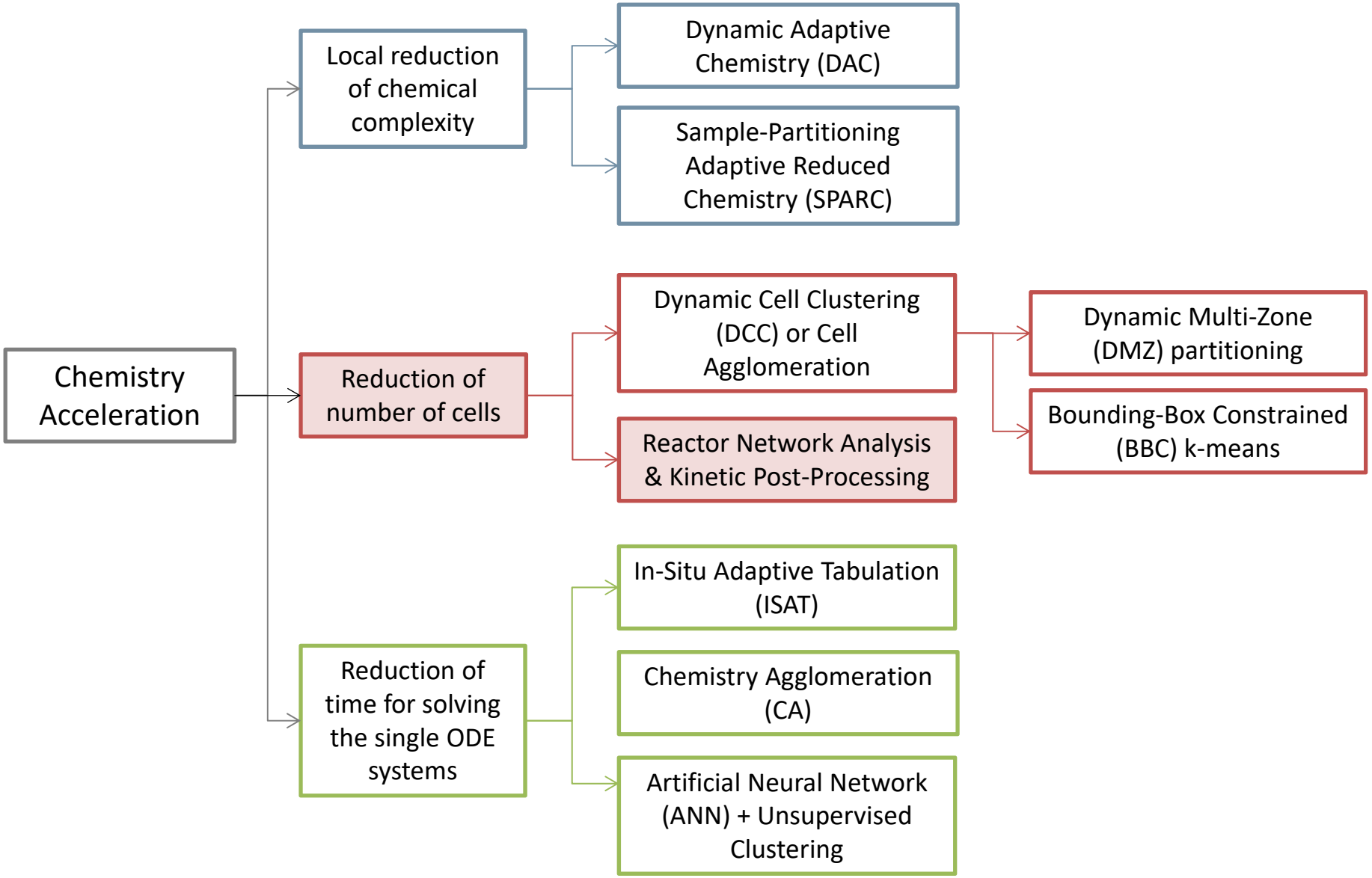

Kinetic Post-Processing (KPP) (I)

CFD simulation

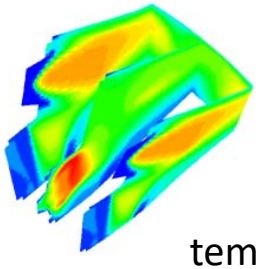

temperature

Post-Processing

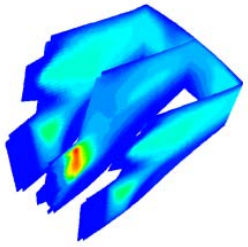

nitrogen oxides
"slow" pollutant species

Detailed chemistry

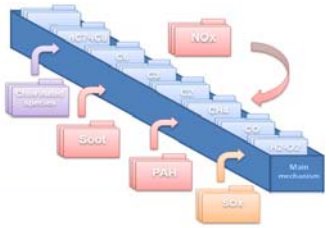

a steady state CFD simulation of the combustion device is performed using a global kinetic mechanism, which allows for the correct prediction of thermal and flow fields, but which cannot give us information on pollutant species

pollutant species usually affect only marginally the main combustion process and consequently do not influence the overall temperature and flow field

Faravelli T. et al., *A new procedure for predicting NOx emissions from furnaces*, Comput. Chem. Eng. 2001, 25 (4–6), 613–618

Skjoth-Rasmussen M. et al., *Post-processing of detailed chemical kinetic mechanisms onto CFD simulations*, Comput. Chem. Eng. 2004, 28 (11), 2351–2361

Fichet, V. et al., *A reactor network model for predicting NOx emissions in gas turbines*, Fuel 2010, 89 (9), 2202–2210.

Kinetic post-processing (KPP) (II)

1. CFD Simulation

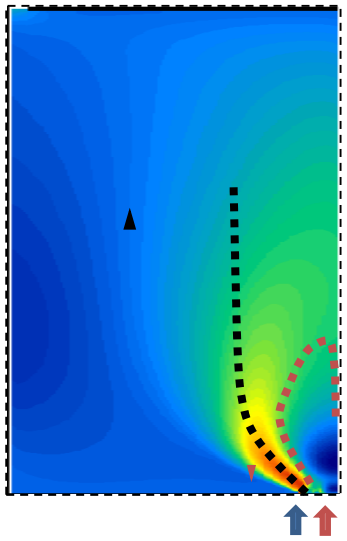

2. Clustering and network construction

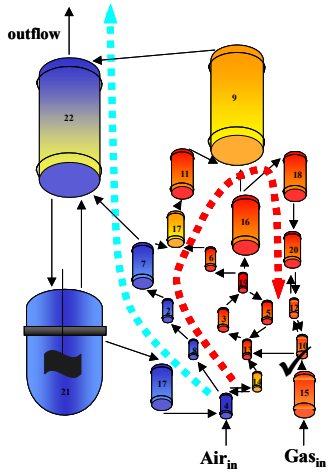

- The clustering reduces the overall dimensions of the problem
- According to the clustering, a complex reactor network is constructed (thousands of reactors)

3. Network solution

- A **detailed kinetic mechanism** is used
- No momentum/energy transport equations to be solved
- **Fully-coupled solution** to ensure high accuracy and reduced CPU time

Simplified kinetic mechanism

Ehrhardt K. et al., *Modeling of NOx reburning in a pilot scale furnace using detailed reaction kinetics*. Combust. Sci. Technol. 1998, 131 (1−6), 131−146

Falcitelli M. et al., *CFD + reactor network analysis: An integrated methodology for the modeling andoptimization of industrial systems for energy saving and pollution reduction*, Appl. Therm. Eng. 2002, 22 (8), 971−979

KPP: Numerical methodology

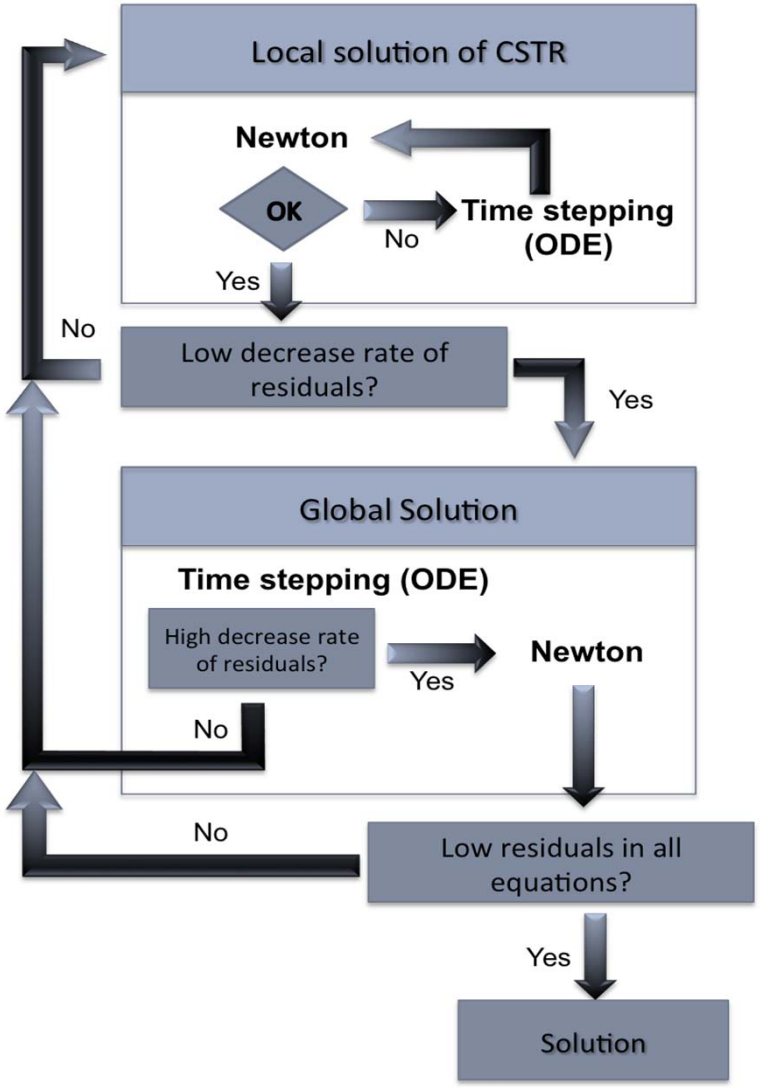

the numerical procedure combines different techniques to obtain the final solution, because the global Newton's method can be successfully applied only if the first-guess solution is close to the real solution.

1. Global Newton's Method
2. Global ODE (Backward Euler)
3. Direct Substitutions (Local solution)
   a. Local Newton's Method
   b. Local ODE system (stiff solver)

Cuoci, A., Frassoldati, A., Stagni, A., Faravelli, T., Ranzi, E., Buzzi-Ferraris, G., *Numerical modeling of NOx formation in turbulent flames using a kinetic post-processing technique* (2013) Energy and Fuels, 27 (2), pp. 1104-1122

Example: low NOx combustor (I)

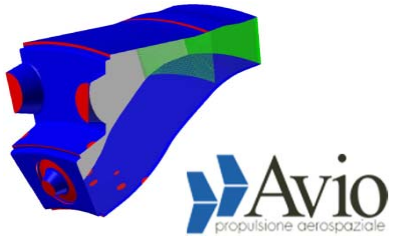

Axially staged combustor equipped with 18 injectors based on the Lean Premixed Prevaporised technology (LPP) for the main stage and 18 conventional pilot injectors

BODY3D Avio code was used to perform the CFD simulation with a global (2 steps) mechanism
Structured mesh (fitted-body) (~1M cells) of a 20° sector

KPP: mechanism with 86 species and 1427 reactions

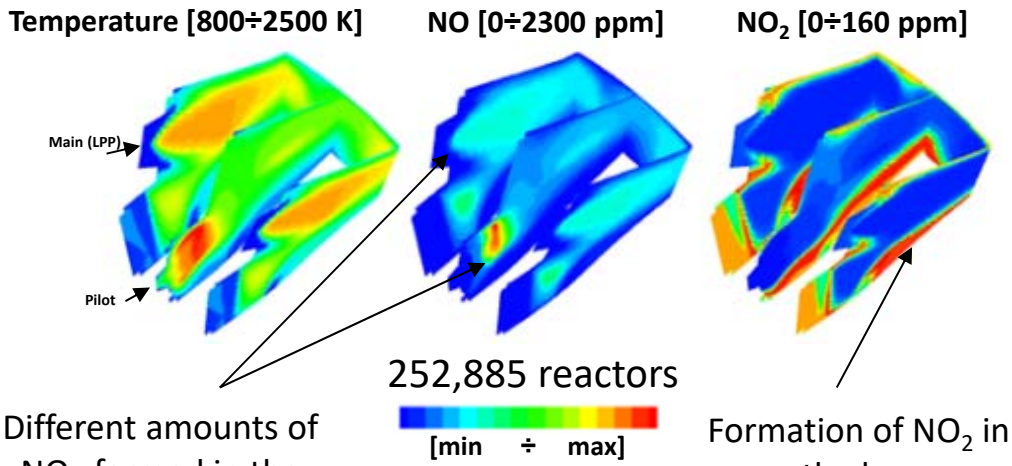

Different amounts of NOx formed in the conventional (pilot) and LPP injectors

Formation of NO_2 in the low temperature region (film cooling)

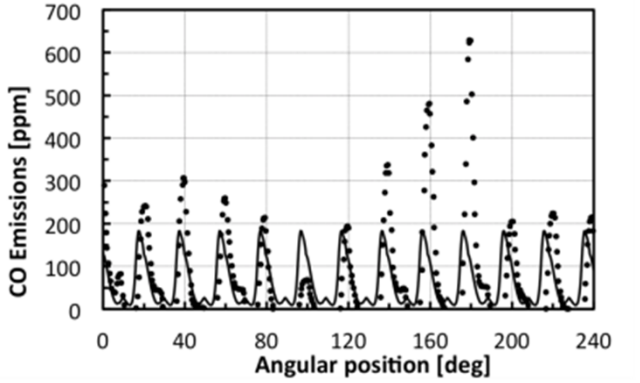

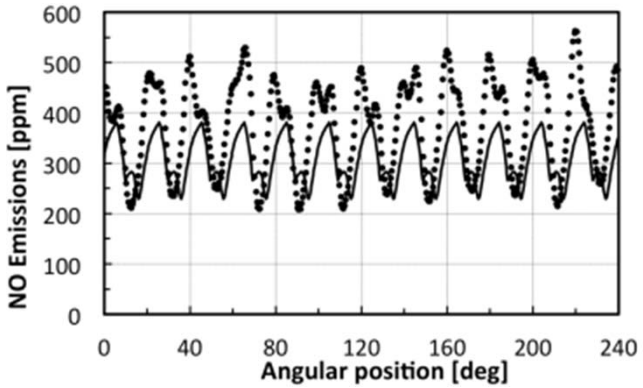

Frassoldati A., Cuoci A., Faravelli T., Ranzi E., Colantuoni S., Di Martino P., Cinque G., Combustion Science and Technology 181, p. 483-495 (2009

Example: low NOx combustor (II)

- A: tubular combustor (56,150 reactors, 4.8M eqs)
- B: aircraft combustor (252,885 reactors, 22M eqs)
- C: aircraft combustor (290,764 reactors, 25M eqs)

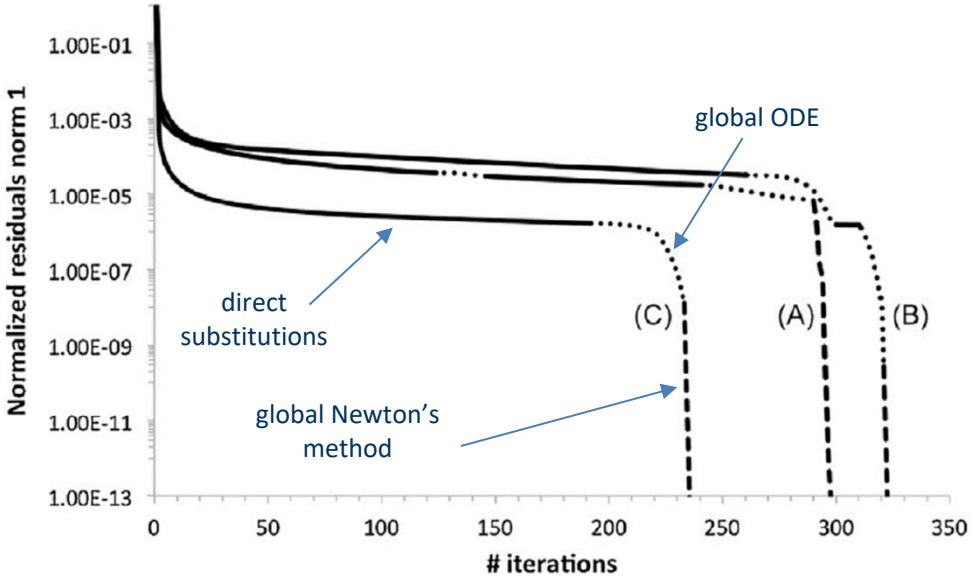

Residuals norm 1 trends, normalized with respect to their initial value (set equal to 1)

Relative importance of the 3 resolution methods in terms of time.

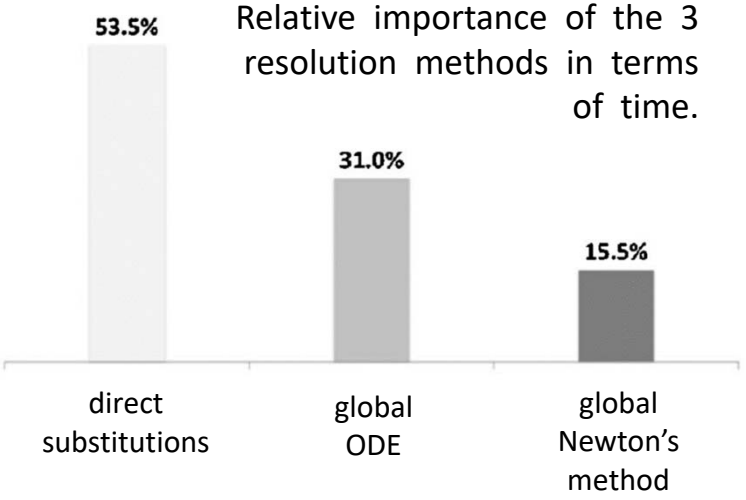

POLIMI NC7 kinetic mechanism
86 species and 1427 reactions

A. Stagni, A. Cuoci, A. Frassoldati, T. Faravelli, *A fully coupled, parallel approach for the post processing of CFD data through reactor network analysis,* Computers and Chemical Engineering, 60, p. 197-212 (2014).

Industrial applications

Turbulent Swirling Nonpremixed Flames

Monaghan et al., *Detailed Emissions Prediction for a Turbulent Swirling Nonpremixed Flame*, Energy & Fuels, 28(2), 1470-1488 (2014)

Gasoil burners

Cuoci et al., *Experimental and Modeling Study of NOx Formation in a Turbulent Gasoil Burner,* 30th Combustion Meeting of the Italian Section of The Combustion Institute, Ischia (2007)

Methane and natural gas burners

Frassoldati et al., *Experimental and modelling study of low-NOx industrial burners*, 31st Combustion Meeting of the Italian Section of The Combustion Institute, Torino (2008)

Combustors for aeroengine applications

Frassoldati et al., *Fluid Dynamics and Detailed Kinetic Modeling of Pollutant Emissions From Lean Combustion Systems,* ASME Turbo Expo 2010: Power for Land, Sea, and Air, Glasgow (2010)

Ultra-low NOX furnaces

Van Goethem et al., *The design of ultra-low NOx critical furnaces*, 10AIChE - 2010 AIChE Spring Meeting

Oxy-combustion furnaces

Cuoci et al., *CFD simulation of a turbulent oxy-fuel flame*, PTSE2010, Processes and Technologies for a Sustainable Energy, Ischia (2010)

Chemistry Acceleration

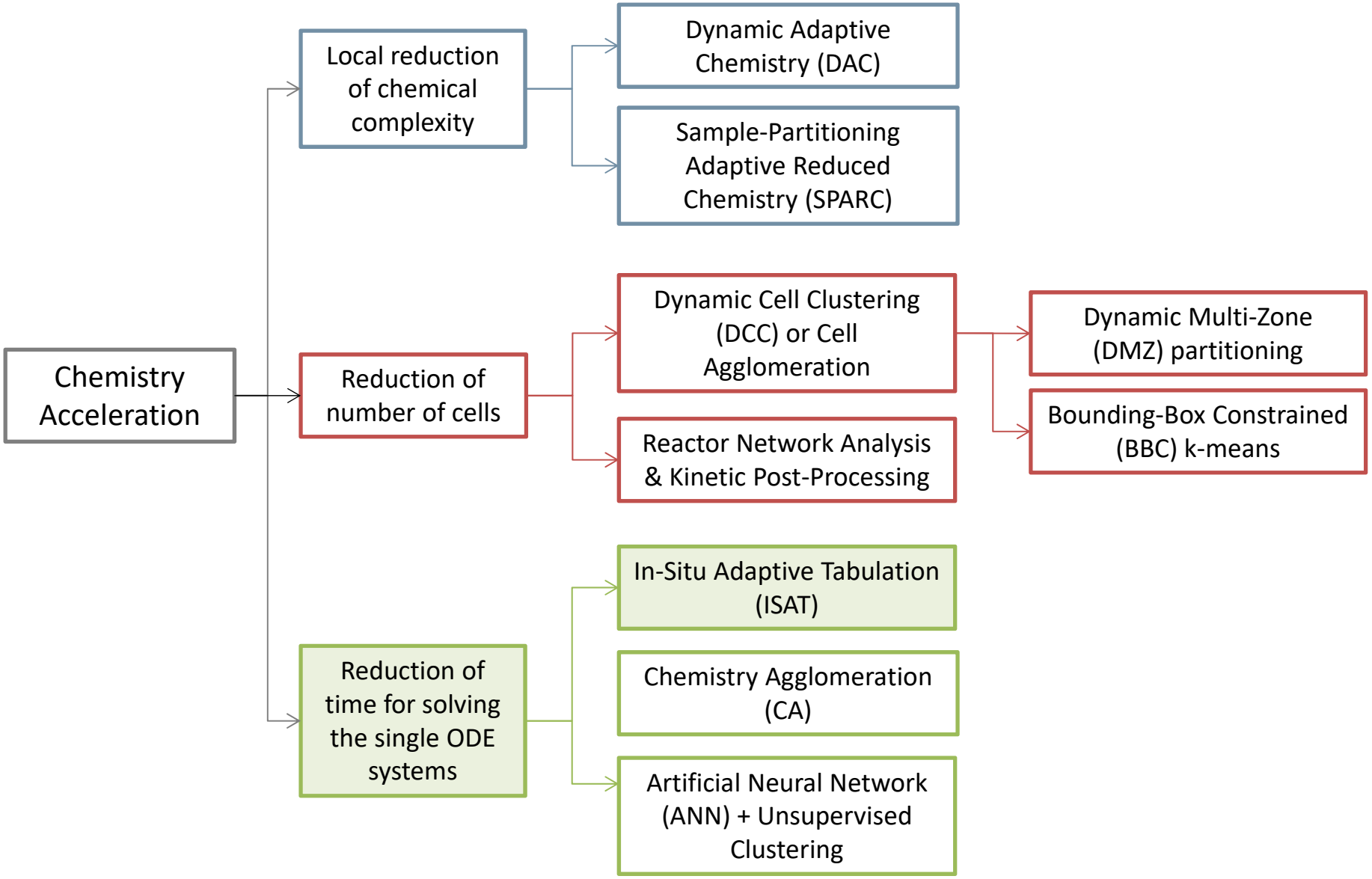

Integration of chemical step

local ODE system

$$\begin{cases} \dfrac{\partial \psi_i}{\partial t} = S_i(\psi_i) \\ \\ \psi_i(t^n) = \psi_i^n \end{cases}$$

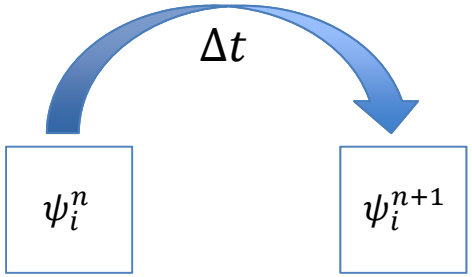

The equations constitute normally a **stiff, highly non-linear system**, which exhibits a wide spectrum of characteristic evolution time-scales. The integration of this ODE system requires **specialized solvers**, which are in general computer-time intensive.

Since a ODE system has to be solved in each cell at every time level, a **direct integration** of the flow and the ODE solvers is very CPU expensive and often impractical.

Tabulation Methods

Many numerical methods resort then to a **pre-calculation of the thermochemistry**, which is stored in the form of a table where the values of the thermochemical variables at the end of a given time step are recorded as a function of the thermochemical state at the beginning of the time step.

Although the thermochemical state is (coarsely) discretized for the tabulation, the **storage requirements quickly grow** as the dimensions of the compositional space increase.

The pre-tabulation can be adopted only in a case of a very small number of species.

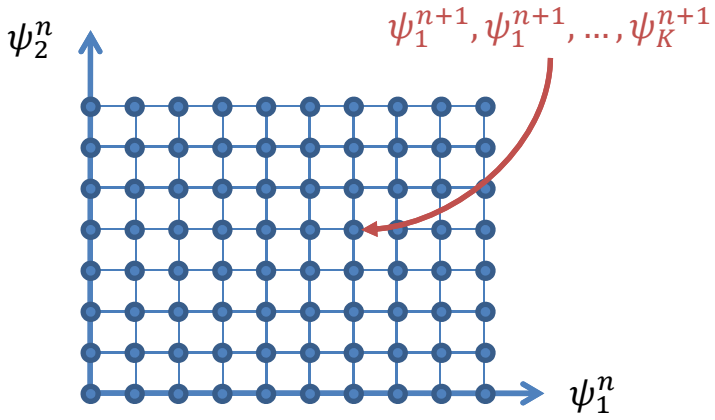

$N_{species}$	N_{points}	N_{tot} [M]	Memory [Gb]
4	10	0.01	0.00032
6	10	1	0.048
8	10	100	6.4
10	10	10^4	800
12	10	10^6	96000

Smart Tabulation Methods

Many numerical methods resort then to a **pre-calculation of the thermochemistry**, which is stored in the form of a table where the values of the thermochemical variables at the end of a given time step are recorded as a function of the thermochemical state at the beginning of the time step.

Although the thermochemical state is (coarsely) discretized for the tabulation, the **storage requirements quickly grow** as the dimensions of the compositional space increase.

The pre-tabulation can be adopted only in a case of a very small number of species.

When the number of species is larger, **smart tabulation methods** or a replacement of tables are needed.

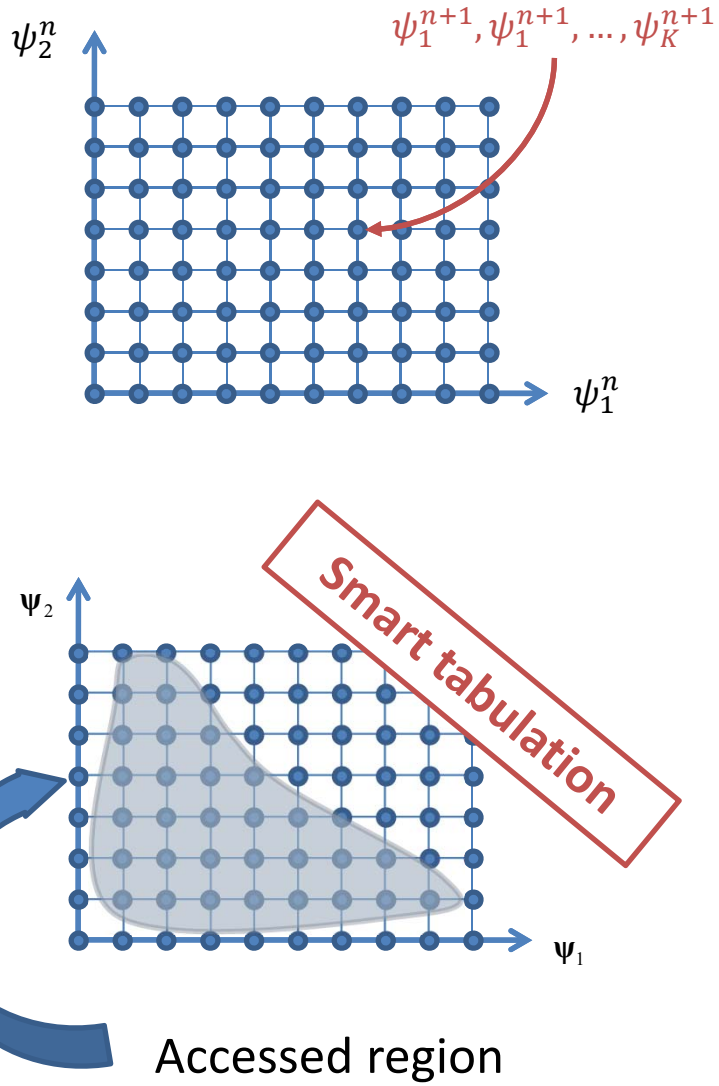

ISAT: In Situ Adaptive Tabulation

1. **In Situ:** Tabulation is carried out only with respect to those points to which the reactive system actually has access (accessed region)

2. **Adaptive:** A specific algorithm is applied in order to minimize the points to be tabulated within the access region, while maintaining good accuracy

3. **Tabulation:** The tabulation is carried out according to a tree structure, in order to ensure good efficiency in updating the map

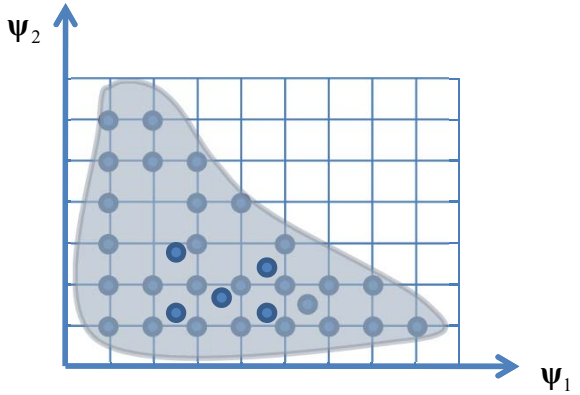

Pope S.B., *"Computationally efficient implementation of combustion chemistry using in-situ adaptive tabulation"*, Combustion Theory and Modeling, 1 (1997) 41-63

Singer M.A., Pope S.B., Najm H.M., *"Operator-splitting with ISAT to model reacting flow with detailed chemistry",* Combustion Theory and Modeling, 10 (2006) 199-217

ISAT: Reaction mapping

Reacting map

$$\mathbf{R}(\boldsymbol{\Psi}_0; t) \stackrel{\text{def}}{=} \boldsymbol{\Psi}(t)$$

Evolution of reacting map

$$\begin{cases} \dfrac{d\boldsymbol{R}}{dt}(\boldsymbol{\Psi}_0; t) = \mathbf{S}\big(\mathbf{R}(\boldsymbol{\Psi}_0; t)\big) \\ \mathbf{R}(\boldsymbol{\Psi}_0; t) = \boldsymbol{\Psi}_0 \end{cases}$$

Reaction-mapping Jacobian matrix

$$\boldsymbol{A}(\boldsymbol{\Psi}_0; t) \stackrel{\text{def}}{=} \frac{\partial \boldsymbol{R}}{\partial \boldsymbol{\Psi}_0}(\boldsymbol{\Psi}_0; t)$$

Sensitivity of **R** with respect to the initial conditions

$$\begin{cases} \dfrac{\partial \boldsymbol{A}}{\partial t}(\boldsymbol{\Psi}_0; t) = \boldsymbol{J}\big(\mathbf{R}(\boldsymbol{\Psi}_0; t)\big)\boldsymbol{A}(\boldsymbol{\Psi}_0; t) \\ \boldsymbol{A}(\boldsymbol{\Psi}_0; t) = \boldsymbol{I} \end{cases}$$

System of ordinary differential equations (ODEs) with initial conditions

ISAT: Direct Integration (DI)

The **direct integration** consists in going to solve directly, through an appropriate algorithm for stiff problems, the differential system starting from an assigned initial condition. At the same time, however, the calculation of matrix $\boldsymbol{A}$ is also carried out:

$$\begin{cases} \dfrac{d\boldsymbol{R}}{dt}(\boldsymbol{\Psi}_0; t) = \mathbf{S}\big(\mathbf{R}(\boldsymbol{\Psi}_0; t)\big) & N \text{ equations} \\ \dfrac{\partial \boldsymbol{A}}{\partial t}(\boldsymbol{\Psi}_0; t) = \boldsymbol{J}\big(\mathbf{R}(\boldsymbol{\Psi}_0; t)\big)\boldsymbol{A}(\boldsymbol{\Psi}_0; t) & N^2 \text{ equations} \end{cases}$$

The ODE system resolution above allows you to have all the information you need to create a node in the reaction map:

$$\boldsymbol{\Psi}_0 \xrightarrow{DI} \begin{cases} \boldsymbol{\Psi}_{\Delta t} = \mathbf{R}(\boldsymbol{\Psi}_0; \Delta t) \\ \boldsymbol{A}(\boldsymbol{\Psi}_0; t) \end{cases}$$

High computational cost

ISAT: linear interpolation

We have a reaction map with a certain number of nodes, calculated through a DI (index i). Let's imagine now to have to integrate the stiff system for new initial conditions (query point):

$\boldsymbol{\psi}_0^{[i]}$ neighboring point

$\boldsymbol{\psi}_0^{q}$ query point

$$\delta\boldsymbol{\psi}_0^q \overset{\text{def}}{=} \boldsymbol{\psi}_0^q - \boldsymbol{\psi}_0^{[i]}$$

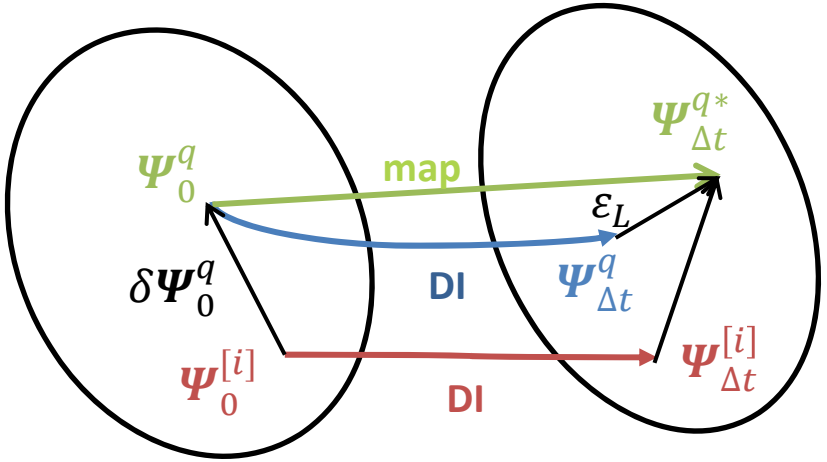

Direct integration

$$\boldsymbol{\psi}_{\Delta t}^q = \mathbf{R}\left(\boldsymbol{\psi}_0^q; \Delta t\right) = \mathbf{R}\left(\boldsymbol{\psi}_0^{[i]} + \delta\boldsymbol{\psi}_0^q; \Delta t\right)$$

Taylor's expansion

$$\delta\boldsymbol{\psi}_{\Delta t}^q \overset{\text{def}}{=} \boldsymbol{\psi}_{\Delta t}^{q*} - \boldsymbol{\psi}_{\Delta t}^{[i]} = \boldsymbol{A}\left(\boldsymbol{\psi}_0^{[i]}; \Delta t\right)\delta\boldsymbol{\psi}_0^q$$

$$\boldsymbol{\psi}_{\Delta t}^{q*} \approx \boldsymbol{\psi}_{\Delta t}^{[i]} + \boldsymbol{A}\left(\boldsymbol{\psi}_0^{[i]}; \Delta t\right)\left(\boldsymbol{\psi}_0^q - \boldsymbol{\psi}_0^{[i]}\right)$$

Difference between linear interpolation and DI

$$\varepsilon_L \overset{\text{def}}{=} \boldsymbol{\psi}_{\Delta t}^{q*} - \boldsymbol{\psi}_{\Delta t}^q$$

ISAT: Ellipsoid of Accuracy (EOA)

The EOA can be estimated from the sensitivity matrix A once a tolerance ε is defined

Retrieve

The query point falls within the EOA and therefore the linear interpolation is adequate

$$\boldsymbol{\Psi}_{\Delta t}^{q*} \approx \boldsymbol{\Psi}_{\Delta t}^{q}$$

Growth

The point is outside of the EOA, but through the DI we have $\varepsilon_L < \varepsilon_{tol}$

The EOA is then expanded to include the new

Addition

If neither the retrieved nor the growth conditions are met, a new node must be tabulated through the DI

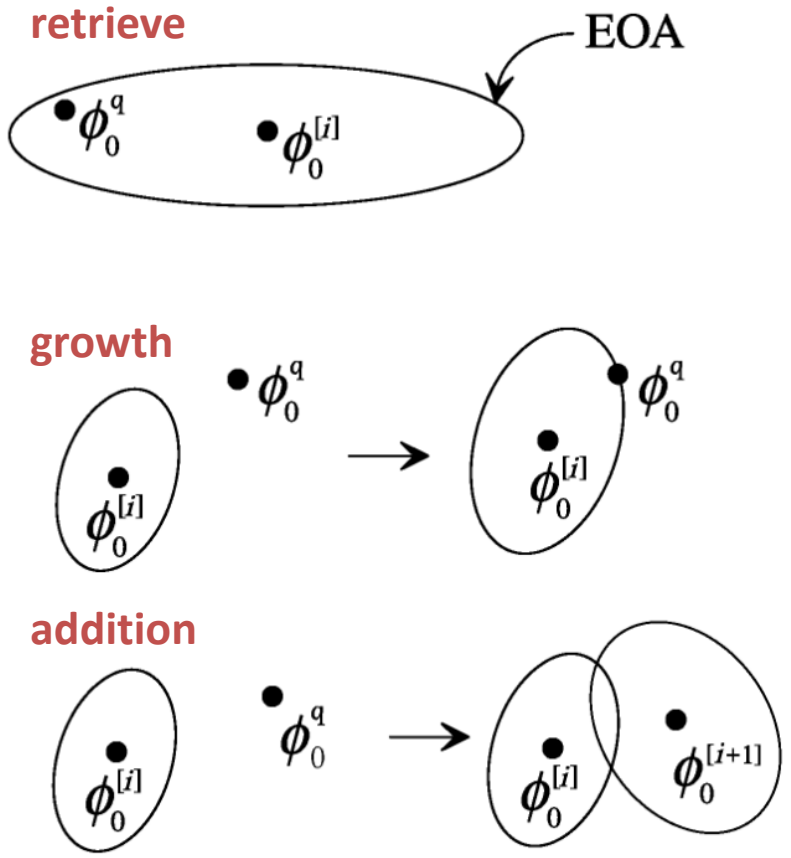

Pope S.B., *"Computationally efficient implementation of combustion chemistry using in-situ adaptive tabulation"*, Combustion Theory and Modeling, 1 (1997) 41-63

ISAT and Steam reforming Packed Bed Reactor (I)

OPERATING CONDITIONS	
CH_4 mass fraction	0.121
H_2O mass fraction	0.829
N_2 mass fraction	0.009
H_2 mass fraction	0.002
Inlet temperature	973 K
Outlet Pressure	14 bar
Flow velocity	3.0 m/s

Conventional Rashig rings

tube diameter 0.015 m

n° cells	Ring	7 Holes
fluid	2.5 M	0.6 M
solid	1.4 M	0.3 M
total	3.9 M	0.9 M

7-Holes Rings

tube diameter 0.04 m

Matros Technologies. Inc. http://www.matrostech.com

BASF The Chemical Company

Simulations performed using a detailed microkinetic mechanism for steam reforming (Deutschmann et al., 2011).
It consists of **42 reactions among 7 gas phase and 13 surface species**.

ISAT and Steam reforming Packed Bed Reactor (II)

ISAT DI

	Rings	7 Holes
Overall Speed-up factor	3.5	2.3
Chemistry Speed-up factor	**28**	**14**
Catalytic Cells [%]	36.2	31.9

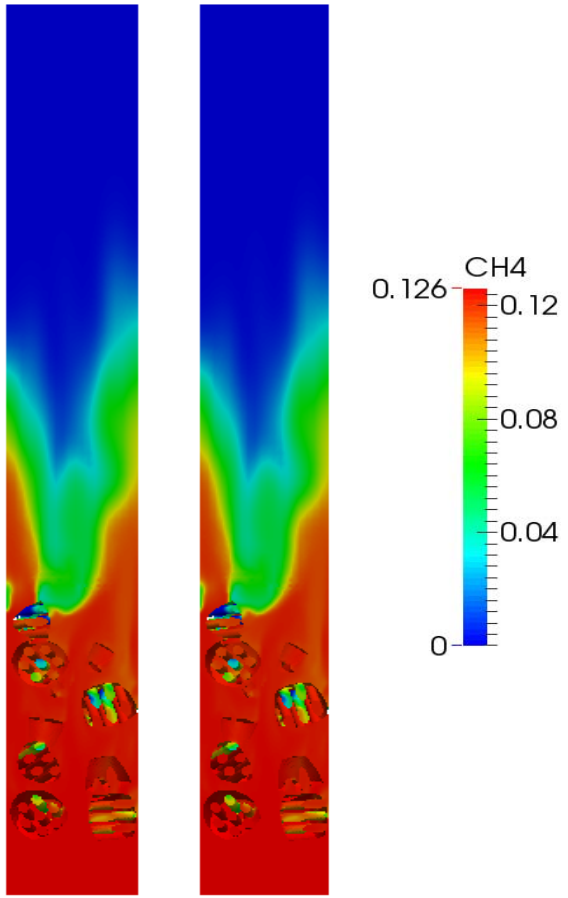

ISAT DI

CatalyticFOAM

Bracconi, M., Maestri, M., Cuoci, A., *In situ adaptive tabulation for the CFD simulation of heterogeneous reactors based on operator-splitting algorithm* (2017) AIChE Journal, 63 (1), pp. 95-104, DOI: 10.1002/aic.15441

ISAT and CPOX of methane (I)

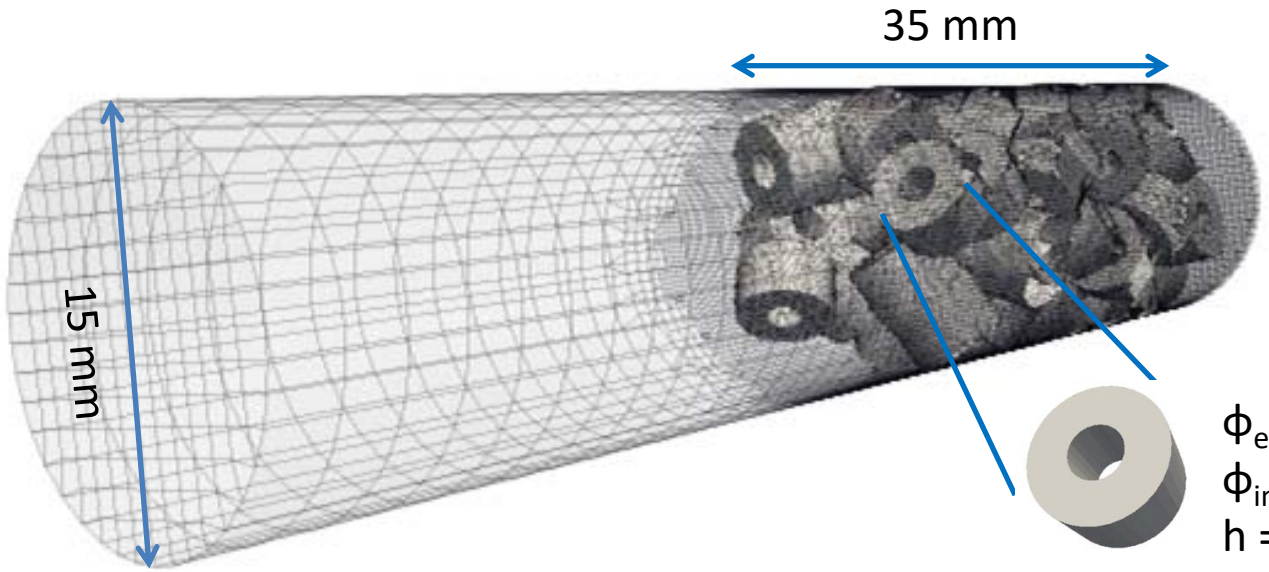

ϕ_{est} = 5 mm
ϕ_{int} = 2 mm
h = 3 mm

- ***Methane (21 gas + 13 surface species, 82 reactions)***
- ***Number of cells:***

	n° cells
fluid	≈ 0.18 M
catalytic	≈ 0.60 M

OPERATING CONDITIONS	
CH_4 mass fraction	0.1565
O_2 mass fraction	0.1753
N_2 mass fraction	0.6682
Inlet temperature	773.15 K
Outlet Pressure	1 bar
Flow velocity	1 m/s

ISAT and CPOX of methane (II)

21 gas species and 13 adsorbed species involved in 82 surface reactions

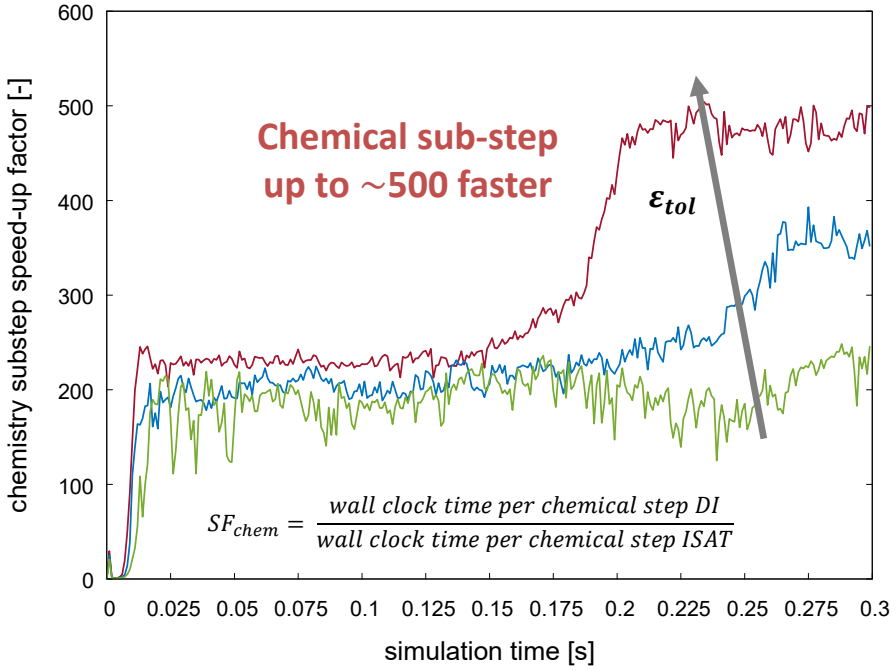

Partial Oxidation (PO) of methane in a heterogeneous catalytic tubular reactor

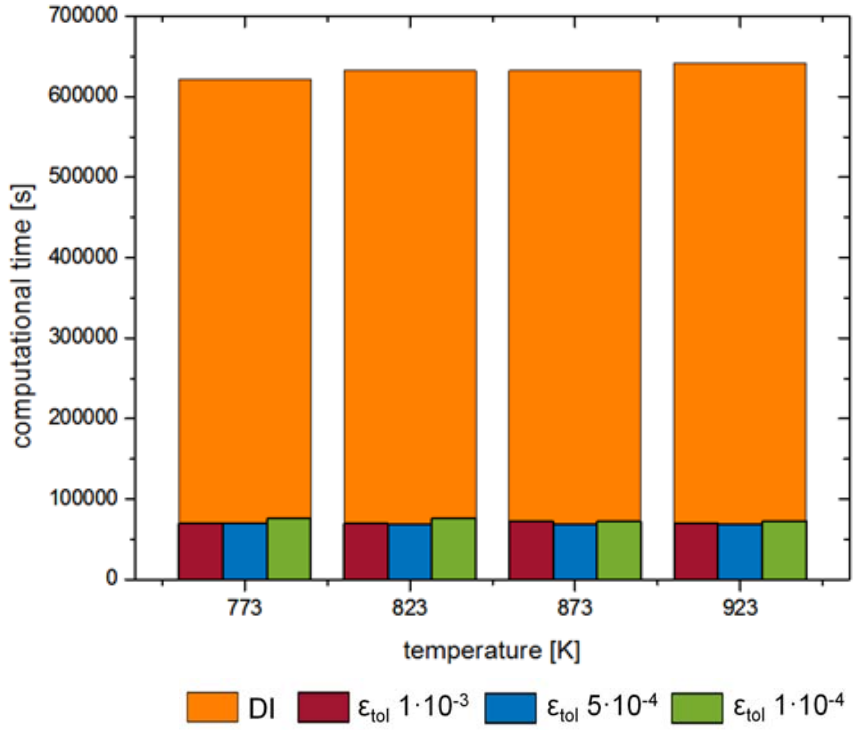

Bracconi, M., Maestri, M., Cuoci, A., *In situ adaptive tabulation for the CFD simulation of heterogeneous reactors based on operator-splitting algorithm* (2017) AIChE Journal, 63 (1), pp. 95-104, DOI: 10.1002/aic.15441

Chemistry Acceleration

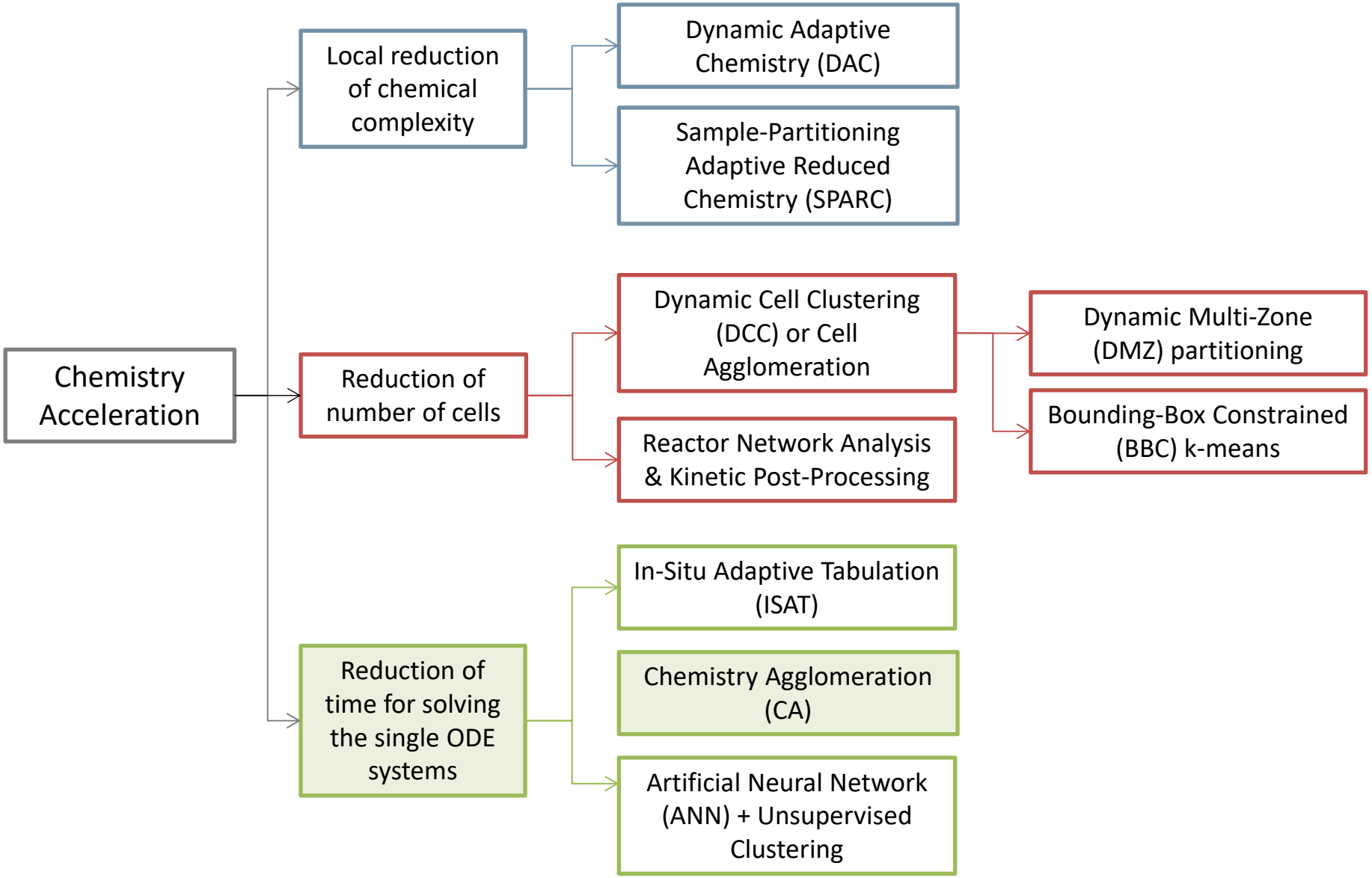

Chemistry Agglomeration (I)

In **Chemistry Agglomeration (CA)** the ODE solution of chemical step is not carried out in a single step, but is split in a sequence of ODE integrations of clusters (groups) of species

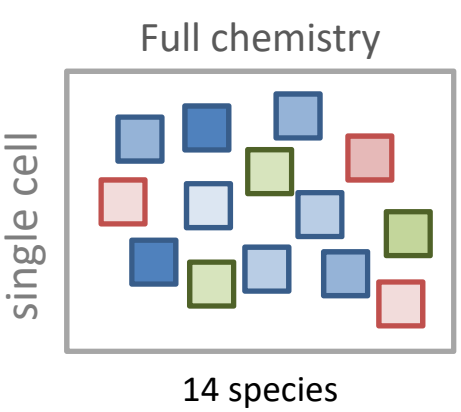

vs

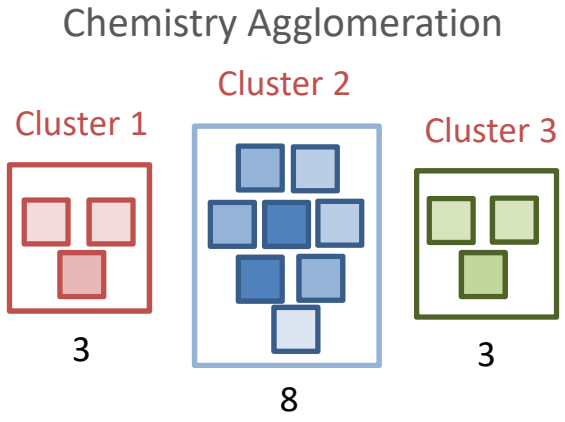

$$\phi^{n+1} = R_{\Delta t}(\phi^n)$$

$$\phi^{n+1} \cong R_{\Delta t}(\phi_1^n) \circ R_{\Delta t}(\phi_2^n) \circ R_{\Delta t}(\phi_3^n)$$

Each subset of species cluster should have no overlap with others, and an almost equal number of species in each subset is assumed.

Wang J.H., Pan S., Hu X.Y., Adams N.A., *A species-clustered splitting scheme for the integration of large-scale chemical kinetics using detailed mechanisms*, Combustion and Flame 205, p. 41-54 (2019)

Chemistry Agglomeration (II)

In **Chemistry Agglomeration (CA)** the ODE solution of chemical step is not carried out in a single step, but is split in a sequence of ODE integrations of clusters of species

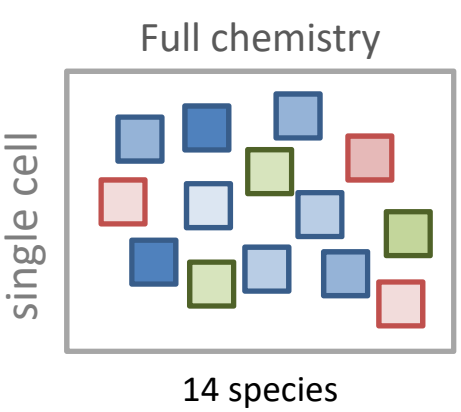

vs

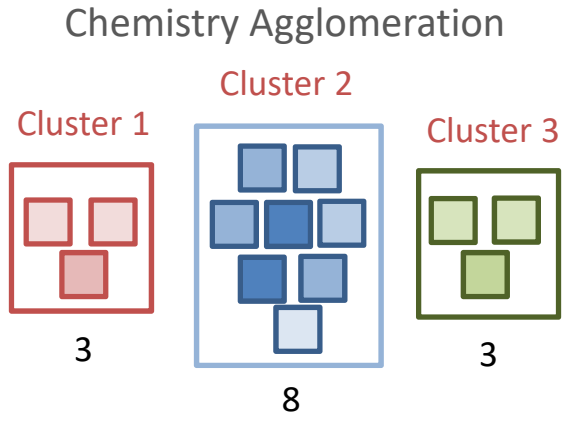

$$\phi^{n+1} = R_{\Delta t}(\phi^n)$$

$$\phi^{n+1} \cong R_{\Delta t}(\phi_1^n) \circ R_{\Delta t}(\phi_2^n) \circ R_{\Delta t}(\phi_3^n)$$

The cost of implicit ODE solution scales as n^2 or n^3 with the number of species n

$$C \sim 14^{2.5} = \sim 700 \longrightarrow C \sim 3^{2.5} + 8^{2.5} + 3^{2.5} = \sim 210$$

Max theoretical speedup = 3.3

An example (I)

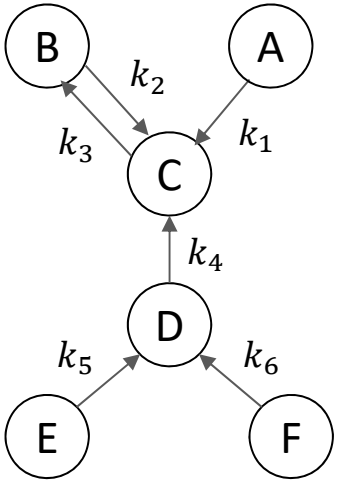

Clustering I

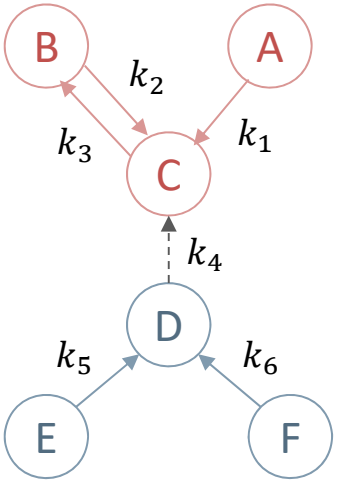

Clustering II

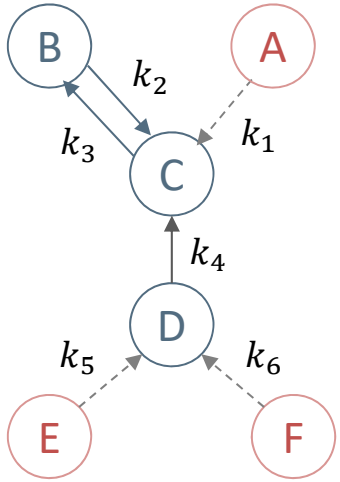

A	B	C	D	E	F	
$-k_1$						A
	$-k_1$	k_3				B
k_1	k_2	$-k_3$	k_4			C
			$-k_4$	k_5	k_6	D
				$-k_5$		E
					$-k_6$	F

A	B	C	D	E	F	
$-k_1$						A
	$-k_1$	k_3				B
k_1	k_2	$-k_3$	k_4			C
			$-k_4$	k_5	k_6	D
				$-k_5$		E
					$-k_6$	F

A	E	F	B	C	D	
$-k_1$						A
	$-k_5$					B
		$-k_6$				C
			$-k_2$	k_3		D
k_1			k_2	$-k_3$	k_4	E
	k_5	k_6			$-k_4$	F

An example (II)

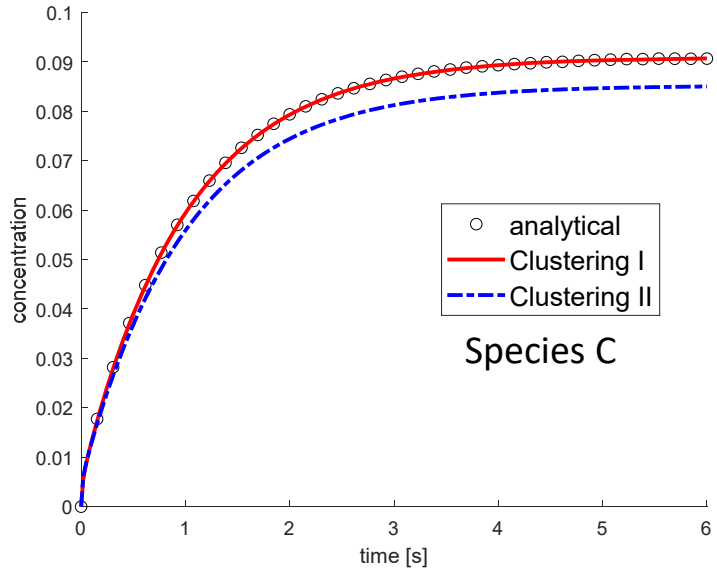

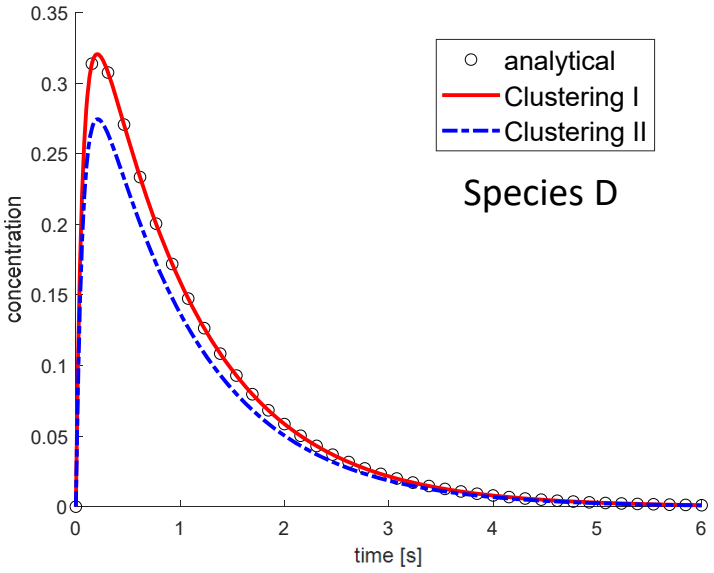

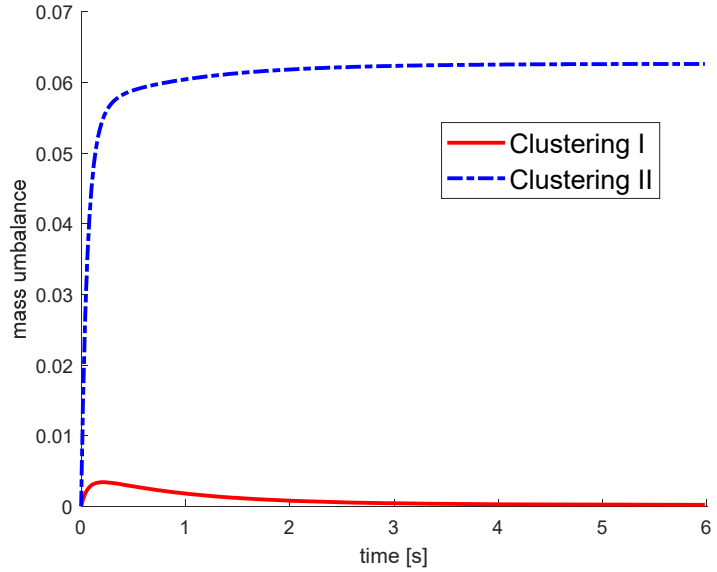

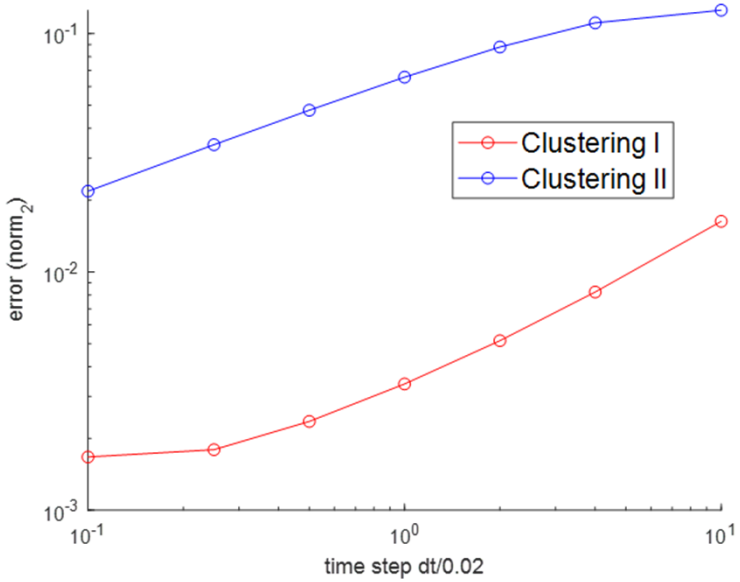

Clustering based on Diffusion Maps

- Given a prescribed number of clusters N, there are many possible clustering combinations.
- A promising strategy is to **cluster all "close" nodes in the graph into a subset**, corresponding to **having species with strong interactions** in the same cluster.
- **Diffusion maps** as a non-linear technique for dimensionality reduction, dataset parameterization and clustering, are a powerful tool reach this goal.
- Different from linear dimensionality reduction methods such as principal component analysis (PCA), diffusion maps is part of the family of **non-linear dimensionality reduction methods** which focus on discovering the underlying manifold that the data has been sampled from.

The weight matrix for diffusion maps

Weight matrix W of **diffusion maps** for the reaction system

$$W(x,y) = \begin{cases} \max(k_j) & \text{if x and y both participate in reaction j} \\ 0 & \text{otherwise} \end{cases}$$

$$W(x,x) = \max(W(x,y)_{y \neq x})$$

Weight matrix of diffusion maps for the reaction system

A	B	C	D	E	F	
k_1	0	k_1	0	0	0	**A**
0	k_3	k_3	0	0	0	**B**
k_1	k_3	k_3	k_4	0	0	**C**
0	0	k_4	k_6	k_5	k_6	**D**
0	0	0	k_5	k_5	0	**E**
0	0	0	k_6	0	k_6	**F**

It is symmetric and component-wise positive

Diffusion maps

Using diffusion maps to analyze the graph based on the weight matrix, we can project the set of species into a **diffusion space** with at most n dimensions, where **the pairwise distance reveals the connectivity between two species**.

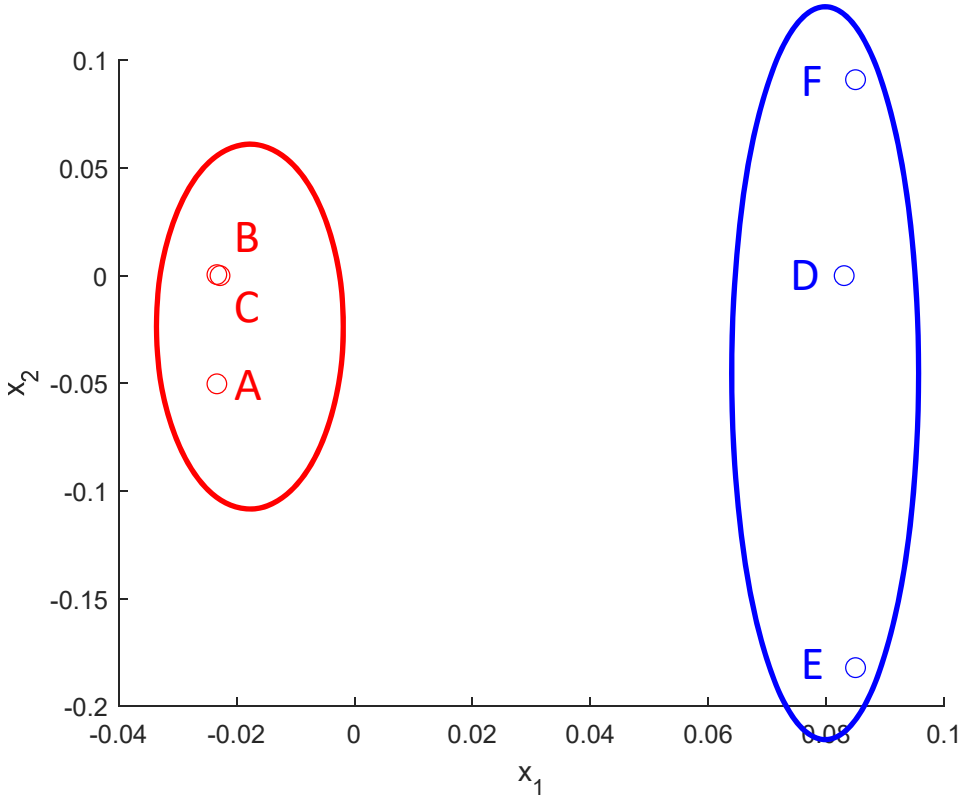

The Diffusion Map applied shows that species A, B and C almost collapse on each other in x_1 and x_2 direction, which are the first two **diffusion map coordinates**

Chemistry Agglomeration for GRI30

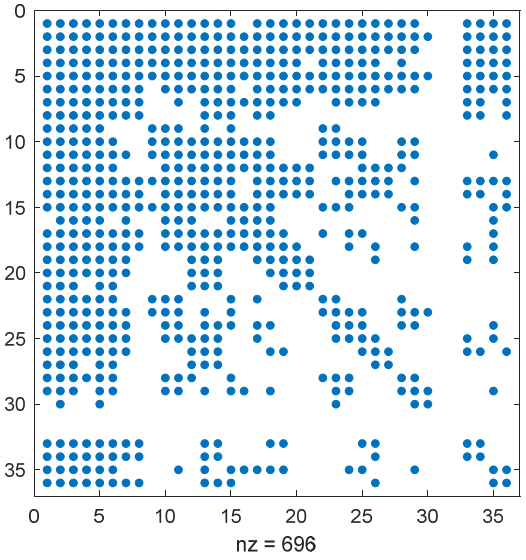

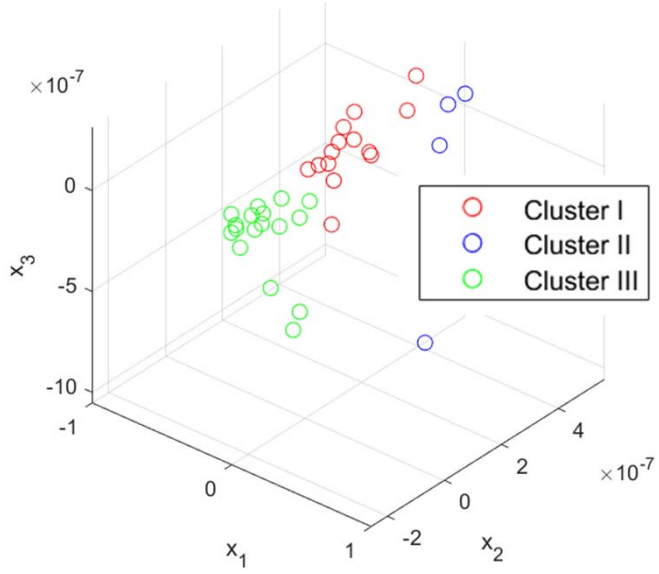

GRI 30 (without NOX), 36 species

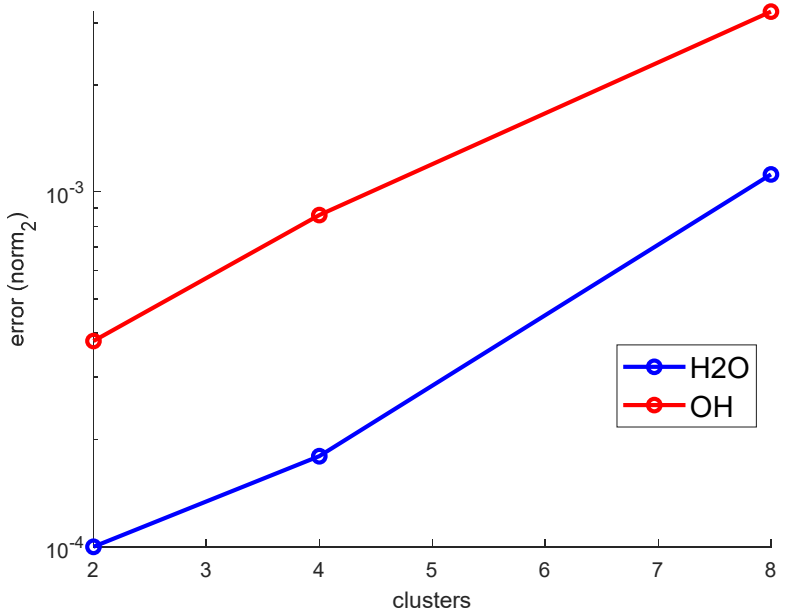

Zero-dimensional auto-ignition of the CH4/air mixture under adiabatic and constant-volume conditions (T = 1200 K, P = 1 bar, Φ = 2)

3 Clusters: 14, 4 and 18 species
Theoretical speed-up: 3.6X

Sparsity of mechanisms

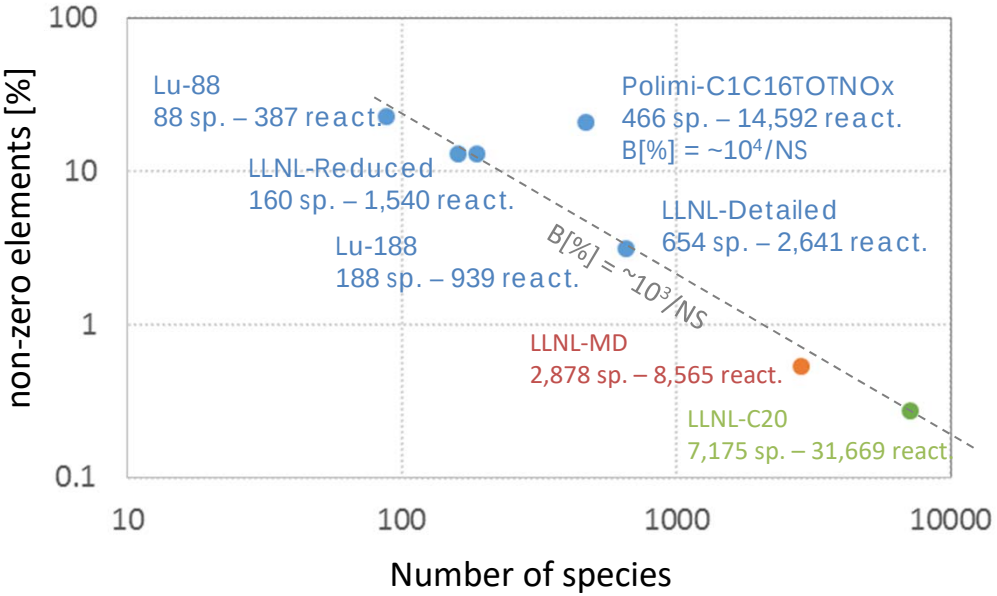

LLNL n-heptane
Species: 658
Reactions: 2827
Non-zeros: 3.03%

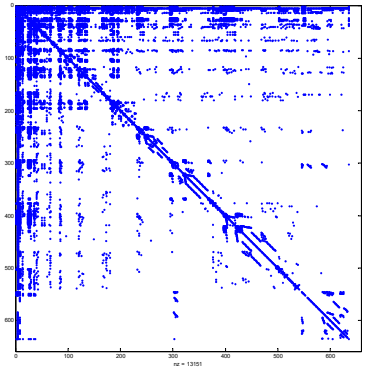

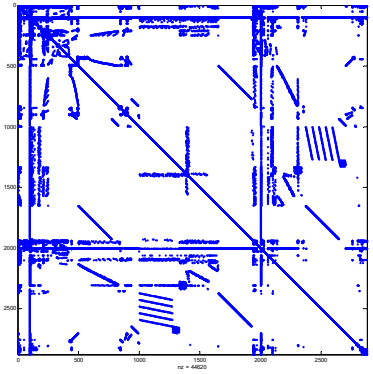

LLNL Methyl-decanoate
Species: 2878
Reactions: 8555
Non-zeros: 0.49%

The sparsity of a wide selection of mechanisms has been assessed and shown in the figure to the left.

It is clear that, the larger then kinetics mechanisms, i.e. the more species, the greater the sparsity.

Observations

- In real cases kinetic constants depend on **temperature of the mixture**. The weight matrix has also take into account the varying reaction rates with temperature.
- Rather than sampling at a single temperature, many temperature samples are collected and averaged in order to construct a **representative weight matrix**.
- The derived clustering by diffusion maps based on such a weight matrix can be **stored and used** for other conditions as long as the same mechanism is involved. In such way, the determination of the weight matrix as well as the clustering procedure can be treated as a preprocessing step instead of costly on-the-fly clustering.
- Since multiple scales of the absolute reaction rates exist, usually spanning several orders of magnitude, **logarithmic scaling** of the reaction rates can be performed to avoid underestimating the slow reactions.
- Also, normalization in each row of the matrix relative to the diagonal species is carried out.

Chemistry Acceleration

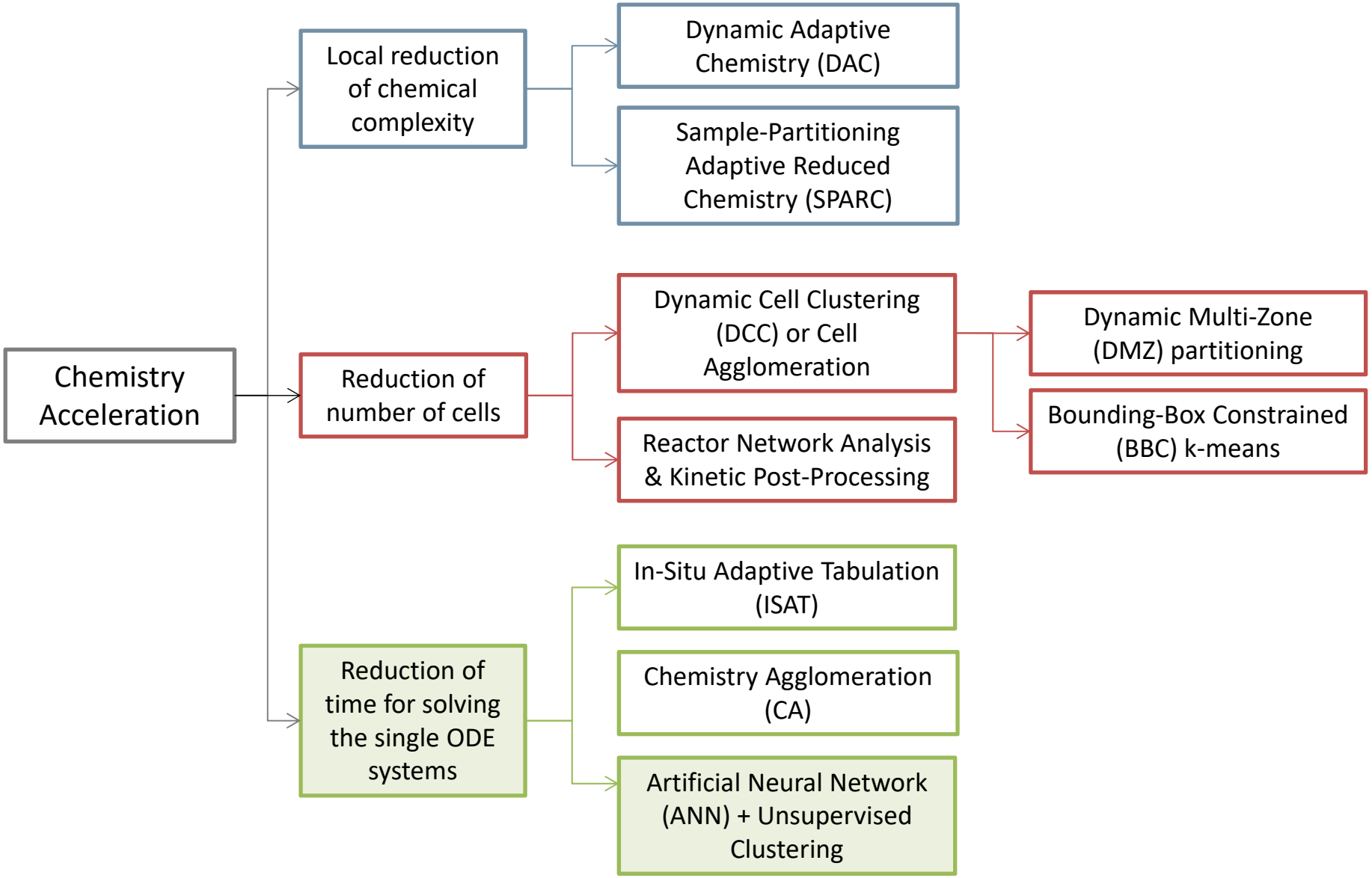

Examples of ANN in combustion

Use **Artificial Neural Networks (ANN)** to replace the expensive solution of local ODE systems

Christo et al. (1996a, 1996b): first example of application of **ANN to replace integration of stiff ODE systems**. Limited to 1-step or 3-steps kinetic mechanisms.

Blasco et al. (1998): first example of systematic analysis of generation of ANN for combustion problems (analysis o scaling, distribution of errors, optimal network topology, etc.)

Blasco et al. (2000): introduction of pre-partitioning of training dataset and generation of multiple ANNs adapted to chemistry

Sen and Menon (2009): first example of ANN adopted in a LES of a turbulent flame to replace the stiff ODE solver in the chemical step

Rigopoulos (2013, 2015): combination of ANN with pre-partitioning of training dataset and reduction of chemical space via RCCE (Rate-Controlled Constrained Equilibrium)

Application of Artificial Neural Networks (ANN)

1. Generation of data (observations)

In order to compute the ANN weights, a set of examples containing input-output data must be generated. The performance of the ANN is very sensitive to the quality of the selected training set

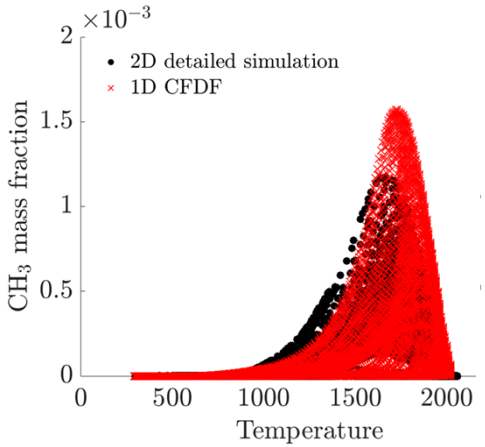

2. Scaling of generated data

Once the training set has been selected and the data have been generated, some preprocessing must be applied to the input and output values before they can be fed to the ANN for training.

3. Selection of ANN topology

The topology or architecture of the ANN can be described in terms of the number of hidden layers of neurons and the number of neurons in each layer. The ANN architecture is to be chosen in a trial-and-error process to maximize the quality of the fitting of the data set.

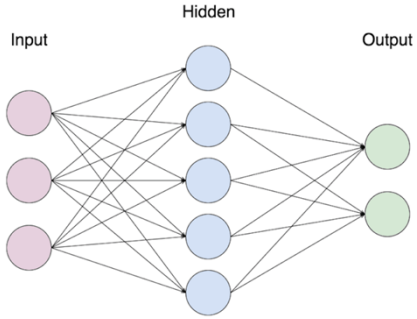

4. Training of ANN

In the training phase, the scaled input and output samples of the generated examples are presented to the ANN and a procedure to adjust the ANN weights is followed.

Modeling time evolution of a chemical system via ANNs

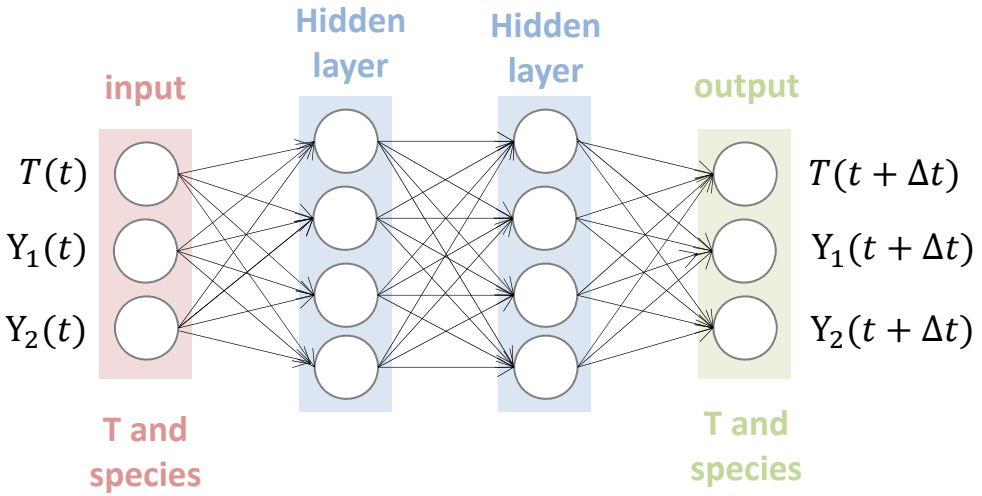

The aim of the reactive-species ANN is to predict, given a composition at the beginning of a time step, the mass fractions of the species at the end of this time step.

- The time step is fixed for the network
- Different ANNs with different time steps are used (for example, $\Delta t = 10^{-5}$, 10^{-3} and 10^{-3} s)
- Intermediate time steps can be simulated by dividing them into smaller ones having the above sizes.

Modeling time evolution of a chemical system via ANNs

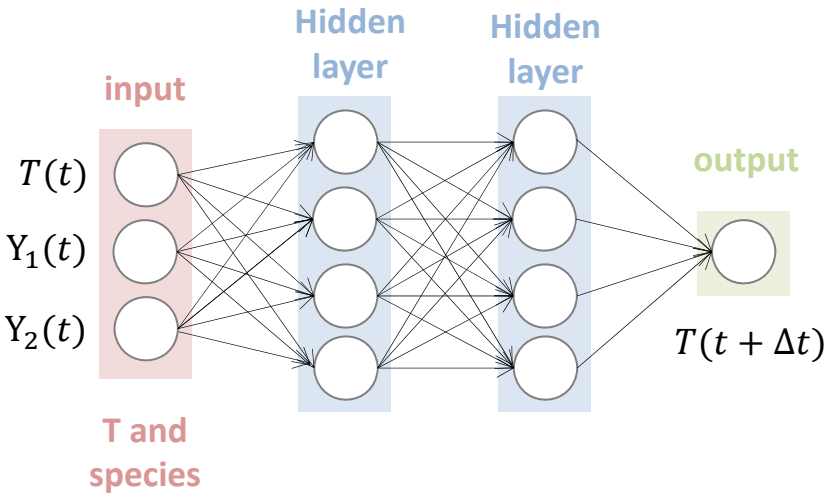

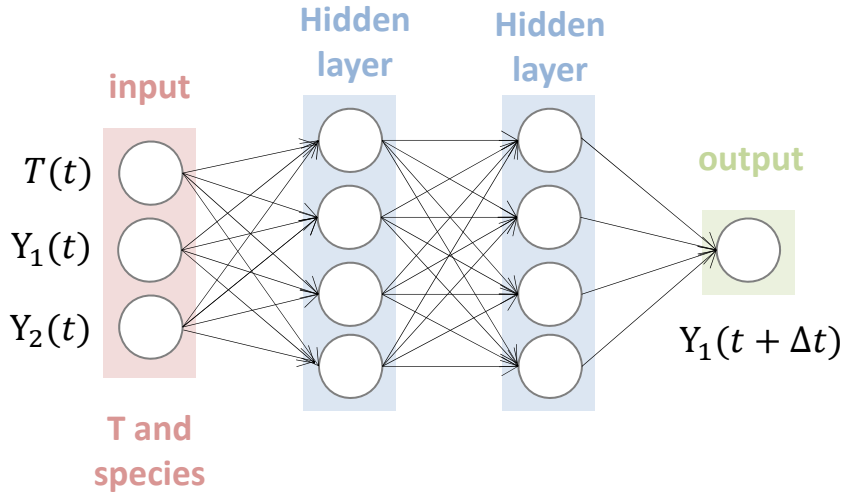

The aim of the reactive-species ANN is to predict, given a composition at the beginning of a time step, the mass fractions of the species at the end of this time step.

- In order to increase the accuracy, multiple ANNs can be considered, dedicated to single species (or groups of species)
- Obviously, the computational cost is expected to increase (linearly) with the number of ANNs

Unsupervised Clustering and ANNs (I)

In a practical flame, for instance, it is possible to identify several zones **(clusters)** with burning regimes where the rate of change of the relevant variables may differ widely (indeed, the relevant variables themselves may also be different)

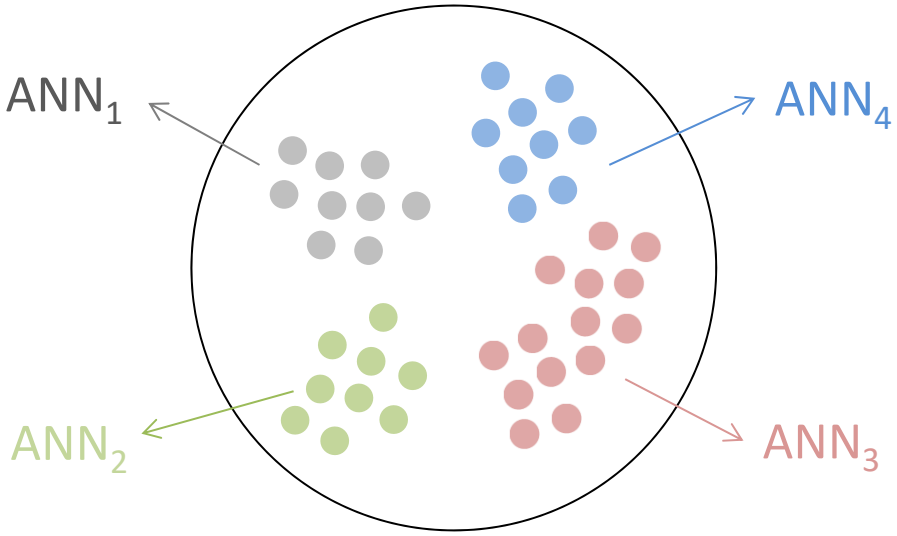

Classification problem

One question that immediately arises is **how to divide the composition space** into parts. With a multidimensional space where only a small part of it is covered by the data set, it would be extremely wasteful to employ a regular grid.

It makes more sense to cluster points in such a way that **compositions that are close to each other** will be allocated to the same ANN.

Unsupervised Clustering and ANNs (II)

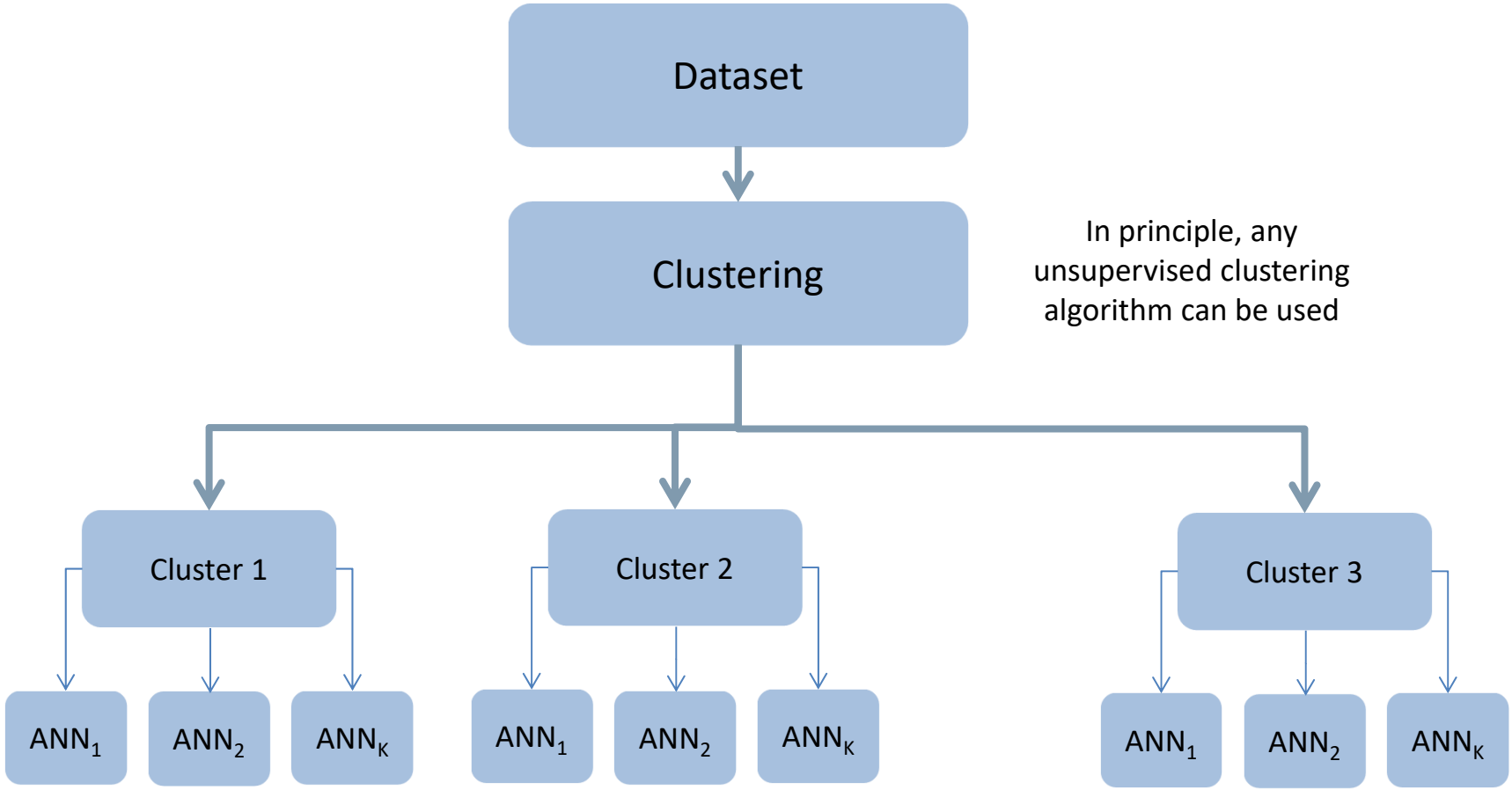

Unsupervised Clustering and ANNs (III)

Diffusion Maps can also be used to group different thermo-chemical scalars together before the ANN training. **Diffusion Maps** help in this respect by identifying scalars that share similar nonlinearity's and groups them together. Such scalar grouping provides additional benefits in terms of building more compact networks and speeding-up training.

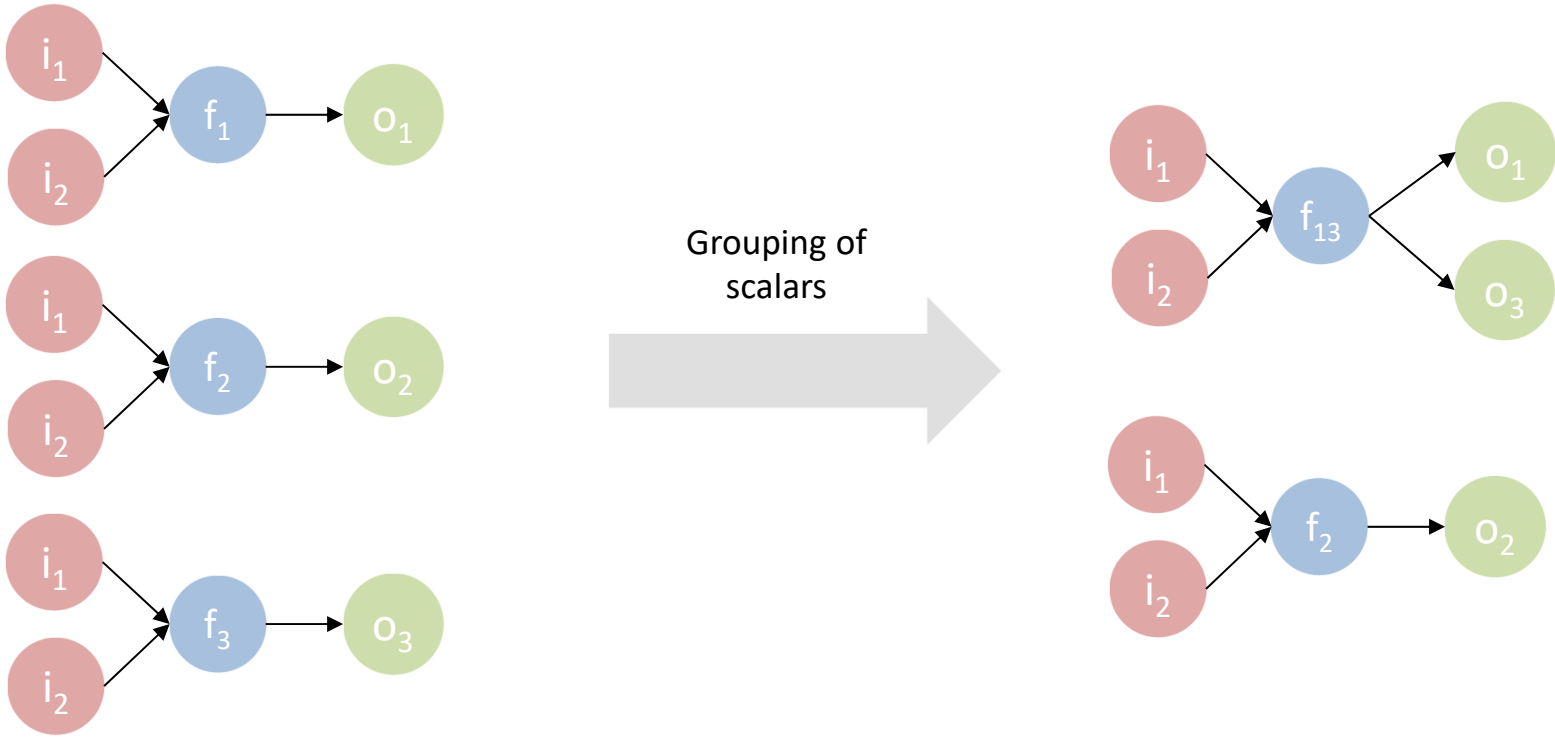

Ranade, R., Li, G., Li, S., Echekki, T., *An Efficient Machine-Learning Approach for PDF Tabulation in Turbulent Combustion Closure,* Combustion Science and Technology (2019)

Unsupervised Clustering and ANNs (IV)

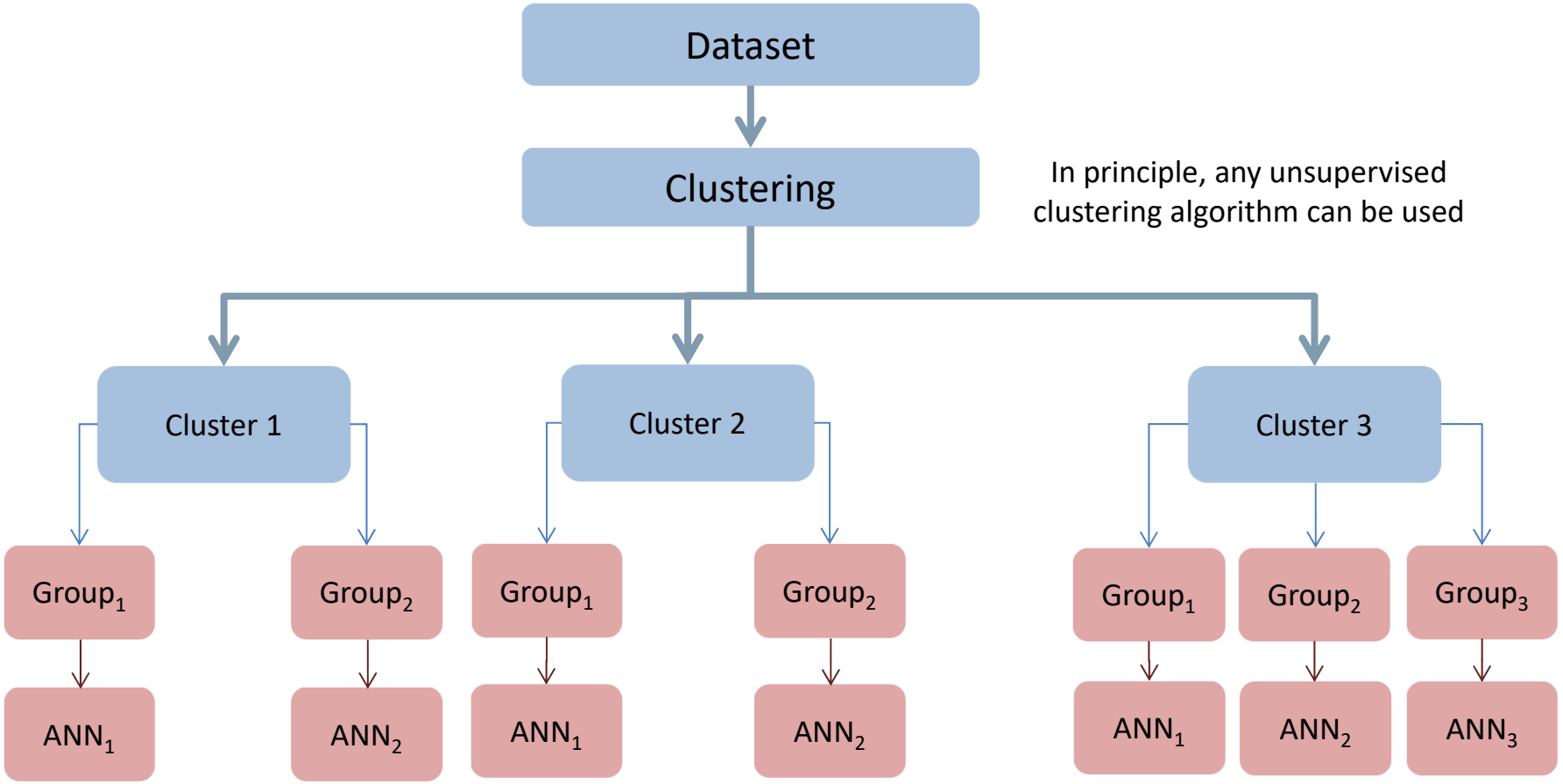

Example: Chemical Vapor Infiltration (CVI) process

Initial preforms

CVI

Final disk brakes

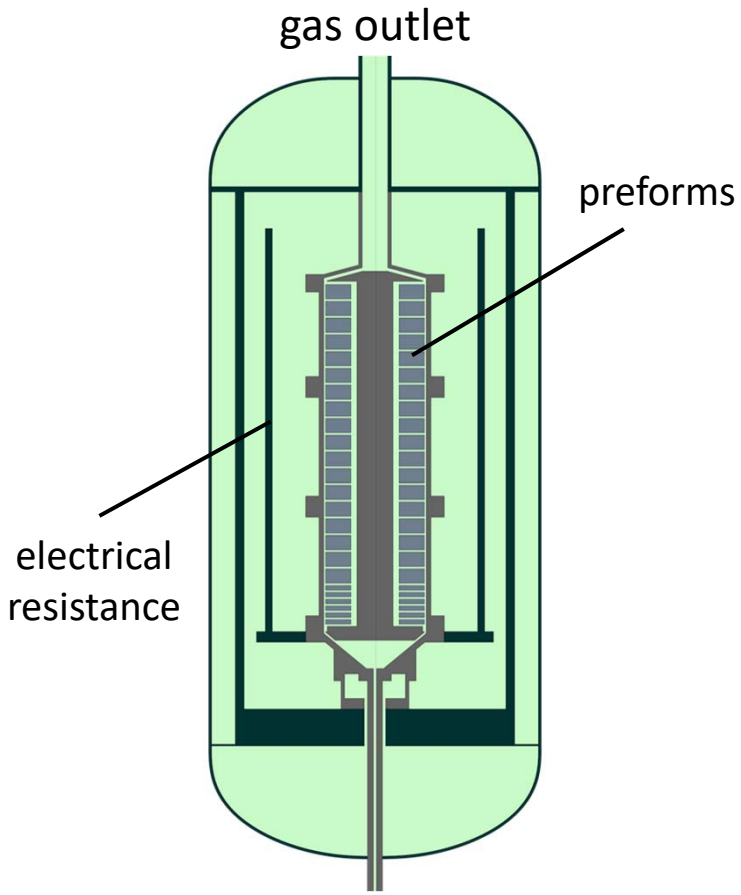

brembo

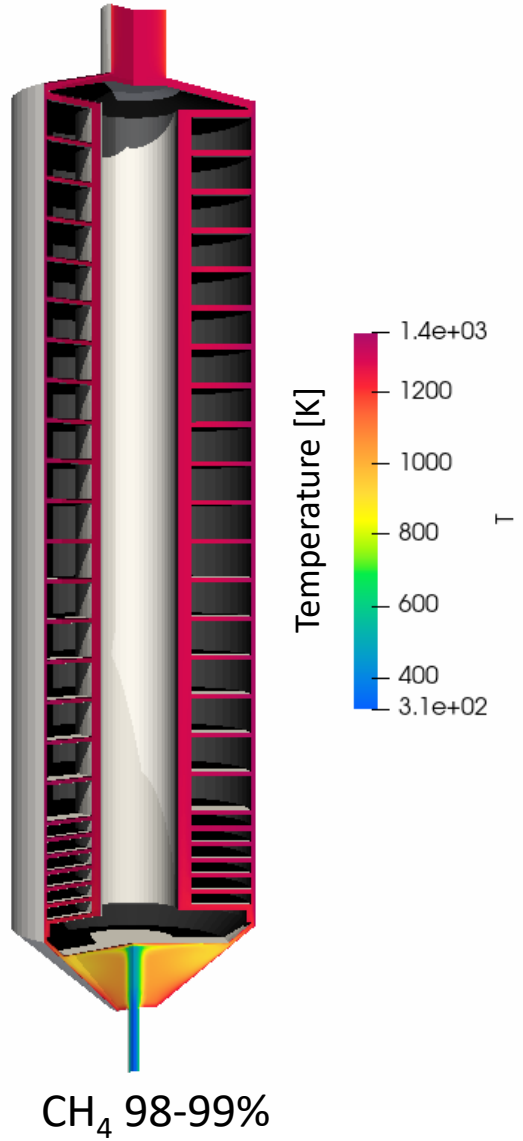

CH_4 98-99%

Chemical Vapor Infiltration (CVI) process

0 hours

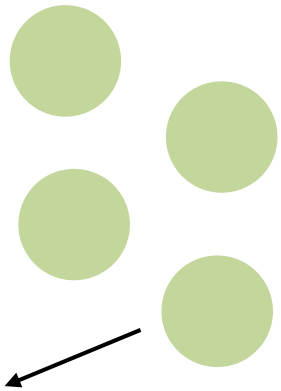

Initial carbon fiber array

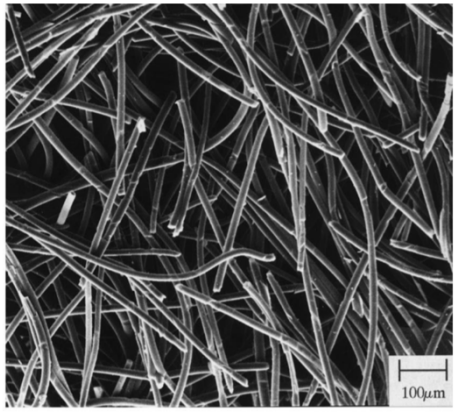

20 hours

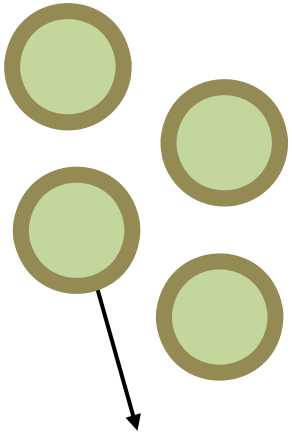

Deposited carbon layer

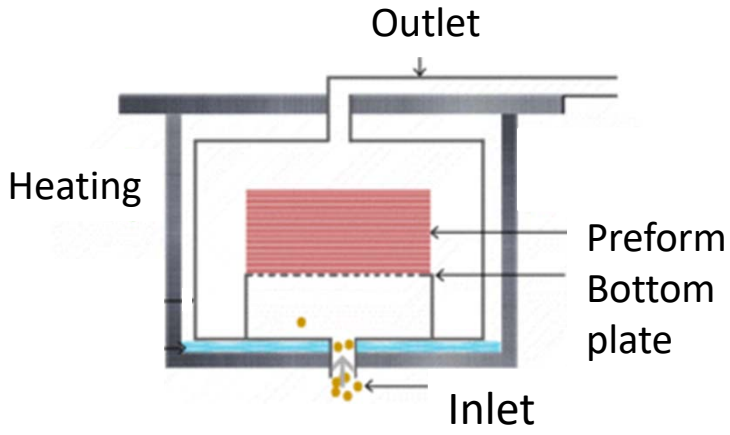

100 hours

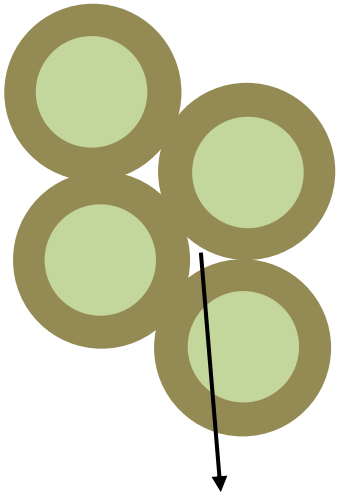

Residual porosity

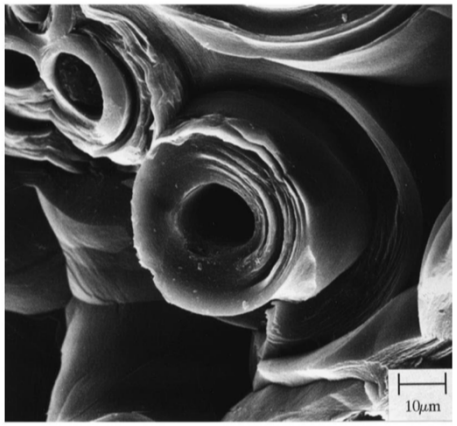

Chemical Vapor Infiltration (CVI) process

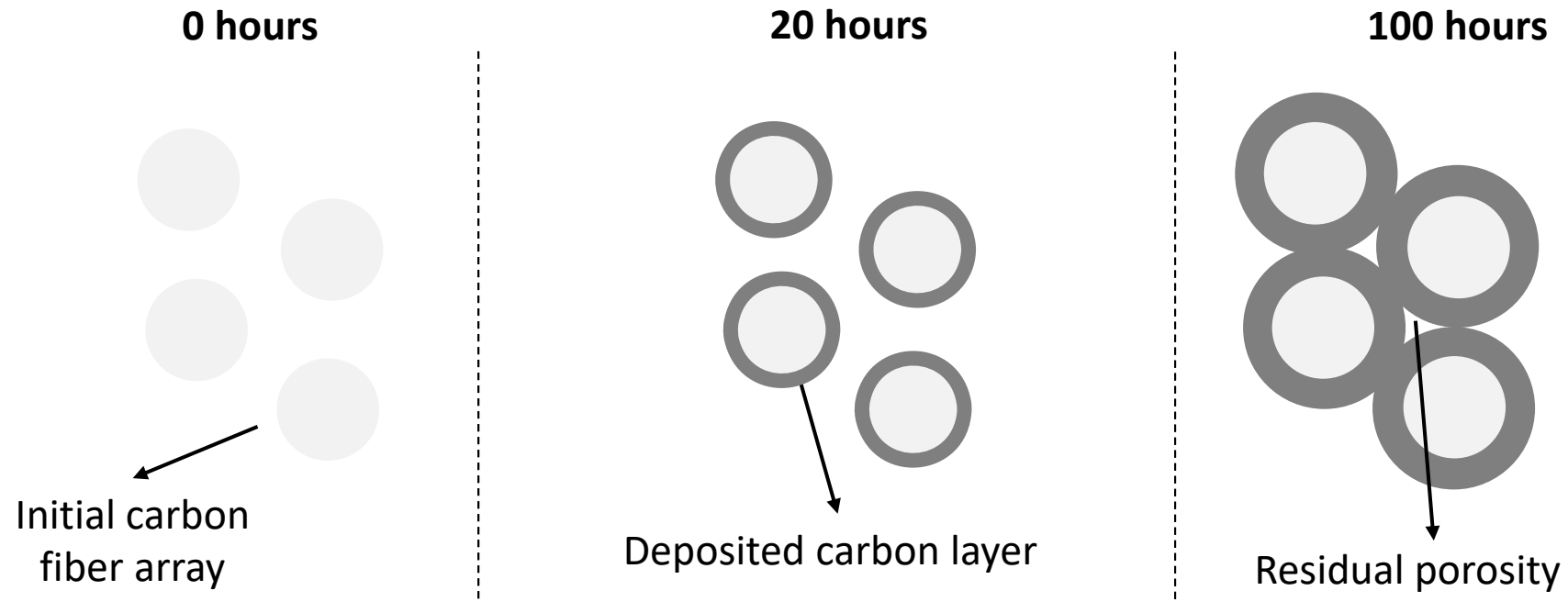

Homogeneous gas phase reactions

CH_4 → C_2 species → C_6 species → C_{6+} species → Soot

Heterogeneous surface reactions

Pyrocarbon C_∞

CVI Reactor Modeling

Homogeneous phase
(240 reactions and 27 species)

Heterogeneous phase*
(275 reactions and 66 surface species)

Methodology

1) Partial decoupling between gas phase and densification process

2) Operator-Splitting technique for CFD simulations and Fully-coupled approach for CVI simulations

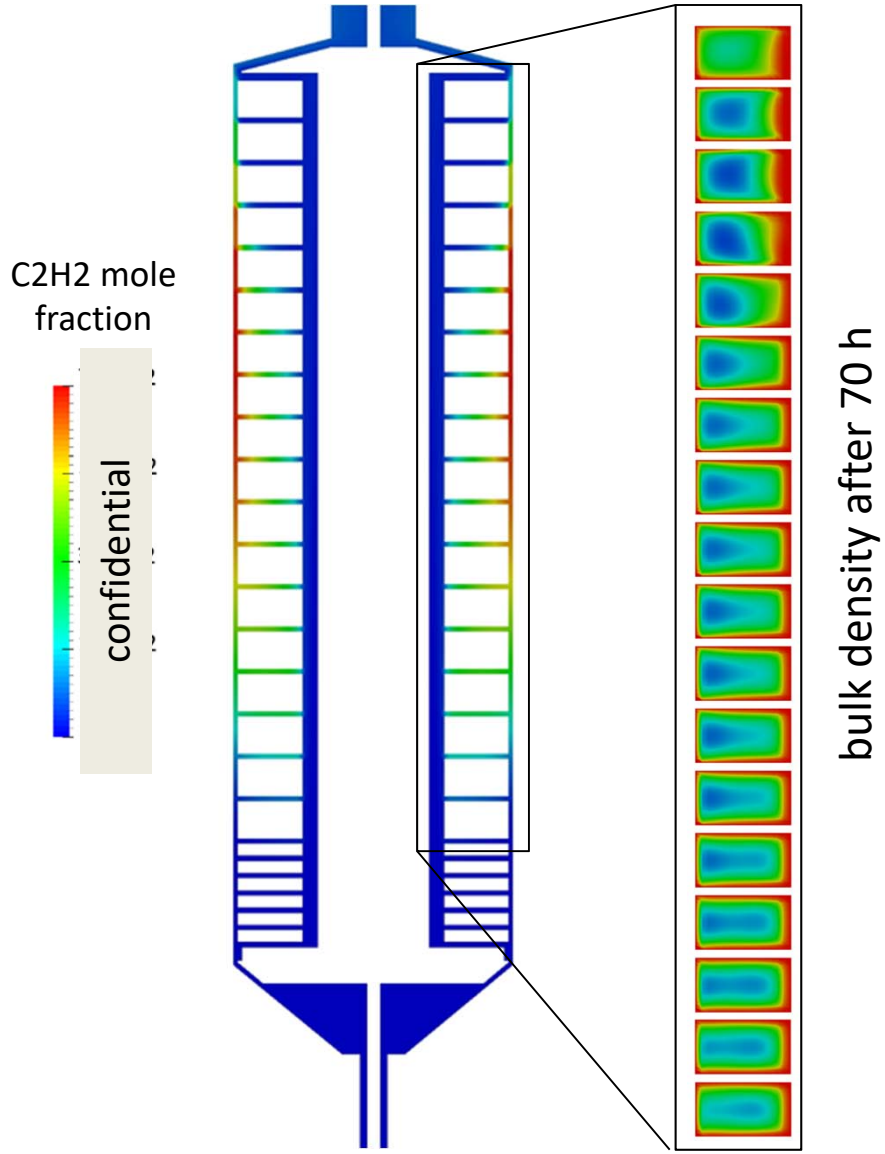

A. Cuoci, A. Frassoldati, T. Faravelli, *Numerical Modeling of reactors for Chemical Vapor Infiltration (CVI) with detailed homogeneous and heterogeneous kinetics*, ISCRE25, Florence (Italy) (2018)

*** Lacroix R, Fournet R, Ziegler-Devin I, et al.** *Kinetic modeling of surface reactions involved in CVI of pyrocarbon obtained by propane pyrolysis,* Carbon, 2010, 48: 132–144

Mean bulk density

Temporal evolution of mean bulk density

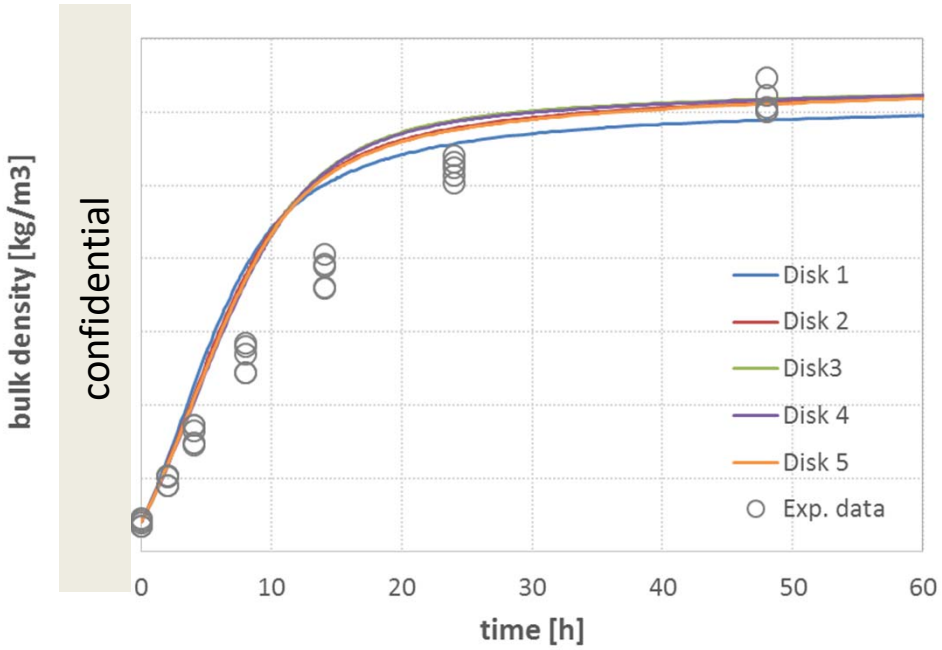

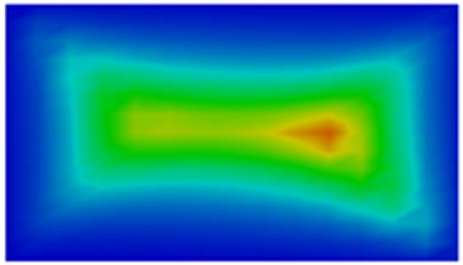

Ratio C2H2/C6H6

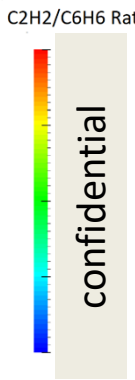

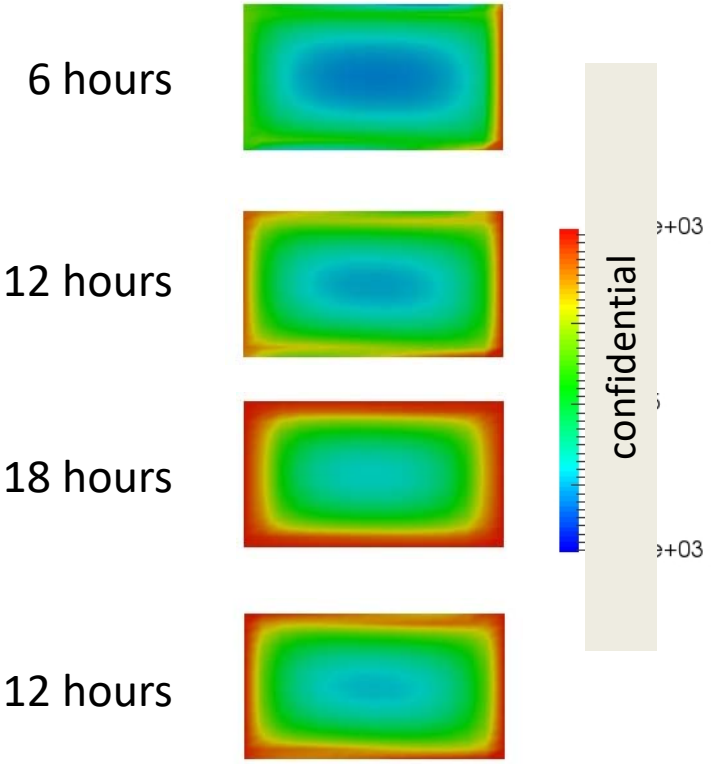

The C2H2/C6H6 is a direct measure of the quality of the graphite

Training dataset: Plug Flow Reactors

Plug Flow Reactors with imposed temperature profile

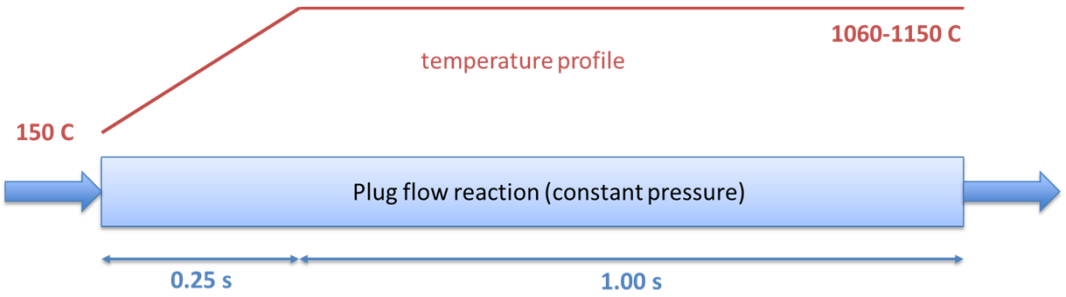

Baseline

Inlet stream (% mol)

CH4	98.84
C2H6	0.11
C3H8	0.01
N2	1.04

Temperature range: 1060-1150 C
Time range (ramp): 0.10-0.50 s

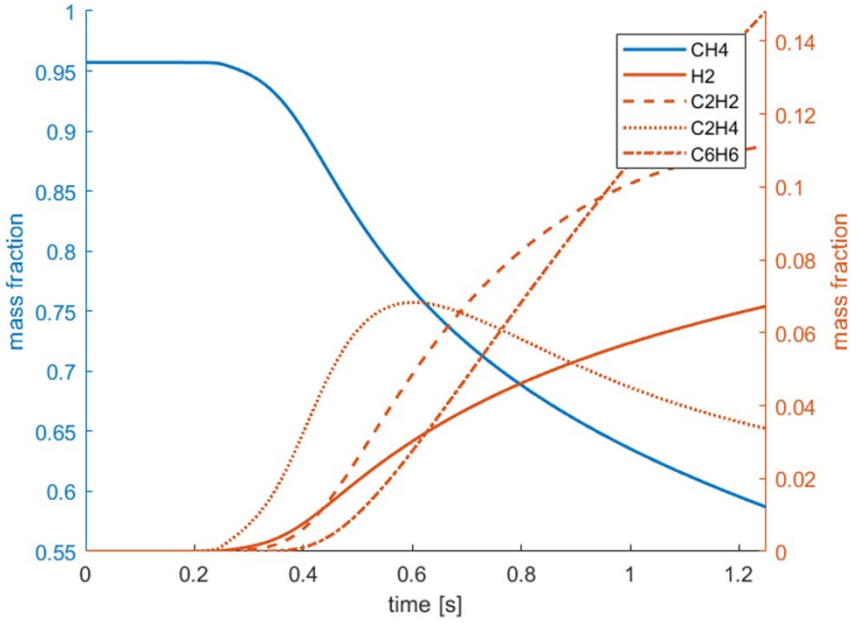

Database

- 500 Plug Flow Reactors
- ~120,000 observations

ANNs training based on Principal Components

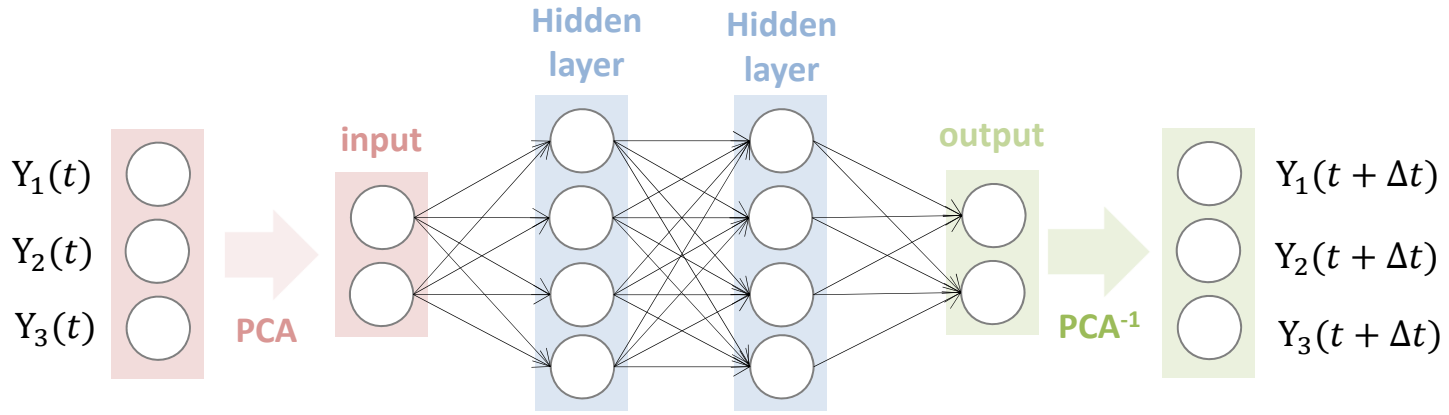

The ANNs are not trained on the composition, but on the first 4 Principal Components

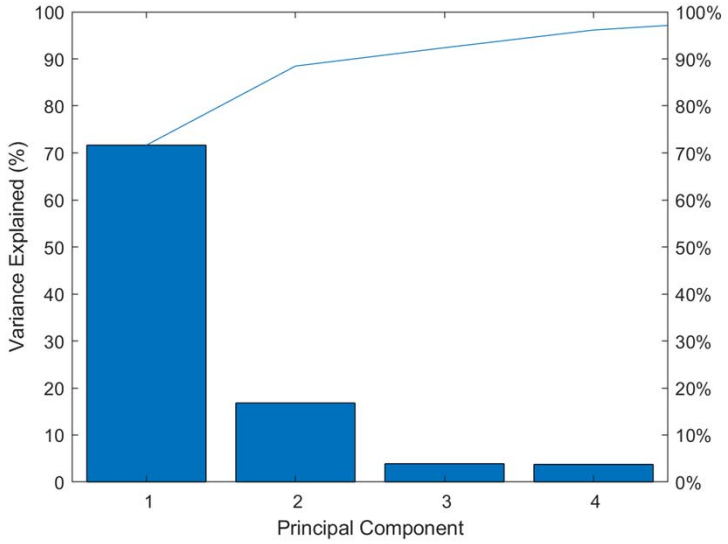

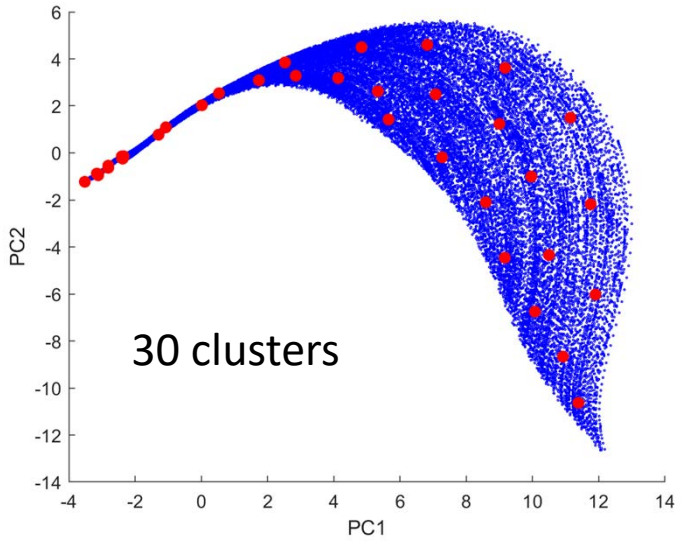

ANNs Training

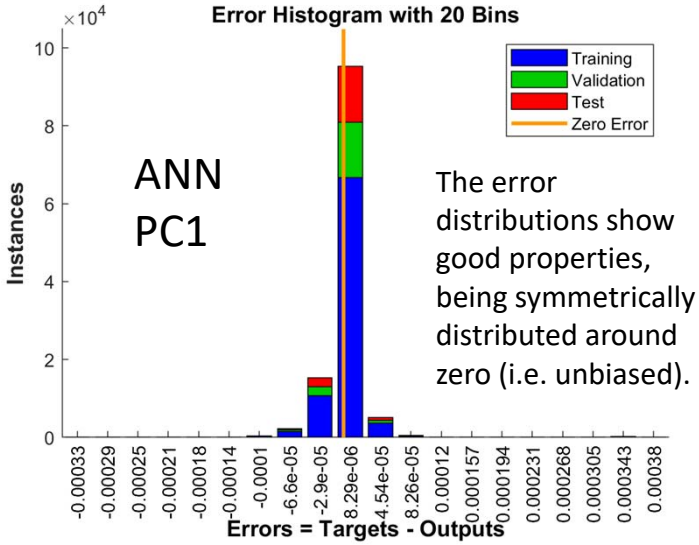

ANN PC1

The error distributions show good properties, being symmetrically distributed around zero (i.e. unbiased).

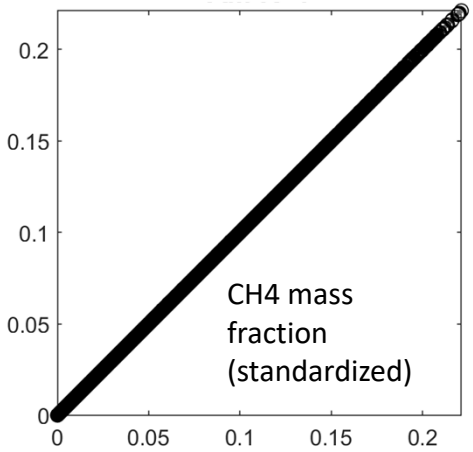

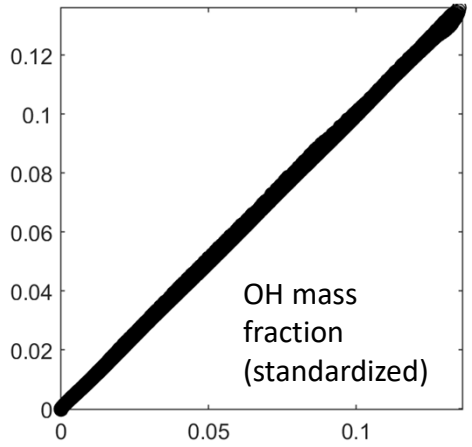

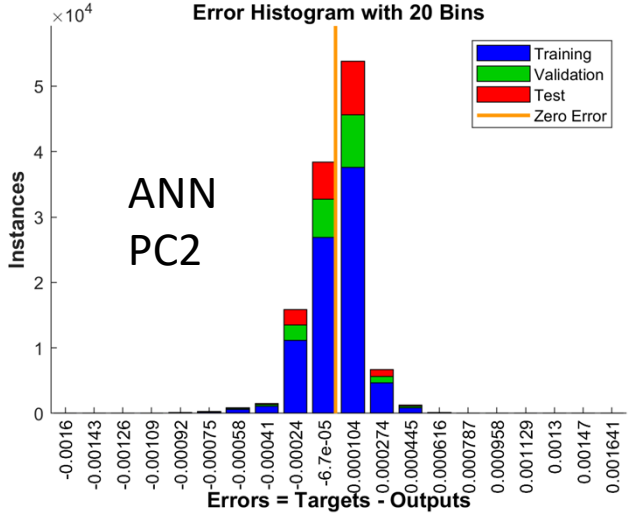

ANN PC2

Several tests were performed to find a suitable network topology (compromise between accuracy and computational cost)

- Number of hidden layers: ~2
- Number of neurons per layer: ~10

Computational performances

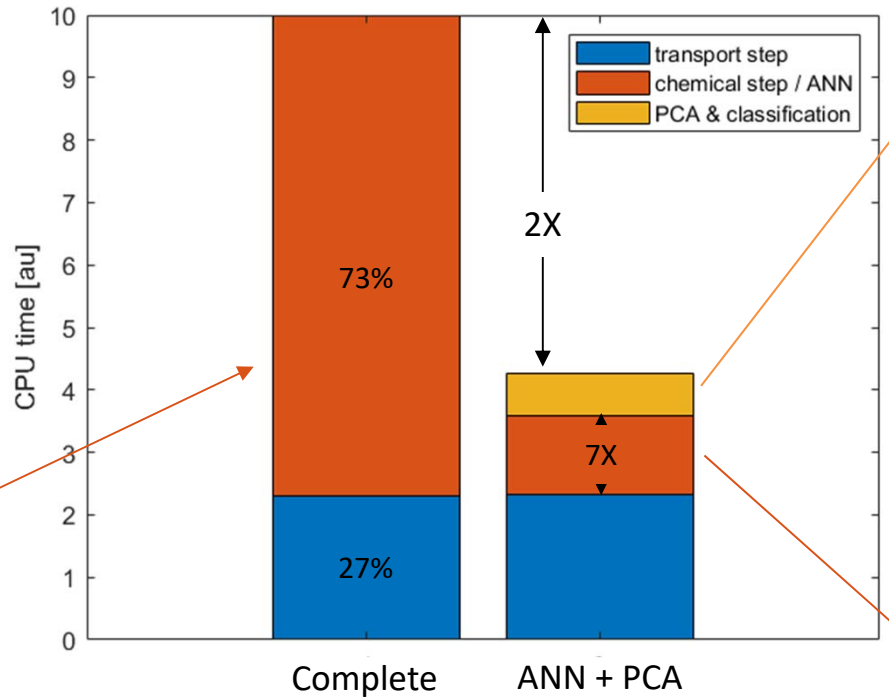

The maximum theoretical speed-up is 3.70

Additional time is required for performing the PCA (projection on the main PCs) and for classifying the cells (30 clusters)

4 different ANNs per cell are solved at each time step

Final remarks

Chemistry Acceleration to enable the adoption of detailed chemistry in CFD of combustion and heterogeneous catalysis can be carried out at different levels:

i. reduction of chemical complexity
ii. reduction of number of reactive environments
iii. replacement of stiff ODE solvers

Chemistry Acceleration techniques can take advantage from Machine Learning:

i. Unsupervised classification (k-means, LPCA)
ii. Regression via feed-forward ANN

Some of the Chemistry Acceleration techniques relies on a **time-consuming trial-and-error process** (especially correct definition of ANN architectures)

Chemistry Acceleration & Machine Learning is a **relatively new field, thus not yet mature**, with significant potential benefits to be better explored.

Acknowledgements

CRECK Modeling Lab @ POLIMI

- Abd Essamade Saufi
- Alessandro Stagni
- Alessio Frassoldati
- Marco Mehl
- Matteo Pelucchi
- Tiziano Faravelli

Laboratory of Catalysis and Catalytic Processes @ POLIMI

Matteo Maestri

Mauro Bracconi

Burn @ ULB

Alessandro Parente

Giuseppe D'Alessio

References (I)

Blasco, J.A., Fueyo, N., Dopazo, C., Ballester, J., Modelling the temporal evolution of a reduced combustion chemical system with an artificial neural network (1998) Combustion and Flame, 113 (1-2), pp. 38-52.
DOI: 10.1016/S0010-2180(97)00211-3

Blasco, J.A., Fueyo, N., Larroya, J.C., Dopazo, C., Chen, Y.-J., A single-step time-integrator of a methane-air chemical system using artificial neural networks (1999) Computers and Chemical Engineering, 23 (9), pp. 1127-1133.
DOI: 10.1016/S0098-1354(99)00278-1

Bracconi, M., Maestri, M., Cuoci, A., In situ adaptive tabulation for the CFD simulation of heterogeneous reactors based on operator-splitting algorithm (2017) AIChE Journal, 63 (1), pp. 95-104.
DOI: 10.1002/aic.15441

Chatzopoulos, A.K., Rigopoulos, S., A chemistry tabulation approach via rate-controlled constrained equilibrium (RCCE) and artificial neural networks (ANNs), with application to turbulent non-premixed CH4/H2/N2 flames (2013) Proceedings of the Combustion Institute, 34 (1), pp. 1465-1473.
DOI: 10.1016/j.proci.2012.06.057

Chen, J.-Y., Blasco, J.A., Fueyo, N., Dopazo, C., An economical strategy for storage of chemical kinetics: Fitting in situ adaptive tabulation with artificial neural networks (2000) Proceedings of the Combustion Institute, 28 (1), pp. 115-121.
DOI: 10.1016/S0082-0784(00)80202-7

Cuoci, A., Frassoldati, A., Faravelli, T., Ranzi, E., Numerical modeling of laminar flames with detailed kinetics based on the operator-splitting method (2013) Energy and Fuels, 27 (12), pp. 7730-7753.
DOI: 10.1021/ef4016334

Contino, F., Jeanmart, H., Lucchini, T., D'Errico, G., Coupling of in situ adaptive tabulation and dynamic adaptive chemistry: An effective method for solving combustion in engine simulations (2011) Proceedings of the Combustion Institute, 33 (2), pp. 3057-3064.
DOI: 10.1016/j.proci.2010.08.002

References (II)

D'Alessio, G., Parente, A., Stagni, A., Cuoci, A., Adaptive chemistry via pre-partitioning of composition space and mechanism reduction (2020) Combustion and Flame, 211, pp. 68-82, DOI: 10.1016/j.combustflame.2019.09.010

Franke, L.L.C., Chatzopoulos, A.K., Rigopoulos, S., Tabulation of combustion chemistry via Artificial Neural Networks (ANNs): Methodology and application to LES-PDF simulation of Sydney flame L (2017) Combustion and Flame, 185, pp. 245-260. DOI: 10.1016/j.combustflame.2017.07.014

Kambhatla, N., Leen, T.K., Dimension Reduction by Local Principal Component Analysis (1997) Neural Computation, 9 (7), pp. 1493-1516.
DOI: 10.1162/neco.1997.9.7.1493

Law, C.K., Combustion at a crossroads: Status and prospects (2007) Proceedings of the Combustion Institute, 31 I (1), pp. 1-29.
DOI: 10.1016/j.proci.2006.08.124

Liang, L., Stevens, J.G., Farrell, J.T., A dynamic multi-zone partitioning scheme for solving detailed chemical kinetics in reactive flow computations (2009) Combustion Science and Technology, 181 (11), pp. 1345-1371.
DOI: 10.1080/00102200903190836

Liang, Y., Pope, S.B., Pepiot, P., A pre-partitioned adaptive chemistry methodology for the efficient implementation of combustion chemistry in particle PDF methods (2015) Combustion and Flame, 162 (9), pp. 3236-3253.
DOI: 10.1016/j.combustflame.2015.05.012

Lu, T., Law, C.K., A directed relation graph method for mechanism reduction (2005) Proceedings of the Combustion Institute, 30 (1), pp. 1333-1341.
DOI: 10.1016/j.proci.2004.08.145

Lu, T., Law, C.K., Toward accommodating realistic fuel chemistry in large-scale computations (2009) Progress in Energy and Combustion Science, 35 (2), pp. 192-215.
DOI: 10.1016/j.pecs.2008.10.002

References (III)

Lu, L., Pope, S.B., An improved algorithm for in situ adaptive tabulation (2009) Journal of Computational Physics, 228 (2), pp. 361-386.
DOI: 10.1016/j.jcp.2008.09.015

Pepiot-Desjardins, P., Pitsch, H., An efficient error-propagation-based reduction method for large chemical kinetic mechanisms (2008) Combustion and Flame, 154 (1-2), pp. 67-81.
DOI: 10.1016/j.combustflame.2007.10.020

Perini, F., High-dimensional, unsupervised cell clustering for computationally efficient engine simulations with detailed combustion chemistry (2013) Fuel, 106, pp. 344-356.
DOI: 10.1016/j.fuel.2012.11.015

Pope, S.B., Computationally efficient implementation of combustion chemistry using in situ adaptive tabulation (1997) Combustion Theory and Modelling, 1 (1), pp. 41-63.
DOI: 10.1080/713665229

Ranade, R., Li, G., Li, S., Echekki, T., An Efficient Machine-Learning Approach for PDF Tabulation in Turbulent Combustion Closure (2019) Combustion Science and Technology
DOI: 10.1080/00102202.2019.1686702

Rebughini, S., Cuoci, A., Dixon, A.G., Maestri, M., Cell agglomeration algorithm for coupling microkinetic modeling and steady-state CFD simulations of catalytic reactors (2017) Computers and Chemical Engineering, 97, pp. 175-182.
DOI: 10.1016/j.compchemeng.2016.11.033

Schwer, D.A., Tolsma, J.E., Green Jr, W.H., Barton, P.I., On upgrading the numerics in combustion chemistry codes (2002) Combustion and Flame, 128 (3), pp. 270-291.
DOI: 10.1016/S0010-2180(01)00352-2

References (IV)

Sen, B.A., Hawkes, E.R., Menon, S., Large eddy simulation of extinction and reignition with artificial neural networks based chemical kinetics (2010) Combustion and Flame, 157 (3), pp. 566-578.
DOI: 10.1016/j.combustflame.2009.11.006

Sen, B.A., Menon, S., Linear eddy mixing based tabulation and artificial neural networks for large eddy simulations of turbulent flames (2010) Combustion and Flame, 157 (1), pp. 62-74.
DOI: 10.1016/j.combustflame.2009.06.005

Sen, B.A., Menon, S., Turbulent premixed flame modeling using artificial neural networks based chemical kinetics (2009) Proceedings of the Combustion Institute, 32 I (1), pp. 1605-1611.
DOI: 10.1016/j.proci.2008.05.077